

DISS. ETH NO. 24744

**MODULATING ENTEROCYTE METABOLISM AFFECTS  
WHOLE BODY GLUCOSE HOMEOSTASIS IN MICE**

A thesis submitted to attain the degree of  
DOCTOR OF SCIENCES of ETH ZURICH

(Dr. sc. ETH Zurich)

presented by

DEEPTI RAMACHANDRAN

MSc, Tata Institute of Fundamental Research, Mumbai (India)

born on 29.05.1987

citizen of India

accepted on the recommendation of

Prof. Dr. Wolfgang Langhans, examiner

Dr. Abdelhak Mansouri, co-examiner

Prof. Dr. Christian Wolfrum, co-examiner

Prof. Dr. Carina Prip-Buus, co-examiner

2017



## ACKNOWLEDGEMENTS

I have many people to thank for being able to make it to the point of writing my thesis acknowledgements and I would like to start with my thesis supervisor Prof. Wolfgang Langhans. Wolfgang, I remember my first phone call with you when I was in India and you inviting me to come see the lab in December 2011. Thank you for that and for all the opportunities you have provided me since then. I don't think any other lab or professor would have given me the kind of scientific freedom you did and I really appreciate it. You also get all the credit for the kind of team you put together here in Schwerzenbach, some of the best people I met in Switzerland are people I met here. Thank you for your encouragement, support and willingness to agree to disagree with your students when it comes to scientific discussions. More importantly, thank you for always treating all of us as adults and independent thinkers - I feel like that simple concept is often lost in the teacher - student relationship, but not with you.

Next, I would like to thank Dr. Abdelhak Mansouri. Thank you Abdelhak for your support and critical input throughout my PhD. You also gave me the freedom to do my research my way and I really appreciate that. We have both discussed and argued about science and beyond and I hope you appreciate the experience as much as I do.

I would like to thank Prof. Christian Wolfrum and Prof. Carina Prip-Buus for being on my doctoral committee and for taking the time out to read this thesis. Christian, I am very grateful for the generous use of your cell culture facility and your molecular biology facility. Much of my research would not have been possible if these labs and equipment were not freely accessible to us. Carina, thank you for generously allowing us the use of your Cpt1mt mice and the plasmid construct. Thank you also for your encouragement and your helpful critique on the manuscript.

I would also like to thank all the Langhans' lab members, past and present. I have learnt a lot from all of you, about science and life. I would especially like to thank Rosi. I have received a lot of help from several people in this lab, but I think you have been instrumental in shaping how my research projects turned out. Thank you for working with me to figure out the enterocyte isolation Rosi. Your enthusiasm for science and for life, and your unbelievable kindness to every single person you meet is something I will never be able to achieve, but have always admired. I would also like to thank Ulli for teaching me how to handle rats and mice, for being the best person I

could possibly sit next to in the office, for listening to all my problems and coming up with real solutions and for always encouraging me to go out and enjoy the sun. I wish I could say I learnt how to be organized from you, I think you are amazing at it, but I am a bad student when it comes to that. I would like to thank Marie, for being the scientific brain I could always pick at any time of the day or night, and for picking mine in turn. I think talking to you forced me to think about things I would never consider otherwise and I learnt more from you than anyone else in all my time here. I am in awe of your brain and your capacity to work thrice as much as anyone else, without losing your motivation. It is very inspiring and I hope you never lose that. I would like to thank Elnaz for her help with the initial phase of my project and for always being honest and appreciating my honesty in return. I do not think I met anyone else who appreciated my blunt talking more. I miss all the fun times we had together, but I am very happy for you and the successes you have achieved now. I would like to thank Shahana, for being my memory bank and for stepping into the void of scientific discussions we faced when Marie and JP left the lab, and really living up to it. Your help in experiments has been invaluable to me and your willingness to help everyone is something I will always admire. Thank you Sharon for also stepping in and helping me out with experiments, support and for lifting the atmosphere in the lab, not many people are able to make others happy the way you do. Thank you JP, for being another science – brain we could all look upto. We started around the same time in the lab, but the skill and acumen with which you finished your PhD and the way you managed to make it look so easy is something I will always envy. Thank you for always helping me with the 10,000 stats questions I kept asking you. Most of all I would like to thank you all for being my friends. No one can ask for a better group of people to work with.

I would also like to thank Nadja, Melanie, Sandra and Nino for their help with experiments or with moral support. Melanie and Sandra, thank you for the great times we shared in our office together. Thank you to Forouhar, Liz and Myrtha for your technical help and support. A special thanks to Forouhar for doing what must be thousands of genotypings for me with no complaints. Also thank you for being such an encouraging and supportive friend to me. Thank you to all the students that I worked with – Flavia, Ladina, Johannes, Mirjam for working with me and for giving me the opportunity to learn from you. Also thank you to every other Langhans lab member with whom I overlapped.

A special thank you to Marcel for being the IT tech through most of my PhD. Your support was so important and much appreciated. Because of your constant work we always had a smooth working environment online and I really appreciate that. Thank you to Silke, Thomas, Simone, Mandy, Michele, and all the other animal care takers. Your work has been invaluable to me and I would never have been able to do my research if not for you Silke and your organization of the entire animal facility. I was really sorry to see you leave. Also, thank you to Ruth for helping me out with all the administrative work at ETH, your work in the background of our research often went unnoticed and unacknowledged.

Thank you to the Wolfrums and the Ristows and the De Bock's for all the support and the fun times we have had together. A special thanks to Abdiel for helping me with the fatty acid oxidation assays - they worked so smoothly because of all the work you did to standardize the technique.

On a personal note, thank you to all my friends in Switzerland- Arpan, Rajlakshmi, Mukul, Dolon, Natasha, Raul, Juliet, Rafa, Foteini and Natalia. There are several more but you guys have been instrumental in making my life in Switzerland a very happy one, so thank you. I would like to thank my friends further away especially Upasana, Sonal and Vasudha for being the people that they are in my life. This space is too small to write down what you girls mean to me so I will not start.

Thank you to my parents who have been the backbone of my life, without whom I would not be anywhere close to where I am today. The past few years have been a lesson in strength for me, a lesson I learnt by watching you both deal with adversity so gracefully. Thank you to Divchi my sister by blood and by soul. You have been incredibly supportive of me while dealing with your own struggles. I am in awe of how much courage you have and I hope you know I will always be there to support you. Thank you to Riya, Nikhิตetta, Pooja and Vinit. You all are the support system I always know I can fall back on, night or day. We don't get to choose family, so I feel incredibly lucky to have you as mine. Thank you also to my extended family of aunts, uncles and cousins all of whom I cannot name here, but who are all a big part of my life.

In my attempts to write this, if I have forgotten to thank anyone, please forgive me and blame it on sleep deprivation and my well-known bad memory. I hope I have thanked you in person to make up for the error.

# TABLE OF CONTENTS

ACKNOWLEDGMENTS	1
LIST OF ABBREVIATIONS	6
SUMMARY	10
ZUSAMMENFASSUNG	12
CHAPTER 1:GENERAL INTRODUCTION	15
1.1 Obesity, a general overview	16
1.2 Causes of obesity	17
1.3 Comorbidities of obesity	17
1.3.1 Type-2 diabetes	18
1.4 Treatments for obesity and diabetes	18
1.4.1 Lifestyle changes	19
1.4.2 Pharmacological treatments	19
1.4.3 Surgical interventions	20
1.5 Mechanisms of RYGB and T2D remission	22
1.6 Structural overview of the small intestine	23
1.7 Metabolic characteristics of the small intestine	24
1.8 Enterocyte fatty acid metabolism	25
1.9 Effects of enterocyte FAO on food intake and metabolism	26
1.10 Sirtuin 3, the global mitochondrial deacetylase	27
1.11 Carnitine palmitoyltransferase-1, the rate-limiting enzyme of fatty acid oxidation	29
1.12 Aims of the thesis	31
1.13 References	33
CHAPTER 2:INTESTINAL SIRT3 OVEREXPRESSION IN MICE IMPROVES WHOLE BODY GLUCOSE HOMEOSTASIS INDEPENDENT OF BODY WEIGHT	43
Abstract	44
2.1 Introduction	45
2.2 Materials and methods	47

2.3	Results	54
2.4	Discussion	62
2.5	References	72
CHAPTER 3:ENTEROCYTE EXPRESSION OF MUTATED CARNITINE PALMITOYLTRANSFERASE-1 INSENSITIVE TO MALONYL COA INHIBITION IN MICE AFFECTS GLYCEMIC CONTROL DEPENDING ON DIETARY FAT		78
	Abstract	79
3.1	Introduction	80
3.2	Materials and methods	81
3.3	Results	90
3.4	Discussion	104
3.5	References	112
CHAPTER 4:GENERAL DISCUSSION		116
4.1	Overview of the main findings	117
4.2	Limitations of our transgenic manipulation	117
4.3	Intestinal ketogenesis	119
	4.3.1 Looking beyond hepatic ketogenesis	119
	4.3.2 Regulation of ketogenesis in pathophysiology	119
	4.3.3 Ketone bodies and glycemic control	121
	4.3.4 Rising ketone body levels - friend or foe?	122
4.4	Intestinal gluconeogenesis	123
	4.4.1 Intestinal gluconeogenesis – physiological relevance	123
	4.4.2 Intestinal gluconeogenesis and glycemic control	123
4.5	Intestinal crosstalk - how does the intestine signal to the rest of the body?	124
4.6	Future prospects	126
4.7	References	128
APPENDIX		134
	<i>Curriculum vitae</i>	135

## LIST OF ABBREVIATIONS

2-DG	2-deoxyglucose
ACC1 or ACACA	acetyl-CoA carboxylase alpha
ACC2 or ACACB	acetyl-Coenzyme A carboxylase beta
AceCS2	acetyl-CoA synthetase-2
AGB	adjustable gastric lap band
Anti+Rot	antimycin and rotenone
ATP	adenosine triphosphate
ATPsyn	ATP synthase
BAT	brown adipose tissue
BHB	$\beta$ -hydroxybutyrate or D- $\beta$ -hydroxybutyrate
BMI	body mass index
CD	(low-fat) control diet
CNS	central nervous system
CoA	coenzyme-A
COX IV	cytochrome-c oxidase subunit-IV
CPT1	carnitine palmitoyltransferase-1
CPT1mt	CPT1a mutant - CPT1m593S
Cpt1mt <sup>fl/fl</sup>	mice with <i>loxP</i> -STOP- <i>loxP</i> -CPT1mt cassette
CPT2	carnitine palmitoyltransferase-2
CT	microcomputed tomography
CVD	cardiovascular disease
DAG	diacylglycerols
DGAT1	acyl-CoA:diacylglycerol acyltransferase-1



DGAT2	acyl-CoA:diacylglycerol acyltransferase-2
DIO	diet-induced obesity
DJB	duodenal-jejunal bypass
ECAR	extracellular acidification rate
ER	endoplasmic reticulum
FAO	fatty acid oxidation
FASN	fatty acid synthase
FAT/CD36	fatty acid translocase/ cluster of differentiation-36
FATP	fatty acid transport protein
FCCP	carbonyl cyanide-4-phenylhydrazone
FCCP	carbonyl cyanide-4-(trifluoromethoxy)-phenylhydrazone
<i>G6pc</i>	glucose-6-phosphatase, catalytic subunit
GABA	gamma-aminobutyric acid
GLP-1	glucagon-like peptide-1
H&E	Hematoxylin and eosin
HFD	high-fat diet
HFHS	high fat-high sucrose
HILIC	hydrophilic interaction chromatography
HK1	hexokinase 1
HMGCS2	3-hydroxy-3-methylglutaryl-CoA synthase-2
iCPT1mt	mice with an enterocyte-specific CPT1mt expression
IDH2	isocitrate dehydrogenase-2
FABP2 or IFABP	intestinal fatty acid binding protein
IP	intraperitoneally

IR	insulin resistance
iSIRT3	mice with an enterocyte-specific SIRT3 overexpression
IST	insulin sensitivity test
KD	ketogenic diets
LCAD	long-chain acyl-CoA dehydrogenase
LCFA	long-chain fatty acids
LC-MS	liquid chromatography–mass spectrometry
FABP1or LFABP	liver fatty acid binding protein
MAG	monoacylglycerol
MCT	monocarboxylate transporters
MGAT	acyl-CoA: monoacylglycerol acyltransferase
MnSOD	manganese superoxide dismutase
NAC	N-acetyl cysteine
NAD	nicotinamide adenine dinucleotide
NEFA	non-esterified fatty acids
OCR	oxygen consumption rate
OEA	oleoylethanolamide
OGTT	oral glucose tolerance test
Oligo	oligomycin
PCOS	polycystic ovarian syndrome
Pen-strep	penicillin and streptomycin
PEPCK1	phosphoenolpyruvate carboxykinase 1
PGC1a	peroxisome proliferative activated receptor gamma, coactivator 1 alpha

PKA	protein kinase
PPAR $\alpha$	peroxisome proliferator activated receptor-alpha
PPIB	peptidylprolyl Isomerase B
PYY	peptide YY
RER	respiratory exchange ratio
ROS	reactive oxygen species
RT-qPCR	Real time quantitative polymerase chain reaction
RYGB	Roux-en-Y gastric bypass
S3fl	mice with <i>loxP</i> -STOP- <i>loxP</i> -Sirt3 cassette
SCFA	short-chain fatty acid
SCOT	Succinyl-CoA: 3-oxoacid CoA transferase
SEM	standard error of the mean
SglT1	sodium-dependent glucose co-transporter
SIRT3	Sirtuin3
SMCT	sodium-coupled monocarboxylate transporters
SOPF	specified and opportunistic pathogen free
T2D	type-2 diabetes
TAG	triacylglycerol
TCA	tri-carboxylic acid
TFAM	transcription factor A, mitochondrial
VDAC	voltage-dependent anion channel
Vil-Cre or Villin-Cre	mice expressing Cre recombinase under Villin promoter
VSG	vertical sleeve gastrectomy
WHO	World Health Organization

## SUMMARY

Obesity and its comorbidities are a growing concern in today's world. Obesity and overweight increase the risk of developing several life threatening diseases, the risks of which are decreased significantly even with a moderate weight loss. The most common comorbidity of obesity is type-2 diabetes which involves a severe dysfunction in glycemic control.

Several studies suggest that gut metabolism plays an important role in whole body energy metabolism. Data from peripheral administration of drugs that reduced food intake in rodents showed that the inhibition of eating was associated with increased fatty acid oxidation (FAO) and ketogenesis in the small intestine, but not in the liver. Gastric bypass studies in humans and rodents indicate that the restructuring of the small intestine leads to morphological and metabolic changes in the gut. These changes are associated with the almost immediate reversal of the diabetic phenotype seen post-surgery, which is absent or less pronounced in surgeries like gastric banding that do not involve these dramatic changes in the small intestine. The intestinal mucosa, or rather the epithelial cells in the small intestine, are the main cells that absorb nutrients from the diet, and redistribute them for storage or to immediately fuel metabolism in the rest of the body. Enteroendocrine cells in the gut epithelium respond to different nutritional and metabolic cues and release gut hormones that also control eating behavior and regulate glucose homeostasis.

All these factors led us to hypothesize that modulating enterocyte metabolism by upregulating FAO in these cells might affect the development of diet-induced obesity (DIO) and impaired glucose homeostasis. To test this we developed two different transgenic mouse models to upregulate enterocyte FAO. Using the *cre-loxP* system, we overexpressed the mitochondrial protein Sirtuin 3 (SIRT3) or expressed a mutant

form of the mitochondrial protein carnitine palmitoyltransferase-1 (CPT1mt) in the enterocytes of mice. We phenotyped these mice under conditions of low-fat control diet (CD) or high-fat diet (HFD) feeding.

Our results show that constitutive (over)expression of SIRT3 or CPT1mt in mouse enterocytes had no effects on body weight gain and the development of DIO. Also, enterocyte SIRT3 expression did not affect glycemic control in CD-fed mice, but improved insulin sensitivity and glucose tolerance in HFD-fed mice, despite the development of DIO. Conversely, enterocyte specific CPT1mt expression led to impaired glucose homeostasis in CD-fed mice, but improved it in HFD-fed mice with DIO. Together our results indicate that modulating enterocyte metabolism can affect whole body glucose homeostasis differentially independent of body weight, but dependent on the nutritional content of the diet.

## ZUSAMMENFASSUNG

Übergewicht und die Komorbiditäten der Adipositas erregen weltweit wachsende Besorgnis. Adipositas und Übergewicht sind hohe Risikofaktoren für die Entwicklung einiger lebensbedrohlicher Krankheiten. Schon moderater Gewichtsverlust führt zu einer signifikanten Reduktion dieser Risikofaktoren. Die häufigste Komorbidität der Adipositas ist Typ-2-Diabetes, definiert durch eine unzureichende glykämische Kontrolle.

Einige frühere Studien weisen darauf hin, dass der Darmstoffwechsel eine wichtige Rolle im Energiestoffwechsel des ganzen Körpers spielt. Bei Nagetieren zeigte die periphere Verabreichung von Medikamenten, welche die Futteraufnahme inhibieren auf, dass die resultierende Verzehrdepression mit einer erhöhten Fettsäureoxidation und Ketogenese im Dünndarm, jedoch nicht in der Leber, assoziiert war. Magenbypass-Studien an Menschen und Nagetieren deuten darauf hin, dass die operationsbedingte Umstrukturierung des Dünndarms zu morphologischen und metabolischen Veränderungen im Darm führt. Diese Veränderungen sind mit der fast unmittelbaren Umkehr des Diabetes-Phänotyps nach der Operation assoziiert. Diese Umkehr ist weniger ausgeprägt oder gar ausbleibend bei Operationen wie dem Magenband, welches keine dramatischen Veränderungen im Dünndarm auslöst. Die Darmschleimhaut, oder genauer gesagt die Epithelzellen des Dünndarms, sind die Zellen, die hauptsächlich die Nährstoffe aus der Nahrung absorbieren. Diese Nährstoffe werden dann zur Speicherung oder für den sofortigen Brennstoffverbrauch des Körperstoffwechsels weiterverteilt. Enteroendokrine Zellen im Darmepithel reagieren auf verschiedene Stimuli aus der Nahrung und aus dem Stoffwechsel und setzen Hormone des Darms frei. Diese Hormone kontrollieren das Essverhalten und regulieren die Glukosehomöostase.

All diese Faktoren führten uns zur Hypothese, dass die Modulation des Enterozytenstoffwechsels durch die Hochregulierung der Fettsäureoxidation einen Effekt auf die Entwicklung der diätinduzierten Adipositas und auf die beeinträchtigte Glukosehomöostase haben könnte. Um dies zu untersuchen, haben wir zwei verschiedene transgene Mausmodelle entwickelt, welche die Fettsäureoxidation der Enterozyten hochregulieren. Mittels des Cre-loxP Systems haben wir in den Enterozyten von Mäusen das mitochondriale Protein Sirtuin-3 (SIRT3) überexprimiert oder eine mutante Form des mitochondrialen Proteins Carnitin-Palmitoyltransferase-1 (CPT1mt) exprimiert. Wir phänotypisierten diese Mäuse auf einer fettarmen Kontrolldiät und einer Hochfettdiät.

Unsere Resultate zeigen, dass die konstitutive (Über)expression von SIRT3 oder CPT1mt in den Enterozyten der Mäuse keinen Effekt auf die Körpergewichtszunahme und auf die Entwicklung von diätinduzierter Adipositas hat. Zudem hatte die Expression von SIRT3 in den Enterozyten keine Auswirkung auf die glykämische Kontrolle bei den Mäusen, wenn sie die fettarme Kontrolldiät konsumierten. Die Expression von SIRT3 in den Enterozyten verbesserte jedoch die Insulinsensitivität und Glukosetoleranz der Mäuse auf Hochfettdiät, trotz der Entwicklung einer diätinduzierten Adipositas. Enterozyten-spezifische Expression von CPT1mt beeinträchtigte hingegen die Glukosehomöostase von Mäusen auf der fettarmen Kontrolldiät, verbesserte sie aber, wenn die Mäuse die Hochfettdiät konsumierten. Zusammengefasst weisen unsere Resultate darauf hin, dass das Verändern des Enterozyten-Stoffwechsels die Glukosehomöostase des ganzen Körpers beeinflussen kann, unabhängig vom Körpergewicht, jedoch abhängig vom Nährstoffgehalt der Diät.





## **CHAPTER 1:**

### **GENERAL INTRODUCTION**

# **OBESITY, TYPE-2 DIABETES AND THE POTENTIAL ROLE OF ENTEROCYTE METABOLISM**

---

## **1.1 Obesity, a general overview**

Obesity, i.e., the accumulation of excessive fat in the body, is one of the primary health concerns in most developed countries as well as in several developing countries [1]. Based on World Health Organization (WHO) statistics, the prevalence of obesity has more than doubled in the world since 1980 (WHO factsheet on Obesity and Overweight, Jun 2016). Obesity and overweight are highly correlated with increased mortality, worldwide [2]. Though not every obese person suffers from obesity-related complications as reviewed in [3], obese people are at a higher risk of developing a wide range of different diseases such as cardiovascular disease (CVD), type-2 diabetes (T2D), cancer, arthritis, infertility, and hypertension [4]. Obesity is defined based on the so-called body mass index (BMI) (Body mass (kg)/height<sup>2</sup> (m<sup>2</sup>)); an individual with a BMI > 30 is considered obese [5]. The BMI, however, has several shortcomings, which is why this definition has come into question [6, 7]. Measuring ectopic and visceral fat content can provide additional and often more accurate information about the increased risk for obesity-related complications or comorbidities [8]. Greater ectopic and visceral fat deposition rather than subcutaneous fat depots are associated with a higher risk of heart disease and other complications [9, 10]. Childhood obesity is probably an even greater health concern than adult obesity [11]. The increasing number of obese children and the decreasing age at which children are diagnosed as obese spells an enormous burden for our health care systems and seems to indicate that obesity is not a condition that is easily regulated and it does not require a long period of time to establish.

## **1.2 Causes of obesity**

What are the causes of obesity? It clearly is the result of a prolonged imbalance between energy intake and energy expenditure. Modern eating habits, which include consumption of many energy dense, easily accessible and highly palatable foods and drinks, tend to increase our caloric intake over what a moderately active person could burn with physical activity. The ever-increasing tendency to lead a sedentary life also adds to the lower energy expenditure that contributes to this imbalance. But, like most diseases, obesity is a complex condition that involves a combination of genetic and environmental factors [12]. The genetic basis of obesity also exists on a wide spectrum. Some genetic causes, such as mutations in the genes for leptin lead to uncontrolled obesity, and the only solution is hormone therapy [13]. In addition to such monogenetic causes of obesity, however, genome wide association studies have identified many genetic variants that are associated with an increased susceptibility to become obese in our current environment [14-16]. Studies in twins or adopted individuals have also helped delineate to a certain extent the contributions of environment vs genetics to the propensity to gain weight [17]. Together these studies seem to indicate that genetic factors could contribute to anywhere from 20 to 70% of an individual's BMI.

## **1.3 Comorbidities of obesity**

A comorbidity is a disease that occurs because of another primary disease - in this case obesity. As mentioned earlier, though the existence of obesity does not necessitate the occurrence of a comorbidity, obese people are at a higher risk of developing several associated diseases. These diseases include T2D, hypertension, CVD, several types of cancer, polycystic ovarian syndrome (PCOS) and osteoarthritis,

to name but a few. A wider waistline, high blood pressure, impaired glucose homeostasis and excessive circulating triglyceride and/or cholesterol levels are the features of the metabolic syndrome, and the occurrence of any three of these features together would classify someone to be suffering from metabolic syndrome. Any one of these features, however, does already increase the risk of a heart attack, stroke or T2D [5].

### **1.3.1 Type-2 diabetes**

T2D is possibly the most common comorbidity of obesity. T2D, also called adult onset diabetes mellitus, is a disease that develops over time, with an initial manifestation of high circulating glucose and insulin levels, also termed prediabetes [18]. The presence of both high circulating glucose and insulin levels is a sign of insulin resistance (IR), i.e., a state in which the  $\beta$ -cells of the pancreas are still able to produce insulin, but the body is unable to respond to insulin properly. To compensate for this loss of sensitivity, the  $\beta$ -cells enhance insulin production. This can go on for years, but slowly, over time, the  $\beta$ -cells begin to lose their ability to produce insulin, leading to long periods of hyperglycemia, which pose several health risks. T2D is highly correlated to obesity, but it also depends on genetic factors, sex and age [19]. Complications of T2D include increased risk of developing CVD, stroke, blindness or kidney failure as well as poor wound healing [20, 21].

## **1.4 Treatments for obesity and diabetes**

Even a moderate amount of weight loss can have beneficial effects on obese patients, by reducing their risk of developing CVD and stroke, and by reducing their blood pressure and circulating cholesterol and triacylglycerol (TAG) levels [22, 23].

Diabetic patients are better able to control their blood glucose levels when they lose weight, which could also reduce their requirement for medicines [24]. The current treatment options for obesity and diabetes include three main strategies - lifestyle interventions, pharmacological therapy and bariatric surgery.

#### **1.4.1 Lifestyle changes**

Lifestyle interventions include attempts to change dietary patterns and increase the amount of physical activity in a regular schedule. Such changes can successfully affect body weight, waist circumference and other parameters, but several factors contribute to the long-term failure of these attempts, such as lack of motivation, difficulty of maintaining the high levels of exercise necessary, and susceptibility to binge on “unhealthy” foods. Changes in dietary patterns are an essential part of controlling the impact of T2D. Low carbohydrate diets, portion size control and eating high fiber and low glycemic index food can help prevent hyperglycemic spikes in prediabetic or diabetic patients. Lack of exercise has been shown to contribute to increased IR, and even moderate regular exercise has been shown to improve insulin sensitivity and peripheral glucose uptake [25]. These interventions, although helpful, are not capable of reversing the diabetic phenotype.

#### **1.4.2 Pharmacological treatments**

Pharmacological drugs that target obesity mostly aim at controlling appetite. The current available appetite suppressants have several different modes of action, some of which are still unclear. Effects of drugs such as Phentermine and Sibutramine are most likely mediated by norepinephrine and dopamine, i.e., they act primarily on the central nervous system (CNS) [26]. Others, such as Orlistat, inhibit gastric and pancreatic lipase, thereby reducing the absorption of fat in the gastrointestinal tract

[27]. Liraglutide is an analogue of the satiating gut peptide glucagon-like peptide-1 (GLP-1) and presumably acts primarily via central GLP-1 receptor signaling [28]. With long-term use, most of these drugs have several side effects, ranging from reduced absorption of fat-soluble vitamins to severe gastrointestinal disorders, as well as hypertension [29]. The dangers of pharmacological treatments became evident when the clinically approved CB1 cannabinoid receptor blocker Rimonabant was introduced into the market. Rimonabant was successful in reducing body weight and improving CVD risk factors, but it also caused side effects such as depression and heightened suicidal tendencies, and was eventually taken off the market [30].

Most drugs for the treatment of T2D are hypoglycemic or insulin sensitizing agents. Several different classes of oral anti-diabetic drugs exist. But long-term use can cause severe side effects such as hypoglycemia, gastrointestinal disorders or even CVD [31]. One of the main problems with drug treatments has been finding a drug or a combination of drugs that works long-term. Currently the most widely used drug for T2D and usually the “first line of defense” is metformin [32]. Metformin improves blood glycemia, by lowering plasma insulin levels and increasing insulin sensitivity. Metformin presumably does so mainly by inhibiting hepatic gluconeogenesis, but it also appears to have an effect on intestinal metabolism [33]. Some doctors also recommend Metformin to female patients suffering from PCOS, with or without obesity. PCOS patients very often show IR, which can be alleviated by metformin [34]. Nevertheless, just like other drugs, metformin also has side effects ranging from nausea and vomiting to lactic acidosis, especially with prolonged use [35].

### **1.4.3 Surgical interventions**

The only intervention that currently leads to sustained weight loss with a comparatively high success rate is bariatric surgery. As an added advantage, bariatric

surgeries lead to the almost immediate reversal of the T2D phenotype in obese and diabetic patients. Different kinds of bariatric surgery with different degrees of surgical severity lead to different degrees of recovery time and varying degrees of weight loss or diabetes reversal depending on the procedure. These surgical procedures include the adjustable gastric lap band (AGB) surgery, vertical sleeve gastrectomy (VSG), and Roux-en-Y gastric bypass (RYGB) surgery (Fig 1) [36]. Of these RYGB involves substantial restructuring of the small intestine leading to malabsorption. The restructuring also causes several metabolic and morphological changes in the small intestine, which are now believed to be involved in the beneficial effects of RYGB surgery [37]. As mentioned earlier, the benefits of bariatric surgery include weight loss, but also the remission of T2D, irrespective of the degree of weight loss. In fact, randomized control human trials showed that RYGB led to the normalization of circulating glucose levels in 75% of the patients, and this effect did not seem to correlate with the degree of weight loss [38]. Considering the improved blood glucose and insulin levels seem to occur almost immediately after surgery, long before any significant weight loss, this indicates that the benefits of bariatric surgery with respect to T2D are independent of weight loss.

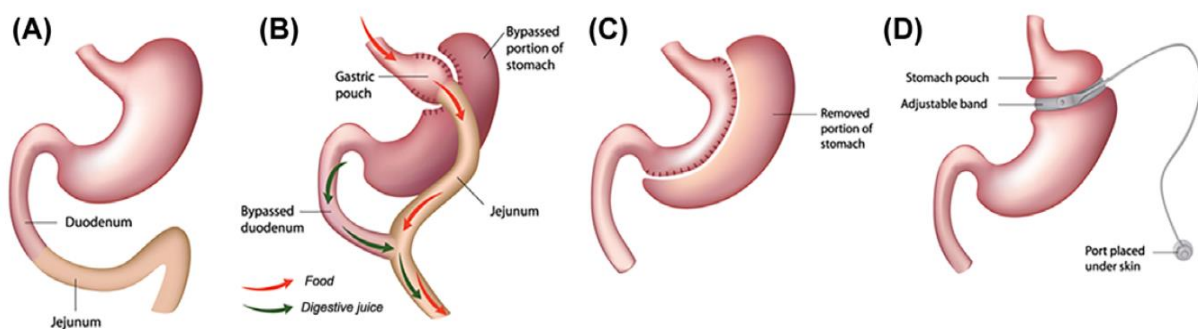


**Figure 1:** Anatomy of the stomach and proximal small intestine before and after bariatric surgery (A) Normal anatomy; (B) Roux-en-Ygastric bypass; (C) vertical sleeve gastrectomy; (D) adjustable gastric banding [36].

## **1.5 Mechanisms of RYGB and T2D remission**

Several studies have tried to identify the mechanisms of the beneficial effects of bariatric surgery. Studies in both human patients and rodent models of RYGB document that the small intestine undergoes dramatic morphological changes after surgery as reviewed in [39]. The jejunum shows an enlargement due to massive hyperplasia and hypertrophy. Specifically the number of enteroendocrine cells increases significantly, contributing to the high levels of the intestinal hormones GLP-1 and peptide YY (PYY) seen in systemic circulation post-surgery [39].

Rodent data also show that the change in nutrient sensing in the jejunum after bypass leads to metabolic reprogramming of the jejunum [40]. Due to bypassing the duodenum and proximal jejunum, the RYGB distal jejunum now encounters comparatively undigested nutrients that it usually does not see prior to surgery. This leads to changes in jejunal glucose metabolism, which in turn affect circulating glucose levels. Experiments with a duodenal-jejunal bypass (DJB) without reducing the stomach size also lowered circulating glucose concentrations in non-obese T2D rats [40]. Another change in RYGB is a modification of bile acid delivery leading to increased plasma bile acids [41]. Experiments in rats that mimicked this rerouting of bile delivery into the gut, led to an improvement in glucose control, by suppressing hepatic gluconeogenesis and enhancing intestinal gluconeogenesis [42, 43]. In fact, rats with this bile acid delivery change also showed lower levels of food intake when fed a high fat-high sucrose diet due to a change in preference for fat rich food [43]. Multiple independent studies in gastric bypass rats showed increased intestinal gluconeogenesis in the distal jejunum after gastric bypass, and reduced gluconeogenesis in the liver, with or without the gastric transection [44, 45].



Bariatric surgery also leads to changes in the gut microbiome of humans as well as rodents, within a week of surgery [46, 47]. All of these alterations might individually or in combination improve glucose homeostasis and reduce body weight, suggesting that bariatric surgery could affect body weight and particularly the diabetic phenotype through multiple mechanisms. In fact, doctors now recommend bariatric surgery as an option for even lean or mildly obese but diabetic patients based on the benefits seen [48]. As is the case with most surgeries, however, along with the pros of gastric bypass come the cons. The most obvious con is the expense. Not all people can afford the high cost of bariatric surgery. But more importantly, these surgeries come with several possible side effects including micronutrient deficiencies mainly due to malabsorption in the intestine, complications related to surgery including mortality, as well as psychological changes such as depression [49, 50]. These are good enough reasons for the attempts to modulate intestinal function noninvasively to accomplish similar beneficial effects as bypass surgery on body weight and glucose homeostasis.

## **1.6 Structural overview of the small intestine**

The small intestine is divided into the duodenum, jejunum and ileum. In the duodenum, which begins right after the pyloric sphincter of the stomach, partially digested food from the stomach (chyme) is mixed with bile and pancreatic juices to further digestion. The jejunum serves as the main region of nutrient absorption. The last section, the ileum, is also involved in nutrient absorption and connects to the large intestine [51].

The small intestine, like the whole alimentary canal, consists of four layers of tissue: (1) the outermost epithelial layer called the serosa, which protects the inner

layers and extends to the mesentery, a thin membrane that anchors the intestine in the abdomen. (2) The muscle layer under the serosa, which consists of an inner circular and outer longitudinal part, and is responsible for the continuous mixing of the contents and the coordinated contractions (peristalsis) that push the chyme through the intestine. (3) The sub-mucosa which consists of connective tissue that supports the overlying mucosa and connects it to the underlying smooth muscle tissue. (4) The mucosa, the innermost layer of epithelial cells, which is specialized for nutrient absorption. Circular folds, villi, and microvilli increase the small intestinal surface area for absorption by more than 120-fold compared to a simple tube of the same length and diameter [51, 52]. The mucosa of the small intestine consists of different cell types with different functions. The intestinal stem cells in the crypts (the invaginations of the mucosal epithelium between the villi) divide to form another stem cell and a daughter cell that differentiates into an absorptive enterocyte, an enteroendocrine cell, a goblet cell or a paneth cell. The cells of the enterocyte lineage divide several times as they migrate up the crypts into the villi. These cells differentiate further into mature absorptive cells that have a lifetime of 3-4 days [53].

## **1.7 Metabolic characteristics of the small intestine**

When food is ingested, carbohydrates, lipids and proteins are broken down in the gastrointestinal tract into monosaccharides, fatty acids and monoacylglycerol (MAG), and amino acids, which in turn are absorbed by the enterocytes. The macronutrient breakdown products serve as energy-yielding substrates for enterocytes or fill nutrient stores in the enterocytes themselves (short-term) or in other body cells, such as adipocytes, hepatocytes and myocytes (short-term and long-term) via shuttling into the circulation. Enterocyte metabolism is mainly active to transfer these nutrients

and water from the intestinal lumen to the systemic circulation. The small intestine contributes to approximately 20% of whole body oxygen consumption indicating that it is highly metabolically active. Data from rats and guinea pigs indicate that only 10 to 20% of this metabolic activity is contributed by the smooth muscle layer of the small intestine [54]. The enterocytes, the main absorptive cells of the intestinal epithelium are capable of oxidizing amino acids, glucose and fatty acids coming from intestinal lumen through their apical membrane, as well as from circulation through their basolateral membrane [55]. Several studies show that diet composition modulates the absorptive capacity of the small intestine [56-58].

## **1.8 Enterocyte fatty acid metabolism**

The main role of the enterocytes in lipid metabolism involves absorbing TAG-derived fatty acids and MAG from the intestinal lumen, resynthesizing TAG, and releasing them into the interstitial fluid, from where they enter the intestinal lymphatics to bypass the liver and eventually end up in the systemic blood circulation [59]. In the intestinal lumen, lipases hydrolyze dietary TAG in a stepwise manner to diacylglycerols (DAG), MAG, and fatty acids. Fatty acids and MAG are transported across the apical membrane of the enterocyte by diffusion or facilitated transport by fatty acid translocase/ cluster of differentiation-36 (FAT/CD36) or other putative transporters such as fatty acid transport protein (FATP) [60]. In the cytosol of the enterocytes, intestinal fatty acid binding protein (IFABP or FABP2) specifically binds fatty acids, whereas liver fatty acid binding protein (LFABP or FABP1) binds fatty acids, fatty acyl-CoA, and MAG [61]. Once absorbed into the enterocyte, fatty acids and MAG are re-esterified via acyl-CoA:monoacylglycerol acyltransferase (MGAT) and acyl-CoA:diacylglycerol acyltransferases (DGAT1 and 2) to TAG, which are temporarily

stored in the enterocyte [62] or assembled to lipoproteins in the endoplasmic reticulum (ER). TAG are processed into mature chylomicrons in the Golgi apparatus. Chylomicrons leave the enterocyte via the basolateral membrane and enter the lymphatic system for delivery into the general circulation [59]. FABP1 may also traffic fatty acids to peroxisome proliferator activated receptor-alpha (PPAR $\alpha$ ), promoting the expression of oxidative genes [61].

### **1.9 Effects of enterocyte FAO on food intake and metabolism**

Enterocytes were mainly considered to use fatty acids as fuel during the suckling period, when the dietary fat content is particularly high [63]. During this period, FAO genes are highly expressed in the enterocytes, whereas their expression decreases significantly as the fat content of the diet decreases post weaning. Several studies revealed, however, that the enterocytes are capable of oxidizing fatty acids and producing ketone bodies even in adulthood when they are exposed to a high-fat diet (HFD) [56, 57]. Evidence from our own lab suggested that even a short-term (3 day) exposure to HFD feeding upregulates the expression of genes and proteins related to FAO and ketogenesis in the enterocytes of the duodenum and jejunum [64]. More importantly, our lab also showed that pharmacological stimulation of FAO in the small intestinal enterocytes was associated with a reduction in food intake. The pharmacological drugs used included an inhibitor of DGAT1, WY14643- an activator of PPAR $\alpha$ , and the endogenous ligand of PPAR $\alpha$  - oleoylethanolamide (OEA) [65-67]. All these drugs led to a reduction of food intake in rats fed standard chow or HFD, when administered at the beginning of their dark phase. DGAT1 is the enzyme involved in the last step of TAG synthesis and is highly expressed in the small intestine. Intragastric infusion of DGAT1 inhibitor led to lower circulating plasma TAG, increased

$\beta$ -hydroxybutyrate (BHB) levels and a lower respiratory exchange ratio with HFD feeding [65]. IP administered WY14643 also led to lower RER, higher BHB levels in the hepatic portal vein plasma, as well as lower lipid droplet accumulation in the jejunum of rats fed HFD [66]. IP infusions of OEA in HFD-fed rats also led to increased circulating BHB and lower circulating levels of the gut peptides GLP-1 and PYY [67]. These effects were accompanied by increases in the protein expressions of genes related to FAO and/or ketogenesis in the small intestinal mucosa, but not in the liver. This led us to hypothesize that increasing the FAO capacity of small intestinal enterocytes could affect body weight.

To target enterocyte metabolism specifically, we decided to use transgenic mouse models to upregulate FAO in the enterocytes. We considered two molecular targets – Sirtuin3 (SIRT3), a mitochondrial protein that regulates FAO post-translationally, and carnitine palmitoyltransferase-1 (CPT1), the rate-limiting enzyme for FAO in the mitochondria.

### **1.10 Sirtuin 3, the global mitochondrial deacetylase**

SIRT3 belongs to a group of proteins called sirtuins, classified as class three histone deacetylases. They were discovered in mammals after their yeast ortholog Sir2 was found to be essential for lifespan extension [68]. Subsequently Sir2 homologues were identified in several other species, including flies and worms [69]. Sir2 is a nuclear protein that is a post-translational histone modifier, thus regulating chromatin structure. Sir2 deacetylates histones and thereby leads to chromatin folding, transcriptional silencing and regulates aging [70]. It is therefore considered an epigenetic regulator of lifespan. Sir2 activity involves the breakdown of one molecule of NAD<sup>+</sup> for every

substrate deacetylated. This function links it to the metabolic status of cells [71]. Mammals have seven sirtuins (SIRT1-7) with different subcellular localizations. SIRT1, 6 and 7 are nuclear proteins, SIRT2 is localized in the cytoplasm, whereas SIRT3, 4 and 5 are mitochondrial proteins [72]. Several studies have shown that all sirtuins are NAD<sup>+</sup>-dependent histone deacetylases *in vitro*, but *in vivo* they have several different non-histone targets that regulate various functions beyond gene silencing [73].

SIRT3 was discovered to be the major mitochondrial protein deacetylase [74]. It is capable of deacetylating various enzymes and, hence, regulating several oxidative metabolic pathways. Targets of SIRT3 include, long-chain acyl-CoA dehydrogenase (LCAD), 3-Hydroxy-3-Methylglutaryl-CoA Synthase-2 (HMGCS2), isocitrate dehydrogenase-2 (IDH2), subunits of complex I and II of the electron transport chain and manganese superoxide dismutase (MnSOD) [75-79]. By deacetylating these proteins, SIRT3 enhances their functions and therefore upregulates FAO, ketogenesis, the TCA cycle, the mitochondrial electron transport chain and reactive oxygen species scavenging. This indicates that SIRT3 upregulation enhances mitochondrial oxidative metabolism and ATP production, but also controls the levels of potentially damaging free radicals generated in the process. SIRT3 also deacetylates and regulates acetyl-CoA synthetase-2 (AceCS2), the enzyme that synthesizes acetyl-CoA [80, 81].

SIRT3 levels are upregulated in adipose tissue, skeletal muscles and liver during caloric restriction [75, 82-84]. Conversely, SIRT3 levels are reduced in these tissues with HFD feeding [83, 85, 86]. Whole body SIRT3 knock out mice developed DIO faster than wild type control mice, when they were fed a HFD. In fact, they developed IR, a hallmark of obesity and metabolic syndrome, even before they developed DIO [87]. Together these data indicate that SIRT3 plays a role in metabolic homeostasis in different tissues. Currently, no data exist on the role of endogenous

SIRT3 in the small intestine, but we considered that it might be a good molecular target to modulate enterocyte mitochondrial metabolism, particularly FAO.

### **1.11 Carnitine palmitoyltransferase-1, the rate-limiting enzyme of fatty acid oxidation**

CPT1 is a protein localized to the outer mitochondrial membrane. It is the key enzyme in the transport of long-chain fatty acids (LCFA) into the mitochondria for  $\beta$ -oxidation [88]. Fatty acids are first linked to coenzyme-A (CoA) by acyl-CoA synthetases. The main function of CPT1 is to attach the CoA esters of LCFA to carnitine to form fatty acyl-carnitine. The fatty-acyl carnitine ester then diffuses into the mitochondrial matrix through the acyl-carnitine/carnitine transporter, carnitine palmitoyltransferase-2 (CPT2), bound to the mitochondrial inner membrane, which releases fatty acyl-CoA and free carnitine into the mitochondrial matrix. Conversion of LCFA into the fatty-acyl carnitine ester commits the fatty acid to  $\beta$ -oxidation. Three separate genes encode three isoforms of CPT1, i.e., CPT1a, CPT1b and CPT1c. CPT1a or the liver isoform is expressed on the mitochondria of all cell types except skeletal muscle cells and brown adipocytes. CPT1b is mainly expressed in cardiac and skeletal muscles and in brown adipose tissue (BAT). CPT1c is considered the brain isoform and is predominantly expressed in the brain and testes [88].

FAO is tightly regulated such that it is usually inhibited under conditions of high nutrient availability. This is mainly achieved by allosteric inhibition of CPT1 by malonyl-CoA, the first intermediate in the cytosolic biosynthesis of fatty acids from acetyl CoA [89]. Food ingestion usually triggers the release of insulin. An insulin-dependent protein phosphatase dephosphorylates and activates the enzyme acetyl-CoA carboxylase

(ACC). ACC is the enzyme that produces malonyl-CoA, which inhibits CPT1, thus preventing the entry of LCFA into the mitochondria for oxidation [90]. Between meals when insulin levels are low and glucagon levels rise, glucagon activates a protein kinase (PKA) that phosphorylates and inactivates ACC. This leads to a drop in the levels of malonyl-CoA, relieving CPT1 from inhibition. Glucagon also induces lipolysis in adipose tissue, which supplies LCFA for  $\beta$ -oxidation [91].  $\beta$ -oxidation is also inhibited by a high NADH/NAD<sup>+</sup> ratio as well as high acetyl-CoA levels in a negative feedback loop [92].

Through extensive experiments, Morillas et al. found a mutation in the CPT1 sequence, which reduces the sensitivity of CPT1 to inhibition by malonyl-CoA [89]. With the expression of the CPT1a mutant - CPT1m593S (CPT1mt), the FAO capacity of cells could be enhanced both *in vitro* and *in vivo* [93-97]. Interestingly, adeno-associated virus mediated overexpression of CPT1mt in the liver of mice could prevent them from developing DIO, hepatic steatosis and IR [98]. Adenoviral-mediated hepatic CPT1mt expression could also reverse an already established glucose intolerance without affecting body weight gain, adiposity or hepatic steatosis [95]. Electrotransfer-mediated overexpression of CPT1mt in skeletal muscle cells led to increased oxidative muscle fibers as well as an increased FAO flux of the muscle cells *in vitro* similar to exercise-induced increased oxidative phenotype seen in the skeletal muscle cells. CPT1mt expression in the skeletal muscle cells of aging mice could also reverse aging-induced muscle cell alterations [96]. Transgenic mice with a skeletal muscle-specific CPT1mt expression had an increased whole body fatty acid utilization *in vivo*, when they were fed standard chow. When fed a high-fat high-sucrose diet, the muscle CPT1mt expressing mice showed reduced muscle lipotoxicity and improved insulin sensitivity, with no changes in body weight or adiposity [97]. Together these data



substantiate our idea that we can increase the FAO capacity of enterocytes using the malonyl-CoA insensitive CPT1mt protein.

## **1.12 Aims of the thesis**

When I first started my PhD, based on the peripheral pharmacological inhibition of food intake and its association with intestinal FAO, we hypothesized that specifically upregulating FAO in the enterocytes might decrease food intake and thereby reduce body weight gain. In order to achieve this enterocyte specific FAO, we decided to use the Cre-*LOXP* system in transgenic mice. Considering the data from gastric bypass humans and rodent models showing that metabolic reprogramming of the small intestine was associated with the reversal of diabetic phenotypes, we also hypothesized that enhancing enterocyte metabolism might affect whole body glucose homeostasis.

Therefore, we settled on two transgenic mouse models, one with an overexpression of SIRT3 in the enterocytes and the other with an expression of CPT1mt in the enterocytes. Using these mouse models, we wanted to address the following questions:

- (1) Does the overexpression/ expression of SIRT3 or CPT1mt in enterocytes lead to an upregulation of the FAO capacity of the cells?
- (2) Does the overexpression/ expression of SIRT3 or CPT1mt in enterocytes lead to a reduction in food intake and body weight gain when the mice consume a low fat diet or a HFD?

- (3) Does the overexpression/ expression of SIRT3 or CPT1mt in enterocytes affect whole body glucose homeostasis and insulin sensitivity in mice consuming low fat diet or HFD?

The present thesis consists of two original research articles written for peer-reviewed journals. The articles are presented in their final form, in which they have been published (Chapter 2) or in which they are ready to be submitted (Chapter 3) for peer-review. In these studies we addressed the main questions stated above and also tried to elucidate the mechanisms of the observed effects. Each chapter has more details on the aims of each study as well as a detailed discussion of the findings. Chapter 4 presents an overall discussion of all findings and puts them into a broader context.

### **1.13 REFERENCES**

- [1] Gonzalez-Muniesa, P., Martinez-Gonzalez, M. A., Hu, F. B., Despres, J. P., Matsuzawa, Y., Loos, R. J. F., et al. Obesity. *Nat Rev Dis Primers*. 2017,3:17034.
- [2] Flegal, K. M., Kit, B. K., Orpana, H., Graubard, B. I. Association of All-Cause Mortality With Overweight and Obesity Using Standard Body Mass Index Categories A Systematic Review and Meta-analysis. *Jama-J Am Med Assoc*. 2013,309:71-82.
- [3] Thomas, E. L., Frost, G., Taylor-Robinson, S. D., Bell, J. D. Excess body fat in obese and normal-weight subjects. *Nutr Res Rev*. 2012,25:150-61.
- [4] Pi-Sunyer, X. The medical risks of obesity. *Postgrad Med*. 2009,121:21-33.
- [5] Engin, A. The Definition and Prevalence of Obesity and Metabolic Syndrome. *Adv Exp Med Biol*. 2017,960:1-17.
- [6] Prentice, A. M., Jebb, S. A. Beyond body mass index. *Obes Rev*. 2001,2:141-7.
- [7] Cetin, D., Lessig, B. A., Nasr, E. Comprehensive Evaluation for Obesity: Beyond Body Mass Index. *J Am Osteopath Assoc*. 2016,116:376-82.
- [8] Levelt, E., Pavlides, M., Banerjee, R., Mahmood, M., Kelly, C., Sellwood, J., et al. Ectopic and Visceral Fat Deposition in Lean and Obese Patients With Type 2 Diabetes. *J Am Coll Cardiol*. 2016,68:53-63.
- [9] Kwon, H., Kim, D., Kim, J. S. Body Fat Distribution and the Risk of Incident Metabolic Syndrome: A Longitudinal Cohort Study. *Sci Rep*. 2017,7:10955.
- [10] Jensen, M. D. Role of body fat distribution and the metabolic complications of obesity. *J Clin Endocrinol Metab*. 2008,93:S57-63.
- [11] Giannini, C., Caprio, S. Islet function in obese adolescents. *Diabetes Obes Metab*. 2012,14 Suppl 3:40-5.
- [12] Qi, L., Cho, Y. A. Gene-environment interaction and obesity. *Nutr Rev*. 2008,66:684-94.

- [13] Farooqi, I. S., O'Rahilly, S. 20 years of leptin: human disorders of leptin action. *The Journal of endocrinology*. 2014,223:T63-70.
- [14] Basile, K. J., Johnson, M. E., Xia, Q., Grant, S. F. Genetic susceptibility to type 2 diabetes and obesity: follow-up of findings from genome-wide association studies. *Int J Endocrinol*. 2014,2014:769671.
- [15] Warrington, N. M., Howe, L. D., Paternoster, L., Kaakinen, M., Herrala, S., Huikari, V., et al. A genome-wide association study of body mass index across early life and childhood. *International journal of epidemiology*. 2015,44:700-12.
- [16] Akiyama, M., Okada, Y., Kanai, M., Takahashi, A., Momozawa, Y., Ikeda, M., et al. Genome-wide association study identifies 112 new loci for body mass index in the Japanese population. *Nat Genet*. 2017,49:1458-67.
- [17] Silventoinen, K., Rokholm, B., Kaprio, J., Sorensen, T. I. The genetic and environmental influences on childhood obesity: a systematic review of twin and adoption studies. *Int J Obes (Lond)*. 2010,34:29-40.
- [18] Kerner, W., Bruckel, J., German Diabetes, A. Definition, classification and diagnosis of diabetes mellitus. *Exp Clin Endocrinol Diabetes*. 2014,122:384-6.
- [19] Kautzky-Willer, A., Harreiter, J., Pacini, G. Sex and Gender Differences in Risk, Pathophysiology and Complications of Type 2 Diabetes Mellitus. *Endocr Rev*. 2016,37:278-316.
- [20] Lin, P. J., Kent, D. M., Winn, A., Cohen, J. T., Neumann, P. J. Multiple chronic conditions in type 2 diabetes mellitus: prevalence and consequences. *Am J Manag Care*. 2015,21:e23-34.
- [21] Khamaisi, M., Balanson, S. Dysregulation of wound healing mechanisms in diabetes and the importance of negative pressure wound therapy (NPWT). *Diabetes Metab Res Rev*. 2017,33.
- [22] Mertens, I. L., Van Gaal, L. F. Overweight, obesity, and blood pressure: the effects of modest weight reduction. *Obes Res*. 2000,8:270-8.

- [23] Magkos, F., Fraterrigo, G., Yoshino, J., Luecking, C., Kirbach, K., Kelly, S. C., et al. Effects of Moderate and Subsequent Progressive Weight Loss on Metabolic Function and Adipose Tissue Biology in Humans with Obesity. *Cell Metab.* 2016,23:591-601.
- [24] Fujioka, K. Benefits of moderate weight loss in patients with type 2 diabetes. *Diabetes Obes Metab.* 2010,12:186-94.
- [25] Way, K. L., Hackett, D. A., Baker, M. K., Johnson, N. A. The Effect of Regular Exercise on Insulin Sensitivity in Type 2 Diabetes Mellitus: A Systematic Review and Meta-Analysis. *Diabetes Metab J.* 2016,40:253-71.
- [26] An, H., Sohn, H., Chung, S. Phentermine, sibutramine and affective disorders. *Clin Psychopharmacol Neurosci.* 2013,11:7-12.
- [27] Hartmann, D., Hussain, Y., Guzelhan, C., Odink, J. Effect on Dietary-Fat Absorption of Orlistat, Administered at Different Times Relative to Meal Intake. *Brit J Clin Pharmacol.* 1993,36:266-70.
- [28] Mehta, A., Marso, S. P., Neeland, I. J. Liraglutide for weight management: a critical review of the evidence. *Obes Sci Pract.* 2017,3:3-14.
- [29] MacDaniels, J. S., Schwartz, T. L. Effectiveness, tolerability and practical application of the newer generation anti-obesity medications. *Drugs Context.* 2016,5:212291.
- [30] Richey, J. M., Woolcott, O. Re-visiting the Endocannabinoid System and Its Therapeutic Potential in Obesity and Associated Diseases. *Curr Diab Rep.* 2017,17:99.
- [31] Chaudhury, A., Duvoor, C., Reddy Dendi, V. S., Kraleti, S., Chada, A., Ravilla, R., et al. Clinical Review of Antidiabetic Drugs: Implications for Type 2 Diabetes Mellitus Management. *Frontiers in endocrinology.* 2017,8:6.
- [32] Hostalek, U., Gwilt, M., Hildemann, S. Therapeutic Use of Metformin in Prediabetes and Diabetes Prevention. *Drugs.* 2015,75:1071-94.
- [33] Foretz, M., Guigas, B., Bertrand, L., Pollak, M., Viollet, B. Metformin: from mechanisms of action to therapies. *Cell Metab.* 2014,20:953-66.

- [34] Naderpoor, N., Shorakae, S., de Courten, B., Misso, M. L., Moran, L. J., Teede, H. J. Metformin and lifestyle modification in polycystic ovary syndrome: systematic review and meta-analysis. *Hum Reprod Update*. 2016,22.
- [35] Pawlyk, A. C., Giacomini, K. M., McKeon, C., Shuldiner, A. R., Florez, J. C. Metformin pharmacogenomics: current status and future directions. *Diabetes*. 2014,63:2590-9.
- [36] Mulla, C. M., Middelbeek, R. J. W., Patti, M. E. Mechanisms of weight loss and improved metabolism following bariatric surgery. *Ann N Y Acad Sci*. 2017.
- [37] Seeley, R. J., Chambers, A. P., Sandoval, D. A. The role of gut adaptation in the potent effects of multiple bariatric surgeries on obesity and diabetes. *Cell Metab*. 2015,21:369-78.
- [38] Mingrone, G., Panunzi, S., De Gaetano, A., Guidone, C., Iaiconelli, A., Leccesi, L., et al. Bariatric surgery versus conventional medical therapy for type 2 diabetes. *N Engl J Med*. 2012,366:1577-85.
- [39] Yarmush, M. L., D'Alessandro, M., Saeidi, N. Regulation of Energy Homeostasis After Gastric Bypass Surgery. *Annu Rev Biomed Eng*. 2017,19:459-84.
- [40] Breen, D. M., Rasmussen, B. A., Kokorovic, A., Wang, R., Cheung, G. W., Lam, T. K. Jejunal nutrient sensing is required for duodenal-jejunal bypass surgery to rapidly lower glucose concentrations in uncontrolled diabetes. *Nat Med*. 2012,18:950-5.
- [41] Pournaras, D. J., Glicksman, C., Vincent, R. P., Kuganlipava, S., Alaghband-Zadeh, J., Mahon, D., et al. The role of bile after Roux-en-Y gastric bypass in promoting weight loss and improving glycaemic control. *Endocrinology*. 2012,153:3613-9.
- [42] Flynn, C. R., Albaugh, V. L., Cai, S., Cheung-Flynn, J., Williams, P. E., Brucker, R. M., et al. Bile diversion to the distal small intestine has comparable metabolic benefits to bariatric surgery. *Nat Commun*. 2015,6.
- [43] Goncalves, D., Barataud, A., De Vadder, F., Vinera, J., Zitoun, C., Duchampt, A., et al. Bile Routing Modification Reproduces Key Features of Gastric Bypass in Rat. *Ann Surg*. 2015,262:1006-15.

- [44] Troy, S., Soty, M., Ribeiro, L., Laval, L., Migrenne, S., Fioramonti, X., et al. Intestinal gluconeogenesis is a key factor for early metabolic changes after gastric bypass but not after gastric lap-band in mice. *Cell Metabolism*. 2008,8:201-11.
- [45] Yan, Y., Zhou, Z., Kong, F., Feng, S., Li, X., Sha, Y., et al. Roux-en-Y Gastric Bypass Surgery Suppresses Hepatic Gluconeogenesis and Increases Intestinal Gluconeogenesis in a T2DM Rat Model. *Obes Surg*. 2016,26:2683-90.
- [46] Furet, J. P., Kong, L. C., Tap, J., Poitou, C., Basdevant, A., Bouillot, J. L., et al. Differential adaptation of human gut microbiota to bariatric surgery-induced weight loss: links with metabolic and low-grade inflammation markers. *Diabetes*. 2010,59:3049-57.
- [47] Liou, A. P., Paziuk, M., Luevano, J. M., Machineni, S., Turnbaugh, P. J., Kaplan, L. M. Conserved Shifts in the Gut Microbiota Due to Gastric Bypass Reduce Host Weight and Adiposity. *Sci Transl Med*. 2013,5.
- [48] Fried, M., Ribaric, G., Buchwald, J. N., Svacina, S., Dolezalova, K., Scopinaro, N. Metabolic surgery for the treatment of type 2 diabetes in patients with BMI <35 kg/m<sup>2</sup>: an integrative review of early studies. *Obes Surg*. 2010,20:776-90.
- [49] Tack, J., Deloose, E. Complications of bariatric surgery: dumping syndrome, reflux and vitamin deficiencies. *Best Pract Res Clin Gastroenterol*. 2014,28:741-9.
- [50] Arman, G. A., Himpens, J., Bolckmans, R., Van Compernelle, D., Vilallonga, R., Leman, G. Medium-Term Outcomes after Reversal of Roux-en-Y Gastric Bypass. *Obes Surg*. 2017.
- [51] Loehry, C. A., Creamer, B. Three-dimensional structure of the human small intestinal mucosa in health and disease. *Gut*. 1969,10:6-12.
- [52] Helander, H. F., Fandriks, L. Surface area of the digestive tract - revisited. *Scand J Gastroenterol*. 2014,49:681-9.
- [53] Crosnier, C., Stamatakis, D., Lewis, J. Organizing cell renewal in the intestine: stem cells, signals and combinatorial control. *Nat Rev Genet*. 2006,7:349-59.

- [54] Sherratt, H. S. The metabolism of the small intestine. Oxygen uptake and L-lactate production along the length of the small intestine of the rat and guinea pig. *Comp Biochem Physiol.* 1968,24:745-61.
- [55] Kiela, P. R., Ghishan, F. K. Physiology of Intestinal Absorption and Secretion. *Best Pract Res Clin Gastroenterol.* 2016,30:145-59.
- [56] McCarthy, D. M., Nicholson, J. A., Kim, Y. S. Intestinal enzyme adaptation to normal diets of different composition. *Am J Physiol.* 1980,239:G445-51.
- [57] Singh, A., Balint, J. A., Edmonds, R. H., Rodgers, J. B. Adaptive changes of the rat small intestine in response to a high fat diet. *Biochim Biophys Acta.* 1972,260:708-15.
- [58] Primeaux, S. D., Braymer, H. D., Bray, G. A. CD36 mRNA in the gastrointestinal tract is differentially regulated by dietary fat intake in obesity-prone and obesity-resistant rats. *Dig Dis Sci.* 2013,58:363-70.
- [59] Mu, H., Hoy, C. E. The digestion of dietary triacylglycerols. *Prog Lipid Res.* 2004,43:105-33.
- [60] Iqbal, J., Hussain, M. M. Intestinal lipid absorption. *Am J Physiol Endocrinol Metab.* 2009,296:E1183-94.
- [61] Gajda, A. M., Storch, J. Enterocyte fatty acid-binding proteins (FABPs): different functions of liver and intestinal FABPs in the intestine. *Prostaglandins Leukot Essent Fatty Acids.* 2015,93:9-16.
- [62] Zhu, J., Lee, B., Buhman, K. K., Cheng, J. X. A dynamic, cytoplasmic triacylglycerol pool in enterocytes revealed by ex vivo and in vivo coherent anti-Stokes Raman scattering imaging. *J Lipid Res.* 2009,50:1080-9.
- [63] Kimura, R. E., Warshaw, J. B. Control of fatty acid oxidation by intramitochondrial [NADH]/[NAD<sup>+</sup>] in developing rat small intestine. *Pediatr Res.* 1988,23:262-5.
- [64] Clara, R., Schumacher, M., Ramachandran, D., Fedele, S., Krieger, J. P., Langhans, W., et al. Metabolic Adaptation of the Small Intestine to Short- and Medium-Term High-Fat Diet Exposure. *J Cell Physiol.* 2017,232:167-75.



- [65] Schober, G., Arnold, M., Birtles, S., Buckett, L. K., Pacheco-Lopez, G., Turnbull, A. V., et al. Diacylglycerol acyltransferase-1 inhibition enhances intestinal fatty acid oxidation and reduces energy intake in rats. *Journal of Lipid Research*. 2013,54:1369-84.
- [66] Azari, E. K., Leitner, C., Jaggi, T., Langhans, W., Mansouri, A. Possible Role of Intestinal Fatty Acid Oxidation in the Eating-Inhibitory Effect of the PPAR-alpha Agonist Wy-14643 in High-Fat Diet Fed Rats. *PLoS One*. 2013,8.
- [67] Azari, E. K., Ramachandran, D., Weibel, S., Arnold, M., Romano, A., Gaetani, S., et al. Vagal afferents are not necessary for the satiety effect of the gut lipid messenger oleoylethanolamide. *Am J Physiol Regul Integr Comp Physiol*. 2014,307:R167-78.
- [68] Kaeberlein, M., McVey, M., Guarente, L. The SIR2/3/4 complex and SIR2 alone promote longevity in *Saccharomyces cerevisiae* by two different mechanisms. *Genes Dev*. 1999,13:2570-80.
- [69] Haigis, M. C., Guarente, L. P. Mammalian sirtuins - emerging roles in physiology, aging, and calorie restriction. *Gene Dev*. 2006,20:2913-21.
- [70] McCleary, D. F., Rine, J. Nutritional Control of Chronological Aging and Heterochromatin in *Saccharomyces cerevisiae*. *Genetics*. 2017,205:1179-93.
- [71] Imai, S., Armstrong, C. M., Kaeberlein, M., Guarente, L. Transcriptional silencing and longevity protein Sir2 is an NAD-dependent histone deacetylase. *Nature*. 2000,403:795-800.
- [72] Kupis, W., Palyga, J., Tomal, E., Niewiadomska, E. The role of sirtuins in cellular homeostasis. *J Physiol Biochem*. 2016,72:371-80.
- [73] Schemies, J., Uciechowska, U., Sippl, W., Jung, M. NAD(+)-Dependent Histone Deacetylases (Sirtuins) as Novel Therapeutic Targets. *Med Res Rev*. 2010,30:861-89.
- [74] Lombard, D. B., Alt, F. W., Cheng, H. L., Bunkenborg, J., Streeper, R. S., Mostoslavsky, R., et al. Mammalian Sir2 homolog SIRT3 regulates global mitochondrial lysine acetylation. *Mol Cell Biol*. 2007,27:8807-14.

- [75] Hirschey, M. D., Shimazu, T., Goetzman, E., Jing, E., Schwer, B., Lombard, D. B., et al. SIRT3 regulates mitochondrial fatty-acid oxidation by reversible enzyme deacetylation. *Nature*. 2010,464:121-U37.
- [76] Shimazu, T., Hirschey, M. D., Hua, L., Dittenhafer-Reed, K. E., Schwer, B., Lombard, D. B., et al. SIRT3 deacetylates mitochondrial 3-hydroxy-3-methylglutaryl CoA synthase 2 and regulates ketone body production. *Cell Metab*. 2010,12:654-61.
- [77] Schlicker, C., Gertz, M., Papatheodorou, P., Kachholz, B., Becker, C. F. W., Steegborn, C. Substrates and regulation mechanisms for the human mitochondrial Sirtuins Sirt3 and Sirt5. *J Mol Biol*. 2008,382:790-801.
- [78] Cimen, H., Han, M. J., Yang, Y., Tong, Q., Koc, H., Koc, E. C. Regulation of succinate dehydrogenase activity by SIRT3 in mammalian mitochondria. *Biochemistry*. 2010,49:304-11.
- [79] Tao, R., Coleman, M. C., Pennington, J. D., Ozden, O., Park, S. H., Jiang, H., et al. Sirt3-mediated deacetylation of evolutionarily conserved lysine 122 regulates MnSOD activity in response to stress. *Mol Cell*. 2010,40:893-904.
- [80] Hallows, W. C., Lee, S., Denu, J. M. Sirtuins deacetylate and activate mammalian acetyl-CoA synthetases. *Proc Natl Acad Sci U S A*. 2006,103:10230-5.
- [81] Schwer, B., Bunkenborg, J., Verdin, R. O., Andersen, J. S., Verdin, E. Reversible lysine acetylation controls the activity of the mitochondrial enzyme acetyl-CoA synthetase 2. *Proc Natl Acad Sci U S A*. 2006,103:10224-9.
- [82] Shi, T., Wang, F., Stieren, E., Tong, Q. SIRT3, a mitochondrial sirtuin deacetylase, regulates mitochondrial function and thermogenesis in brown adipocytes. *J Biol Chem*. 2005,280:13560-7.
- [83] Palacios, O. M., Carmona, J. J., Michan, S., Chen, K. Y., Manabe, Y., Ward, J. L., 3rd, et al. Diet and exercise signals regulate SIRT3 and activate AMPK and PGC-1alpha in skeletal muscle. *Aging*. 2009,1:771-83.
- [84] Schwer, B., Eckersdorff, M., Li, Y., Silva, J. C., Fermin, D., Kurtev, M. V., et al. Calorie restriction alters mitochondrial protein acetylation. *Aging cell*. 2009,8:604-6.

- [85] Bao, J., Scott, I., Lu, Z., Pang, L., Dimond, C. C., Gius, D., et al. SIRT3 is regulated by nutrient excess and modulates hepatic susceptibility to lipotoxicity. *Free Radic Biol Med.* 2010,49:1230-7.
- [86] Kendrick, A. A., Choudhury, M., Rahman, S. M., McCurdy, C. E., Friederich, M., Van Hove, J. L., et al. Fatty liver is associated with reduced SIRT3 activity and mitochondrial protein hyperacetylation. *Biochem J.* 2011,433:505-14.
- [87] Hirschey, M. D., Shimazu, T., Jing, E., Grueter, C. A., Collins, A. M., Auouizerat, B., et al. SIRT3 deficiency and mitochondrial protein hyperacetylation accelerate the development of the metabolic syndrome. *Mol Cell.* 2011,44:177-90.
- [88] Zammit, V. A. Carnitine palmitoyltransferase 1: central to cell function. *IUBMB Life.* 2008,60:347-54.
- [89] Morillas, M., Gomez-Puertas, P., Bentebibel, A., Selles, E., Casals, N., Valencia, A., et al. Identification of conserved amino acid residues in rat liver carnitine palmitoyltransferase I critical for malonyl-CoA inhibition - Mutation of methionine 593 abolishes malonyl-CoA inhibition. *Journal of Biological Chemistry.* 2003,278:9058-63.
- [90] Wakil, S. J., Abu-Elheiga, L. A. Fatty acid metabolism: target for metabolic syndrome. *J Lipid Res.* 2009,50 Suppl:S138-43.
- [91] Duncan, R. E., Ahmadian, M., Jaworski, K., Sarkadi-Nagy, E., Sul, H. S. Regulation of lipolysis in adipocytes. *Annu Rev Nutr.* 2007,27:79-101.
- [92] Pietrocola, F., Galluzzi, L., Bravo-San Pedro, J. M., Madeo, F., Kroemer, G. Acetyl coenzyme A: a central metabolite and second messenger. *Cell Metab.* 2015,21:805-21.
- [93] Akkaoui, M., Cohen, I., Esnous, C., Lenoir, V., Sournac, M., Girard, J., et al. Modulation of the hepatic malonyl-CoA-carnitine palmitoyltransferase 1A partnership creates a metabolic switch allowing oxidation of de novo fatty acids. *Biochem J.* 2009,420:429-38.
- [94] Henique, C., Mansouri, A., Fumey, G., Lenoir, V., Girard, J., Bouillaud, F., et al. Increased mitochondrial fatty acid oxidation is sufficient to protect skeletal muscle cells from palmitate-induced apoptosis. *J Biol Chem.* 2010,285:36818-27.

[95] Monsenego, J., Mansouri, A., Akkaoui, M., Lenoir, V., Esnous, C., Fauveau, V., et al. Enhancing liver mitochondrial fatty acid oxidation capacity in obese mice improves insulin sensitivity independently of hepatic steatosis. *Journal of Hepatology*. 2012,56:632-9.

[96] Henique, C., Mansouri, A., Vavrova, E., Lenoir, V., Ferry, A., Esnous, C., et al. Increasing mitochondrial muscle fatty acid oxidation induces skeletal muscle remodeling toward an oxidative phenotype. *FASEB J*. 2015,29:2473-83.

[97] Vavrova, E., Lenoir, V., Alves-Guerra, M. C., Denis, R. G., Castel, J., Esnous, C., et al. Muscle expression of a malonyl-CoA-insensitive carnitine palmitoyltransferase-1 protects mice against high-fat/high-sucrose diet-induced insulin resistance. *Am J Physiol Endocrinol Metab*. 2016,311:E649-60.

[98] Orellana-Gavalda, J. M., Herrero, L., Malandrino, M. I., Paneda, A., Sol Rodriguez-Pena, M., Petry, H., et al. Molecular therapy for obesity and diabetes based on a long-term increase in hepatic fatty-acid oxidation. *Hepatology*. 2011,53:821-32.

## **CHAPTER 2:**

# **INTESTINAL SIRT3 OVEREXPRESSION IN MICE IMPROVES WHOLE BODY GLUCOSE HOMEOSTASIS INDEPENDENT OF BODY WEIGHT**

Deepti Ramachandran<sup>1</sup>, Rosmarie Clara<sup>1</sup>, Shahana Fedele<sup>1</sup>, Junmin Hu<sup>2</sup>, Endre Lackzo<sup>2</sup>, Jing-Yi Huang<sup>3</sup>, Eric Verdin<sup>3</sup>, Wolfgang Langhans<sup>1</sup>, Abdelhak Mansouri<sup>1</sup>

<sup>1</sup>Physiology and Behavior Laboratory, ETH Zurich, Schwerzenbach, Switzerland

<sup>2</sup>Functional Genomics Center Zurich (FGCZ), ETH Zurich and University of Zurich,  
Zurich, Switzerland

<sup>3</sup>Gladstone Institute of Virology and Immunology, University of California, San  
Francisco, California, USA.

## **STATUS**

Published in *Molecular Metabolism* 6 (2017) pp. 1264-1273, *In press*.

---

## ABSTRACT

**Objective:** Intestinal metabolism might play a greater role in regulating whole body metabolism than previously believed. We aimed to enhance enterocyte metabolism in mice and investigate if it plays a role in diet-induced obesity (DIO) and its comorbidities.

**Methods:** Using the *cre-loxP* system, we overexpressed the mitochondrial NAD<sup>+</sup> dependent protein deacetylase SIRT3 in enterocytes of mice (iSIRT3 mice). We chronically fed iSIRT3 mice and floxed-SIRT3 control (S3fl) mice a low-fat, control diet (CD) or a high-fat diet (HFD) and then phenotyped the mice.

**Results:** There were no genotype differences in any of the parameters tested when the mice were fed CD. Also, iSIRT3 mice were equally susceptible to the development of DIO as S3fl mice when fed HFD. They were, however, better able than S3fl mice to regulate their blood glucose levels in response to exogenous insulin and glucose, indicating that they were protected from developing insulin resistance. This improved glucose homeostasis was accompanied by an increase in enterocyte metabolic activity and an upregulation of ketogenic gene expression in the small intestine.

**Conclusion:** Enhancing enterocyte oxidative metabolism can improve whole body glucose homeostasis.

## 2.1 INTRODUCTION

Type-2 diabetes (T2D), a leading global health concern, is a major cause of premature deaths worldwide [1]. Overweight and obesity massively increase the risk of developing T2D, which involves a progressive rise in insulin resistance (IR), due in part to ectopic fat accumulation. The pancreas tries to compensate for the rising IR by overproducing insulin, which ultimately leads to pancreatic  $\beta$ -cell dysfunction [2]. Current pharmacological treatments for T2D mainly involve a combination of insulin and hypoglycemic or insulin sensitizing agents. The most efficient treatment for T2D and morbid obesity so far is surgical intervention such as Roux-en-Y gastric bypass (RYGB) [3]. In fact, gastric bypass surgery leads to an immediate reversal of the diabetic phenotype, even before any substantial weight loss [4, 5]. A large part of this success is supposedly due to morphological and functional changes in the small intestine [6]. Data from gastric bypass rat and mouse models support this theory, i.e., postsurgical morphological and/or metabolic changes in the small intestine might play a role in improving glycemic control in these animals [7-9].

Genetic [10] and pharmacological [11, 12] inhibition of intestinal triacylglycerol (TAG) re-esterification prevented diet-induced obesity (DIO) and/or improved glycemic control in rodents. Pharmacological studies have also implicated enterocyte fatty acid oxidation (FAO) in the control of food intake and energy expenditure [13, 14]. Intestines of obesity resistant mice show an increase in FAO genes in response to HFD feeding compared to obesity prone mice [15]. A recent study also revealed that within three days of HFD exposure, mouse enterocytes increase their capacity to oxidize fat and to produce ketone bodies [16]. Together, these studies suggest that enterocyte metabolism might play an important role in the development of obesity and the metabolic syndrome.

In this study, we aimed to examine whether genetically enhancing enterocyte mitochondrial metabolic functions, such as FAO, affects DIO and whole body glucose homeostasis. We therefore overexpressed the mitochondrial protein Sirtuin 3 (SIRT3) in the enterocytes of mice and tested the effects of this manipulation on the development of DIO and IR. All sirtuins require NAD<sup>+</sup> to be catalytically active, which directly links their function to the metabolic status of a cell [17]. SIRT3, primarily expressed in mitochondria, deacetylates and activates global mitochondrial proteins leading to increased mitochondrial function, including FAO, TCA cycle flux, and ketogenesis [18, 19].

We found that SIRT3 overexpression in the enterocytes did not produce any effects when the mice were on control diet (CD). On HFD, however, SIRT3 overexpression protected the mice from developing glucose intolerance and IR. This was accompanied by an increased gene expression of the ketogenic marker 3-hydroxy-3-methylglutaryl-CoA synthase 2 (*Hmgcs2*) in the duodenal and jejunal enterocytes of these mice. In addition, in control mice, postprandial systemic ketone body levels were lower on the HFD than on the CD, whereas in mice with the enterocyte specific SIRT3 overexpression, this difference was not significant. Intestinal SIRT3 overexpression in mice chronically fed HFD led to an increase in small intestinal enterocyte metabolic activity in response to an oral load of oleic acid. SIRT3 overexpression did not affect body weight, body composition, fat distribution, or small intestinal morphology. These findings suggest that an increase in the metabolic flux of enterocytes is sufficient to improve whole body glucose homeostasis in DIO, independent of body weight, body composition, or fat distribution.



## 2.2 MATERIALS AND METHODS

### 2.2.1 Animals

Mice with an enterocyte-specific SIRT3 overexpression (iSIRT3) were generated by crossing transgenic mice with a floxed stop cassette preceding the *Sirt3* gene (S3fl) [20] with mice expressing Cre recombinase under the enterocyte-specific promoter *Villin* (VilCre) [21] (stock number 004586 from the Jax cre repository), so that an additional copy of *Sirt3* was expressed in the epithelial cells of the intestine. The S3fl mice served as controls. All mice had a C57Bl6/J background. All breedings were carried out in our in-house specified and opportunistic pathogen free (SOPF) animal facility. At 8 to 10 weeks of age, male mice of the appropriate genotype were moved into the experimental room with controlled temperature and humidity ( $22 \pm 2^\circ\text{C}$ ,  $55 \pm 5\%$ ) and a 12 h/12 h dark/light cycle. All animals were group-housed (2-4 animals per cage) and had ad libitum access to food and water unless otherwise specified. Their body weights were monitored regularly as indicated. All animal experiments were approved by the Cantonal Veterinary Office of Zurich.

### 2.2.2 Diets

In the SOPF breeding facility, mice were fed standard chow diet (Kliba Nafag, Switzerland). In the experimental room, they were switched to either refined low-fat control diet (CD, #S9213-E001, 10 kJ% fat) or high-fat diet (HFD, # E15742-34, 60 kJ% fat) from Ssniff Spezialdiäten GmbH, Germany.

### 2.2.3 Body composition

Awake mice were scanned at the start and after 2, 4, 8, and 11 weeks of CD and HFD feeding using the EchoMRI 3-in-1 analyzer (EchoMRI™, Singapore and

Houston, USA) to assess fat and lean mass. After 16 weeks on the diets, mice were scanned under isoflurane anesthesia using high-resolution microcomputed tomography (CT; La Theta LCT-100; Hitachi-Aloka Medical Ltd, Japan) scanner to determine fat distribution in addition to body composition.

#### **2.2.4 Energy intake and indirect calorimetry**

Measurements were carried out in PhenoMaster/LabMaster metabolic cages (TSE systems, Bad Homburg, Germany). Mice were fed CD and adapted over 1 week to single housing in cages similar to the PhenoMaster cages before measurements. Data displayed were collected after an additional 2 days of habituation in the system. After 2 days of data collection on CD, mice were switched to HFD, and data were recorded for 2 more days. Food intake was measured manually every 12 h, at the beginning of the light or dark phases. Energy intake was calculated by multiplying the absolute food intake values with the energy density of the diets (1 g of CD = 15.25 kJ; 1 g of HFD = 21.53 kJ). Mice were returned to group caging at the end of the PhenoMaster experiments, and their body compositions were measured using the Echo-MRI analyzer [22, 23].

#### **2.2.5 Insulin sensitivity test (IST)**

After 8 weeks on the diets, mice were fasted for 4-5 h in the middle of the dark phase with ad libitum access to water. Actrapid HM human insulin (Novo Nordisk, Denmark) was injected intraperitoneally (IP), and tail blood glucose levels were monitored at the time points indicated using the Accu-Chek Aviva blood glucose monitor (Roche, Switzerland). Insulin dose: 0.4 and 0.8 mU/g body weight for CD and HFD-fed mice, respectively.

### **2.2.6 Oral glucose tolerance test (OGTT)**

After 10 weeks on the diets, mice were fasted for 6 h at the onset of dark phase with ad libitum access to water [24]. They received a 20% glucose solution in water by gavage (glucose dose: 2 g/kg body weight). Tail blood glucose levels were monitored at the time points indicated.

### **2.2.7 Animal sacrifice and tissue collection**

After 17 or 20 weeks on the diets, mice were food deprived for 2 h in the dark phase (postprandial) or overnight, respectively, with ad libitum access to water until sacrifice. All animals were sacrificed in the dark phase by decapitation; trunk blood was collected and processed as described later in the plasma metabolite analysis section (method 2.11). The intestine and liver were dissected out. Enterocytes were isolated as described below. Livers were flash frozen in liquid nitrogen and stored at -80°C until required.

### **Intestinal epithelial cell isolation**

Intestinal epithelial cells were isolated using a modified version of a protocol described earlier [16, 25]. The small intestines were dissected out, divided into duodenum and jejunum, flushed with ice-cold PBS, and then inverted. Each jejunal section was divided into 2 pieces and together with the duodenum, each intestinal section was tied to the end of a 12.5 mL Glison DistriTip Maxi syringe with the plunger pulled out partially and the barrel filled with air. To secure the intestine in place, we inserted a piece of plastic tubing onto the end of the syringe and below the knotted string. To prevent the intestine from floating in the solution when inflated, we tied a small metal washer with string at the lower end of the intestinal section. These tissues

were submerged in ice-cold Cell Recovery Solution (Corning #354253), in 5 mL polystyrene tubes and placed on ice. The intestinal sections were then inflated and deflated by pushing down and pulling up the plunger in a series of 4 inflations and deflations every 5 minutes (min). After 20 min, the intestine still attached to the syringe was laid out on a petri dish containing ice cold PBS, inflated and the epithelium was scraped off carefully with a pair of thin blunt forceps to avoid pricking the intestinal tube. The cells were then transferred into Falcon tubes and pelleted. The pellets were flash frozen in liquid nitrogen and stored at -80°C until subsequent analyses. Further mentions of the duodenum or jejunum in this manuscript (with the exception of the histological analysis) refer to the enterocytes isolated from these regions.

### **2.2.8 Histology**

Two cm pieces of jejunum were collected into tissue processing/embedding cassettes and fixed overnight in 4% paraformaldehyde at 4°C. They were transferred to 65% ethanol in an automatic paraffin-embedding processor (STP 120 spin Tissue Processor, Thermo Fischer, Waltham, MA, USA). The tissues were embedded in paraffin blocks with an automatic embedding system (Automatic Embedding System Bio-optica, Milano, Italy). Paraffin sections were cut with a motorized rotary microtome (Hyrax M55, Zeiss, Oberkochen, Germany) and disposable microtome razor blades (S-22 blades, Feather, Osaka, Japan).

### **Hematoxylin and eosin (H&E) stain**

Paraffin sections were stained automatically using an H&E-staining machine (Shandon Varistain, Thermo Fischer Scientific, Waltham, MA, USA). The stained sections were mounted in embedding medium (Entellan® New, DPX mountant, Sigma-Aldrich, St. Louis, MO, USA). The sections were scanned with the Axio Scope.A1

(Zeiss, Oberkochen, Germany). The desired pictures were taken with an integrated camera and the pictures were analyzed with the software AxioVision (Zeiss, Oberkochen, Germany). Additionally, the villi lengths of the jejunal sections were measured using the software AxioVision.

### **2.2.9 Mitochondrial isolation and western blotting**

Mitochondria were isolated from frozen duodenum and jejunum using a method described previously [26]. Mitochondria were lysed in RIPA buffer containing protease inhibitors and protein concentrations were determined using the DC Protein assay kit (BioRad # 5000112). Equal amounts of proteins were denatured with 6X Laemmli containing DTT and run on SDS PAGE gels. Alternatively, the samples were processed and run in precast BOLT-Bis-Tris Plus gels (Thermo Fisher Scientific, Switzerland) according to manufacturer's instructions. Gels were transferred to PVDF membranes, which were blocked with milk, probed with the appropriate primary antibody dilutions overnight at 4°C. They were washed, incubated in the appropriate HRP linked secondary antibody dilutions, washed, and then developed using a homemade chemiluminescent developing substrate. The blots were imaged using ImageQuant software. Antibodies used are listed in Sup table 1.

### **2.2.10 Real time quantitative polymerase chain reaction (RT-qPCR) analysis**

RNA was extracted from the duodenum and jejunum using Trizol reagent (Life Technologies #15596018) following the manufacturer's protocol and treated with DNase (Qiagen #79254). cDNA was synthesized using the High-Capacity cDNA Reverse Transcription Kit (Applied Biosystems #4368813) and used for RT-qPCR reactions using FAST SYBR green and the Vii7 Real Time PCR system (Applied

Biosystems). Each sample was run in triplicate and analysed using the  $2^{-\Delta\Delta C_T}$  method [27] with *Ppib* as the reference gene [28]. Primers used are listed in Sup table 2.

### **2.2.11 Plasma metabolite and insulin analysis**

Postprandial trunk blood samples were collected in microtubes containing 0.5 M EDTA after a 2 h fast in the dark phase; fasting blood samples (approximately 50 $\mu$ L) were collected from the lateral tail vein in EDTA coated microtubes (Sarstedt, Switzerland), after 6 h of fasting beginning at the onset of dark phase. Blood samples were centrifuged at 8700 g for 10 min at 4°C, and plasma were collected and stored at -80°C until required. Plasma TAG, free glycerol, non-esterified fatty acids (NEFA), and  $\beta$ -hydroxybutyrate (BHB) concentrations were measured using standard colorimetric and enzymatic methods adapted for the Cobas MIRA auto analyzer (Hoffman LaRoche, Basel, Switzerland) [29]. Final TAG values were obtained by subtracting the free glycerol values from the measured TAG values. Plasma insulin levels were measured using the Mouse/Rat Insulin Kit (catalog no. K152BZC-2) according to manufacturer's instructions (Meso Scale Discovery, USA).

### **2.2.12 Metabolomics**

#### **Sample preparation**

After 20 weeks on HFD, mice were fasted overnight and gavaged with a 500  $\mu$ L bolus of 150 mM  $^{13}\text{C}_2$  Oleic acid (SIGMA #646466) in a 0.5 % methylcellulose solution. The mice were sacrificed 2 h post gavage and duodenum, jejunum, and livers were collected and frozen in liquid nitrogen. Tissue samples were pulverized in liquid nitrogen and pre-weighed samples (approximately 100 mg) were lysed in 1 mL of 80% methanol and incubated on a thermoshaker at 4°C for 1 h at 1000 rpm. The samples were centrifuged at 14000 g and 4°C for 15 min, and 900  $\mu$ L of the supernatants were

transferred to fresh glass vials and sealed with Teflon/PTFE caps. These 80% methanol extracts were stored at -20°C until further processing. Fifty µL of each extract were transferred to an Eppendorf vial, dried completely under N<sub>2</sub>, re-dissolved with 20 µL water, and diluted with 80 µL of 50 mM ammonium acetate in acetonitrile/ methanol/ water/ saturated aqueous ammonium hydroxide (900: 88: 10: 2, v/v, pH 9). The final dilutions were centrifuged at 16100 g and 4°C for 15 min. The supernatants were transferred into glass vials for liquid chromatography–mass spectrometry (LC-MS) analyses [30].

### **LC-MS analyses**

Hydrophilic interaction chromatography (HILIC) was performed on a nano-UPLC system (Waters Inc. Milford, USA) coupled by a nano-ESI source to a Synapt G2 HDMS (Waters, Manchester, UK) as described in [31] with slight modification in the flow rate. The initial flow rate was 3.5µl/min and went down to 2.5µl/min during the gradient for 10min. A pooled sample consisting of a mix of every sample collected was repeatedly analyzed after every fifth sample in order to monitor the LC-MS performance and to assess the technical variance. Along with the pooled samples, a standard reference compound mix was analyzed containing the targeted metabolites glutamate, citrate, isocitrate, NAD<sup>+</sup>, ATP, ADP, acetyl-CoA, malonyl CoA, and palmitoyl-CoA, each at 5 µM concentration. Relative quantifications of the targeted metabolites were done by using the module QuanLynx of the mass spectrometry software MassLynx (version 4.1, Waters, United Kingdom).

#### **2.2.13 Statistical analysis**

All data are presented as mean ± standard error of the mean (SEM) of absolute values, % changes or fold changes as indicated in the figures. Data normality was verified using the Shapiro-Wilk test (when  $n \geq 7$ ) and Kolmogorov-Smirnov test (when

$5 \leq n \leq 6$ ). Non-parametric tests were used when the data were not normally distributed. Outliers were identified using the Grubb's test and removed. Statistical tests used are mentioned in the figure legends. When  $P < 0.05$ , the differences were considered statistically significant.

## 2.3 RESULTS

### 2.3.1 iSIRT3 mice overexpressed SIRT3 in the small intestine.

A western blot analysis of mitochondria isolated from the enterocytes of the duodenum and jejunum of S3fl and iSIRT3 mice showed that SIRT3 protein levels were higher in the small intestine of iSIRT3 mice (Fig 1), thus validating the intended transgenic manipulation. The mitochondrial proteins cytochrome-c oxidase subunit-IV (COX IV) and voltage-dependent anion channel (VDAC) were used as loading controls.

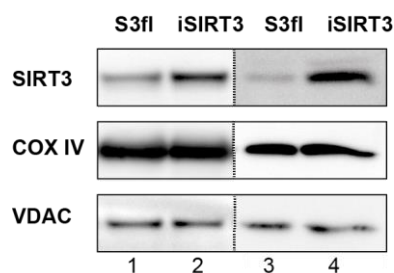


**Figure 1: iSIRT3 mice overexpressed SIRT3 in the small intestine.**

Western blot analysis of mitochondrial fractions isolated from the duodenum (lanes 1 and 2) and jejunum (lanes 3 and 4) of S3fl and iSIRT3 mice. Antibodies used are for sirtuin 3 (SIRT3), cytochrome-c oxidase subunit-IV (COX IV), and voltage-dependent anion channel (VDAC). The dotted line separates discontinuous blots. [Lanes 1 and 2,  $n = 3$  (pooled samples); lanes 3 and 4,  $n = 1$ ].



### 2.3.2 iSIRT3 and S3fl control mice had similar body weight, body composition, energy intake, and whole body energy metabolism.

All animals irrespective of genotype gained weight similarly on the HFD over time (diet,  $P < 0.0001$ ; time,  $P < 0.0001$ ; time x diet,  $P < 0.0001$ ) (Fig 2A). Monitoring the body composition of awake animals every few weeks using the EchoMRI scanner revealed that all animals showed similar increases in fat and lean mass over time (Sup Fig 1A). All animals on HFD gained more fat mass over time compared to those on CD (fat mass: diet,  $P < 0.0001$ ; fat and lean mass: time,  $P < 0.0001$ ; time x diet,  $P < 0.0001$ ). After 16 weeks on the diets, a CT scan of anesthetized mice also revealed a diet effect, such that there was a similar increase in lean mass ( $P < 0.05$ ), overall fat mass ( $P < 0.0001$ ), and visceral fat mass ( $P < 0.0001$ ) in S3fl and iSIRT3 mice on HFD compared to those on CD (Fig 2B). Both S3fl and iSIRT3 mice also showed an increase in subcutaneous fat on HFD versus (vs) CD ( $P < 0.0001$ ), with an interaction between the independent parameters, genotype, and diet ( $P < 0.05$ ); however, a *post hoc* analysis did not reveal any significant differences between the genotypes on either diet.

Both S3fl and iSIRT3 mice had lower energy intake ( $P < 0.01$ ) (Fig 2C), respiratory exchange ratio (RER) ( $P < 0.0001$ ) (Fig 2D), and locomotor activity ( $P < 0.001$ ) (Fig 2E) when switched from CD to HFD. No genotype differences were observed. Also, no diet or genotype effects in energy expenditure were observed in these mice (Fig 2F and Sup fig 1B).

Histological analyses of the jejunum of the mice revealed no visible differences between the genotypes. All animals on HFD showed a significant increase in villi length vs those on CD ( $P < 0.05$ ) (Sup fig 1C and D).

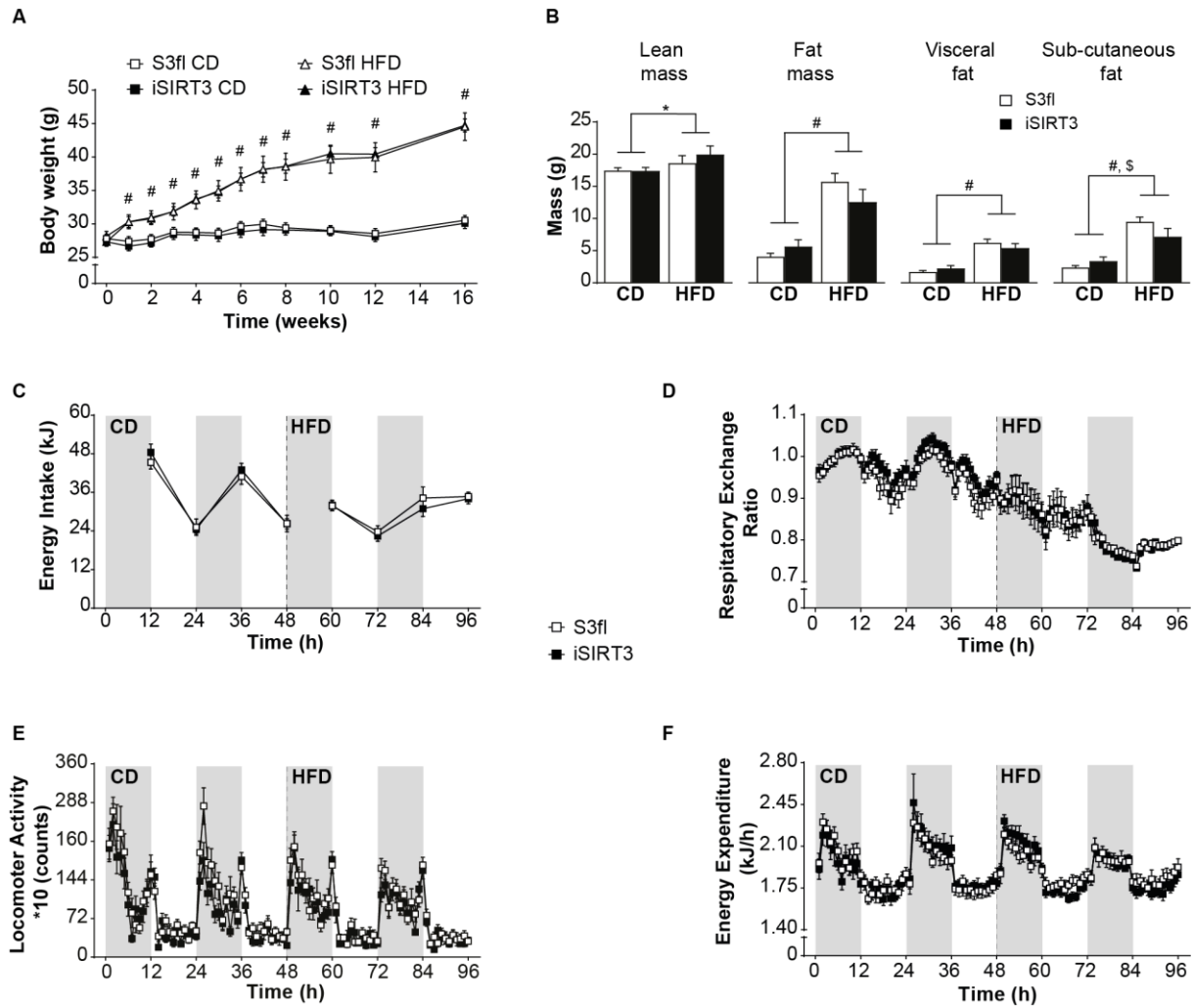


**Figure 2: iSIRT3 and S3fl control mice had similar body weight, body composition, energy intake, and whole body energy metabolism.**

(A) Body weights of iSIRT3 and S3fl mice on control diet (CD) or high fat diet (HFD) monitored over time. [n = 8-10; 3-way RM ANOVA (time x diet x genotype), time x diet,  $P < 0.0001$ : followed by a restricted 2-way ANOVA (diet x genotype) at each time point; diet,  $\#P < 0.0001$ . (B) CT scan analyses of S3fl and iSIRT3 mice fed CD or HFD. [n = 6-8; 2-way ANOVA (diet x genotype) with Tukey's multiple comparisons *post hoc* test. For lean mass, fat mass, visceral fat, and subcutaneous fat; diet effects,  $*P < 0.05$ ,  $\#P < 0.0001$ . Subcutaneous fat; diet x genotype,  $\$P < 0.05$ ]. (C-F) Indirect calorimetry data. The grey and white bars in the background represent the dark and light phases, respectively. (C) Energy intake measured every 12 hours. (D) Respiratory exchange ratio (RER) (E) Locomotor Activity and (F) Energy expenditure (EE) values plotted as mean values of 1 h time bins. (C-F) [n = 8-9; mixed RM ANOVA (genotype x diet x days x phases) with measurements over time compacted into diet (CD and HFD), days (day 1 and 2) and phases (dark and light)]. Data are presented as mean values  $\pm$  SEM.

### **2.3.3 iSIRT3 mice on HFD showed improved glucose homeostasis compared to S3fl mice.**

S3fl and iSIRT3 mice on CD were similarly sensitive to insulin given IP (Fig 3A) and similarly tolerant to an oral load of glucose (Fig 3E). iSIRT3 mice on HFD, however, showed an increased sensitivity to insulin (time x genotype,  $P < 0.01$ ) (Fig 3B), with lower circulating glucose levels compared to controls 90 min post injection ( $P < 0.05$ ). iSIRT3 mice on HFD also showed improved glucose clearance compared to S3fl mice, in response to an oral glucose load (time x genotype,  $P < 0.05$ ) with lower levels of glucose 30 ( $P < 0.01$ ) and 60 min ( $P < 0.05$ ) post gavage (Fig 3F). The fasting levels of plasma glucose and insulin were increased in both S3fl and iSIRT3 mice on HFD ( $P < 0.0001$ ), compared to those on CD, with no genotype differences on either diet (Sup fig 2).

### **2.3.4 iSIRT3 mice on HFD showed an induction of the ketogenic gene *Hmgcs2* in the small intestine, but not in the liver.**

There was an induction of *Hmgcs2* ( $P < 0.0001$ ), *Cpt1a* ( $P < 0.0001$ ) and *Lcad* ( $P < 0.001$ ) mRNA and a downregulation of *Pgc1a* mRNA ( $P < 0.001$ ) in the duodenum of all animals on HFD compared to those on CD (Fig 4 A). A similar increase in *Hmgcs2*, *Cpt1a*, and *Lcad* mRNA, as well as a downregulation of *Pgc1a* mRNA was seen in the jejunum of all the HFD fed mice compared to CD fed mice, irrespective of genotype ( $P < 0.0001$ ) (Fig 4B). iSIRT3 mice on HFD showed an even greater upregulation of *Hmgcs2* expression in the duodenum and jejunum compared to all the other groups (duodenum,  $P < 0.01$  vs S3fl on HFD; jejunum,  $P < 0.05$  vs S3fl on HFD) (Fig 4A and B). Livers of S3fl and iSIRT3 mice also showed an upregulation of *Hmgcs2*, *Cpt1a*, *ATPsyn*, and *Lcad* mRNA on HFD vs CD, with no genotypes differences.

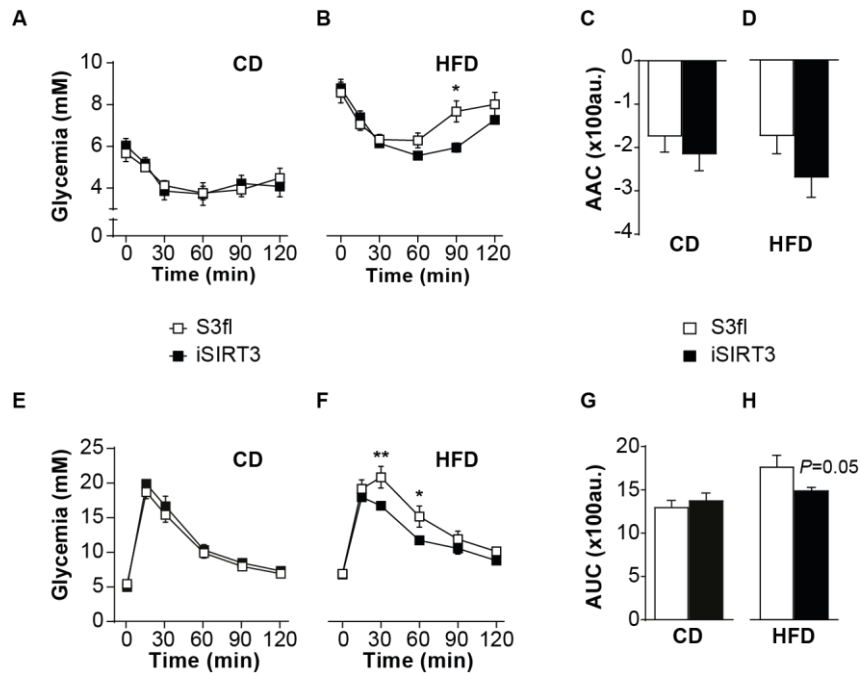


**Figure 3: iSIRT3 mice on HFD showed improved glucose homeostasis compared to S3fl mice.**

(A-B) Tail blood glucose values of insulin sensitivity test (IST) for S3fl and iSIRT3 mice on CD and HFD, respectively; (A) CD [n = 7-8; 2-way RM ANOVA (time x genotype)]. (B) HFD [n = 7-10; 2-way RM ANOVA (time x genotype) with Bonferroni's multiple comparisons *post hoc* test; time x genotype,  $P < 0.01$ ; genotype effect at time point 90 min,  $^*P < 0.05$ ]. (C) Area above the curve (AAC) of IST curves in A [n = 7-8; Mann-Whitney test]. (D) AAC of IST curves in B [n = 7-10; Unpaired *t* test]. (E-F) Tail blood glucose values of oral glucose tolerance test (OGTT) for S3fl and iSIRT3 mice on CD and HFD respectively. (E) CD [n = 9-10; 2-way RM ANOVA (time x genotype)]. (F) HFD [n = 6-7; 2-way RM ANOVA (time x genotype) with Bonferroni's multiple comparisons *post hoc* test; time x genotype,  $P < 0.05$ ; genotype effects at time point 30 min,  $^{**}P < 0.01$  and 60 min,  $^*P < 0.05$ ]. (G) Area under the curve (AUC) for OGTT curves in E [n = 9-10; Unpaired *t* test]. (H) AUC for OGTT curves in F [n = 6-7; Mann-Whitney test; genotype, ns]. Data are presented as mean values  $\pm$  SEM.

### 2.3.5 iSIRT3 mice on HFD did not show the lower systemic plasma ketone body levels compared to CD seen in S3fl mice.

The plasma NEFA, TAG, and glucose levels were similar in S3fl and iSIRT3 mice on CD or HFD with all animals on HFD showing lower NEFA ( $P < 0.0001$ ) and TAG levels ( $P < 0.0001$ ) (Fig 5A and B) and higher plasma glucose levels ( $P < 0.0001$ ) (Fig 5C) compared to mice on CD. Interestingly, the plasma BHB levels were lower in HFD fed mice compared to CD fed mice ( $P < 0.0001$ ), but the *post hoc* analysis showed that this difference was significant only in S3fl and not in iSIRT3 mice.

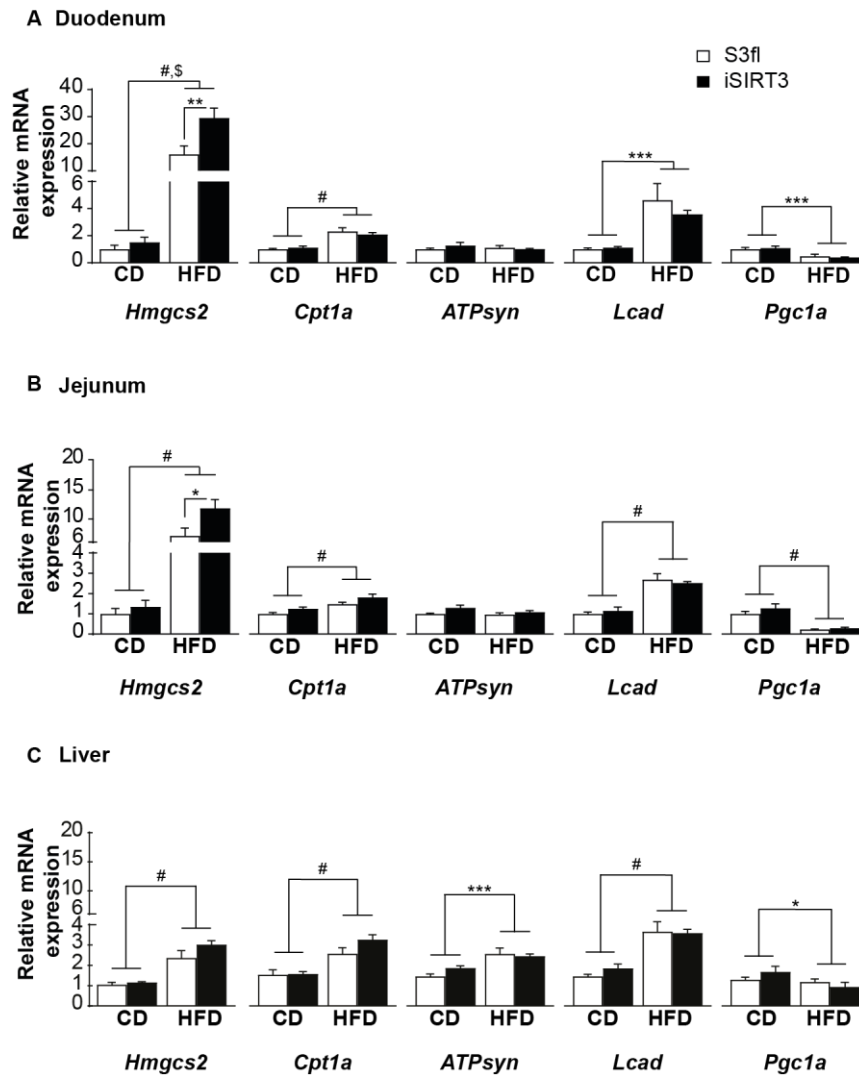


**Figure 4: iSIRT3 mice on HFD showed an induction of the ketogenic gene *Hmgcs2* in the small intestine but not in the liver.**

(A-C) Relative mRNA expression of *Hmgcs2*, *Cpt1a*, *ATPsyn*, *Lcad*, and *Pgc1a* in the duodenum, jejunum, and liver of S3fl and iSIRT3 mice on CD or HFD. (A) Duodenum [n = 6-8; 2-way ANOVA (diet x genotype) with Tukey's multiple comparison *post hoc* test. *Hmgcs2*, diet, #*P* < 0.0001; genotype, *P* < 0.05; diet x genotype, \$*P* < 0.05; S3fl HFD vs iSIRT3 HFD, \*\**P* < 0.01. *CPT1a*, diet, #*P* < 0.0001. *Lcad*, diet, \*\**P* < 0.001. *Pgc1a*, diet, \*\*\**P* < 0.001]. (B) Jejunum [n = 5-8; 2-way ANOVA (diet x genotype) with Tukey's multiple comparison *post hoc* test. *Hmgcs2*, genotype, *P* < 0.05; diet, #*P* < 0.0001; diet x genotype, *P* = 0.06, ns; S3fl HFD vs iSIRT3 HFD, \**P* < 0.05. *CPT1a*, genotype, *P* < 0.05; diet, #*P* < 0.0001, diet x genotype, ns. *ATPsyn*, genotype, *P* < 0.05; diet, ns; diet x genotype, ns. *Lcad*, genotype, ns; diet, #*P* < 0.0001, diet x genotype, ns. *Pgc1a*, genotype, ns; diet, #*P* < 0.0001, diet x genotype, ns]. (C) Liver [n = 6-9; 2-way ANOVA (diet x genotype) with Tukey's multiple comparison *post hoc* test. *Hmgcs2*, diet, #*P* < 0.0001. *CPT1a*, diet, #*P* < 0.0001. *ATPsyn*, diet, \*\*\**P* < 0.001. *Lcad*, diet, #*P* < 0.0001. *Pgc1a*, diet, \**P* < 0.05]. Data are presented as mean values ± SEM.

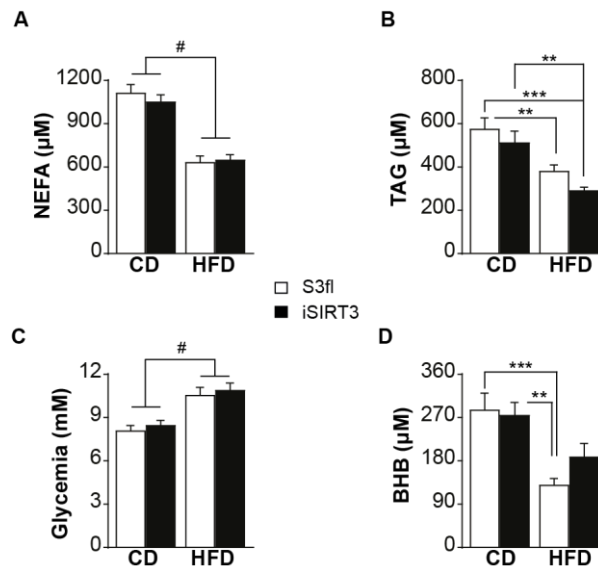


**Figure 5: iSIRT3 mice on HFD did not show the lower systemic plasma ketone body levels compared to CD seen in S3fl mice.**

(A-D) Post prandial trunk blood plasma metabolite levels of S3fl and iSIRT3 mice on CD and HFD [n = 13-18; 2-way ANOVA (diet x genotype) with Tukey's multiple comparison *post hoc* test]. (A) Non-esterified fatty acids (NEFA); diet, # $P < 0.0001$ . (B) Triacylglycerol (TAG); diet,  $P < 0.01$ ; S3fl CD vs S3fl HFD and iSIRT3 CD vs iSIRT3 HFD, \*\* $P < 0.01$ ; S3fl CD vs iSIRT3 HFD, \*\*\* $P < 0.001$ . (C) Glucose; diet, # $P < 0.0001$ . (D)  $\beta$ -hydroxybutyrate (BHB); diet,  $P < 0.0001$ ; S3fl CD vs S3fl HFD, \*\*\* $P < 0.001$ ; iSIRT3 CD vs S3fl HFD, \*\* $P < 0.01$ . Data are presented as mean values  $\pm$  SEM.

### 2.3.6 iSIRT3 mice showed a differentially regulated metabolic activity of jejunal enterocytes in response to an oral gavage of long-chain fatty acid.

We could not detect the  $^{13}\text{C}_2$  label from the oleic acid gavage in any of the metabolites tested in the duodenum, jejunum, or liver of S3fl and iSIRT3 mice on HFD. Interestingly, the jejunum of iSIRT3 mice showed lower levels of  $\text{NAD}^+$ , as well as palmitoyl CoA and malonyl CoA levels, compared to S3fl mice ( $P < 0.05$ ) (Fig 6A and D, Sup Fig 3B). There were no differences in the levels of these compounds in the duodenum or the liver, or in the NADH levels and ATP/ADP ratios of all three regions tested (Fig 6A-E). We also saw no differences in acetyl CoA, glutamate, citrate, and isocitrate levels in the intestinal samples (Sup Fig 3A-B). Of these, only acetyl CoA and

glutamate were detectable in the liver, with no differences between the two genotypes (Sup fig 3C).

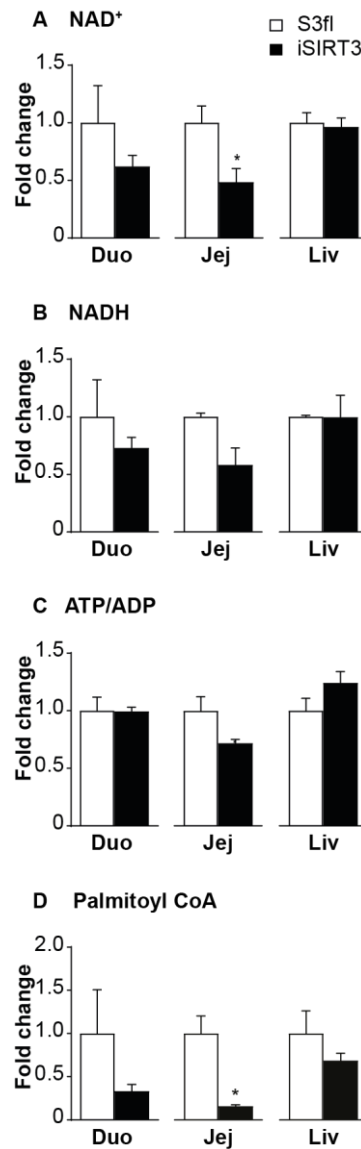


**Figure 6: iSIRT3 mice showed a differentially regulated metabolic activity of jejunal enterocytes in response to an oral gavage of fatty acid.**

LC-MS analyses of metabolites from the duodenum, jejunum, and liver of S3fl and iSIRT3 mice after oleic acid gavage, represented as fold change compared to S3fl controls. (A) NAD<sup>+</sup>, (B) NADH, (C) ATP/ADP, (D) Palmitoyl CoA [n = 3-5; Mann-Whitney test, \* $p < 0.05$ ]. Data are presented as mean values  $\pm$  SEM.

## 2.4 DISCUSSION

The major aim of this study was to examine if enhancing the metabolic flux of the enterocytes in mice could influence DIO and its comorbidities. Using the *cre-loxP* system, we genetically overexpressed the mitochondrial NAD<sup>+</sup> dependent protein deacetylase SIRT3, in the epithelial cells of the intestine. We characterized both *iSIRT3* and *S3fl* mice fed CD or HFD for several weeks and found that an overexpression of SIRT3 in the enterocytes did not lead to differences in any of the parameters tested when these mice were on CD. On HFD, both *S3fl* and *iSIRT3* mice showed similar manifestations of DIO, but *iSIRT3* mice were better able to regulate their blood glucose levels in response to exogenous insulin or glucose. This indicates that *iSIRT3* mice on HFD were protected from developing IR, one of the major comorbidities of DIO. *iSIRT3* mice also showed increased ketogenic gene expression in the small intestine as well increased enterocyte metabolic activity. Our findings suggest that enterocyte oxidative metabolism plays a role in the regulation of whole body glucose metabolism under conditions of DIO.

As post-translational regulator of several mitochondrial proteins, SIRT3 has been shown to upregulate multiple metabolic pathways including FAO, the TCA cycle, and ketogenesis [19]. Here we show that in chronic HFD fed *iSIRT3* mice, after an oral bolus of oleic acid, SIRT3 activity was upregulated in the small intestine but not in the liver. The decrease in the NAD<sup>+</sup> levels in the jejunum is indirect evidence for increased SIRT3 activity. NAD<sup>+</sup> is the cosubstrate for several enzymes, one of which is SIRT3 [17]. SIRT3 breaks down a molecule of NAD<sup>+</sup> during every deacetylation reaction [32], and an upregulation of SIRT3 activity would in turn reduce the NAD<sup>+</sup> levels. The reverse is true when NAD<sup>+</sup> consuming enzymes are inhibited or downregulated. For example, PARP1 inhibition leads to an increase in NAD<sup>+</sup> levels as shown in [33].



iSIRT3 mice also showed a decrease in malonyl CoA and palmitoyl CoA levels in the jejunum. Malonyl CoA is an intermediate of fatty acid synthesis, while palmitoyl CoA is its end product. Malonyl CoA is also an inhibitor of the mitochondrial long-chain fatty acid transport protein CPT1a, and thereby an inhibitor of FAO. A decrease in the levels of these two metabolites implies a downregulation of *de-novo* fatty acid synthesis and an upregulation of FAO [34, 35]; further indicating that FAO is enhanced in the enterocytes of iSIRT3 mice on HFD. Together, these data demonstrate that an overexpression of SIRT3 in enterocytes of HFD fed mice enhanced the mitochondrial metabolic activity of small intestinal epithelial cells.

Data from whole body SIRT3 knock out mice showed that the absence of SIRT3 led to an accelerated development of DIO and metabolic syndrome on chronic HFD feeding [36]. This was attributed to increased mitochondrial dysfunction due to the hyperacetylation of mitochondrial proteins in the absence of SIRT3. Subsequent studies on SIRT3 overexpression mice showed that increased SIRT3 expression protected mice from developing noise induced hearing loss, as well as ageing associated tissue fibrosis [20, 37]; however, they did not study the effects of whole body or tissue specific SIRT3 overexpression on the development of DIO or metabolic syndrome in response to chronic HFD feeding. We here show that an increase in SIRT3 expression and function in the enterocytes had no impact on body weight, body composition, or fat distribution, and iSIRT3 mice on HFD developed DIO similar to S3fl mice. Both S3fl and iSIRT3 mice also showed increased jejunal villi length and had similarly high circulating levels of fasting glucose and insulin after chronic HFD feeding. These effects are consistent with previous observations in animals fed HFD that develop DIO [38, 39]. Indirect calorimetry data also showed no differences between S3fl and iSIRT3 mice on CD or when switched to HFD. The reductions in energy intake,

RER, and activity, seen in both S3fl and iSIRT3 mice on exposure to HFD, were in line with previous studies about HFD feeding in mice [40-42].

Despite these similarities though, iSIRT3 mice showed distinct differences from S3fl controls in their ability to regulate systemic glucose. After IP insulin, iSIRT3 mice on HFD showed prolonged hypoglycemia and a slow rise in blood glucose levels. This indicates that iSIRT3 mice were less resistant to insulin than S3fl controls, even after several weeks on HFD. iSIRT3 mice were also able to rapidly uptake and clear the high circulating blood glucose levels in the OGTT, compared to S3fl mice. These results clearly indicate that iSIRT3 mice on HFD developed less IR than S3fl mice, despite similar DIO. Conversely, the whole body SIRT3 knock out mice on HFD developed IR and DIO faster than control mice; this was attributed mainly to hepatic dyslipidemia caused by increased lipogenesis [36]. Mice deficient in LCAD as well as malonyl CoA carboxylase showed reduced fatty acid oxidation in the liver and skeletal muscle, respectively, and developed IR [43, 44]. These data suggest that decreased fatty acid oxidation in the liver and muscle caused peripheral IR. Here we show that increased SIRT3 (and therefore increased FAO in the enterocytes), contributes to protection from developing IR.

At the molecular level, both S3fl and iSIRT3 mice showed an upregulation of genes involved in FAO (*Cpt1a* and *Lcad*) and ketogenesis (*Hmgcs2*) in the duodenum, jejunum, and liver on HFD compared to CD. Of note was the nearly 10 to 20-fold increase in *Hmgcs2* mRNA expression in the duodenum and jejunum of all HFD fed mice vs CD fed mice, compared to the smaller, 3-fold increase in the liver. This is consistent with previous data showing that exposure to HFD for two weeks increased the expression of fat oxidation and mainly ketogenic genes in the duodenum [16]. Our data indicate that after 17 weeks of HFD feeding, these increases in gene expression

occur in the duodenum and jejunum as well as in the liver. HFD fed iSIRT3 mice showed an even greater increase in *Hmgcs2* expression in the duodenum and jejunum than S3fl mice (15 to 30-fold increase vs CD fed mice), but not in the liver, indicating that intestinal SIRT3 overexpression further upregulates ketogenic genes in the small intestine of mice fed HFD. SIRT3 is a posttranslational regulator of proteins that deacylates several genes in the FAO pathway, thereby enhancing fat oxidation [45]. Hence, it is not surprising that we see an upregulation of FAO in the enterocytes of iSIRT3 mice, with no changes at the gene expression level, compared to S3fl mice on HFD. SIRT3 is also known to deacylate and upregulate HMGCS2 and thereby ketogenesis [46]. The increased gene expression of *Hmgcs2* in the enterocytes of iSIRT3 mice suggests that this might be an indirect mechanism of upregulation rather than an activation by direct deacetylation, though we cannot rule out the latter possibility based on our results.

Despite the upregulation of *Hmgcs2* mRNA expression in the duodenum, jejunum, and liver of all mice on HFD, systemic postprandial plasma BHB levels in control S3fl mice on HFD were lower than on CD. The overall decrease in BHB levels in the trunk blood plasma of HFD fed mice is consistent with previous findings showing that long-term obesity or HFD feeding leads to reduced circulating ketone body levels in humans as well as rodents [47-50]. These studies suggest that while mild IR leads to an upregulation of hepatic ketogenesis, severe IR leads to blunted hepatic ketogenesis even under conditions of high-fat oxidation in the liver. The plasma BHB levels of iSIRT3 mice fed HFD were not different from those of mice fed CD and showed an increasing trend compared to S3fl mice on HFD, which did not reach statistical significance. This might be because the blood samples from our mice were trunk blood samples collected after decapitation, which represent a diluted pool of

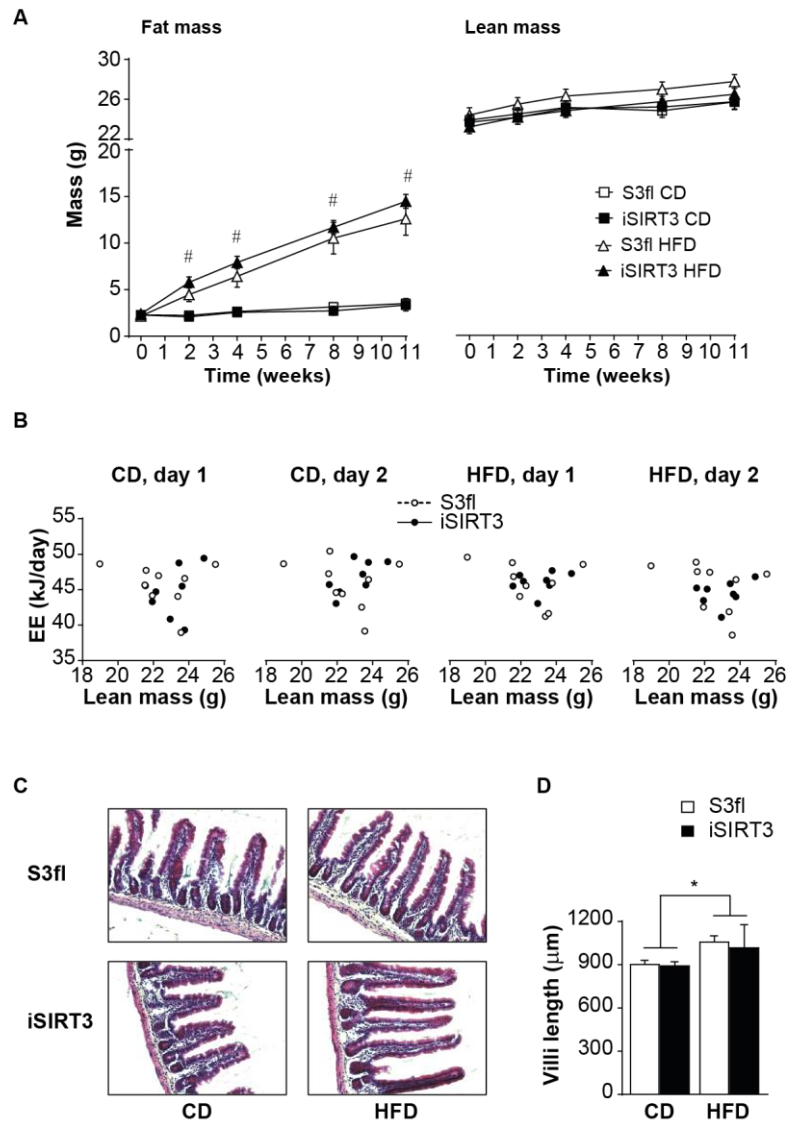
blood coming from the intestine. Analysis of plasma BHB levels from the hepatic portal vein would have allowed for a better estimate of the amount of ketone bodies generated in the small intestine [11, 51, 52]. Our results suggest that SIRT3 overexpression in the enterocytes led to an increase in ketone body production in the intestine but not in the liver of iSIRT3 mice on HFD. This is consistent with pharmacological studies in rats, where peripheral administration of FAO stimulators showed an upregulation of FAO and ketogenic markers in the small intestine, but not the liver, as well as increased BHB levels in the hepatic portal vein blood plasma [11, 51, 52]. Both S3fl and iSIRT3 mice on HFD also showed reduced NEFA and TAG levels under fed conditions compared to CD fed mice, with no genotype effect. These HFD-induced reductions in plasma NEFA and TAG levels are consistent with previous findings, which show that there is a species-specific decrease in circulating TAG and free fatty acids in mice with DIO [53].

Traditionally, ketone bodies were mainly thought of as an alternative fuel source for the brain and other peripheral organs, in conditions of prolonged fasting. More recently, BHB has been proposed as a signaling metabolite even under conditions of nutrient abundance (as reviewed in [54] and [55]) and thereby might protect against the development of IR and T2D. These reviews mainly focus on the liver as the main organ contributing to circulating ketone bodies. In line with previous findings [15, 16], our data suggest that the gut also has the capacity to contribute to circulating ketone levels and, in fact, might be an interesting extra-hepatic target to manipulate whole body glucose homeostasis, especially in DIO.

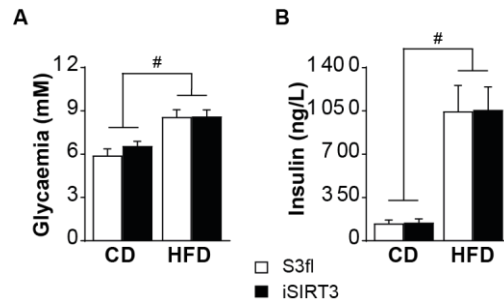
Studies addressing the effects of peripheral administration of FAO stimulators suggest that enhanced FAO and ketogenesis in the small intestine might reduce energy intake and body weight [51, 52]. Our results seem to indicate otherwise

because enhanced FAO and ketogenesis in enterocytes did not lead to changes in energy intake or body weight, on CD -or on HFD. This difference might be due to the fact that the pharmacological studies looked at the acute effects of peripherally administered FAO stimulators. Our transgenic mice overexpressed SIRT3 under the constitutive expression of Cre recombinase, downstream of the Villin promoter. This might have caused compensatory changes during development and, hence, blunted any changes in food intake. The use of an inducible Cre mouse model that would allow for the initiation of SIRT3 overexpression in a specific time window might help to answer this question. In addition, our mouse model expressed only one extra copy of the Sirt3 gene. A homozygous knock-in mouse model could presumably cause a greater overexpression of SIRT3 with stronger or different phenotypic effects.

Further studies should try to identify the exact mechanisms of the observed effects in HFD-fed iSIRT3 mice. In any case, targeting intestinal metabolism in obese patients through non-surgical interventions might be an interesting new approach to fight IR and T2D.

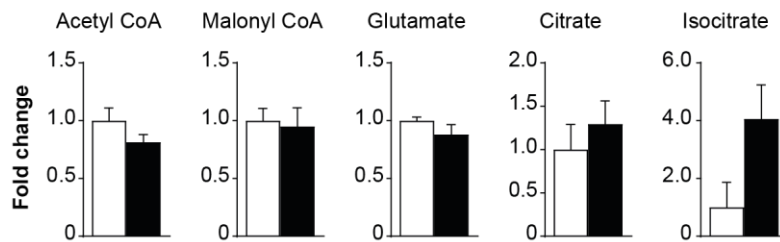


**Supplementary Figure 1:** (A) MRI scan measurements of fat mass (left) and lean mass (right) of S3fl and iSIRT3 mice before (week 0) and after 2, 4, 8 and 11 weeks on CD and HFD. [ $n = 7-10$ ; three-way RM ANOVA; genotype, ns; diet,  $P < 0.0001$ ; time,  $P < 0.0001$ ; time  $\times$  diet,  $P < 0.0001$ ; genotype  $\times$  diet, ns; genotype  $\times$  time, ns; genotype  $\times$  diet  $\times$  time, ns. Two-way ANOVA at each time point; diet,  $\#P < 0.0001$ . (B) Energy expenditure (EE) per day as a function of lean mass for S3fl and iSIRT3 mice [ $n=8-9$ ; ANCOVA for EE with lean mass as the covariate; genotype, ns for each day; lean mass, ns for each day]. (C) Representative images of bright field microscopy images of H&E stained jejunal sections of S3fl and iSIRT3 mice, on CD and HFD for 16 weeks at 20X magnification. (D) Measurements of the villi lengths of S3fl and iSIRT3 mice from B. [ $n = 3-5$ ; two-way ANOVA with Tukey's multiple comparisons *post hoc* test; genotype, ns; diet,  $\ast P < 0.05$ ; diet  $\times$  genotype, ns]. Data are presented as mean values  $\pm$

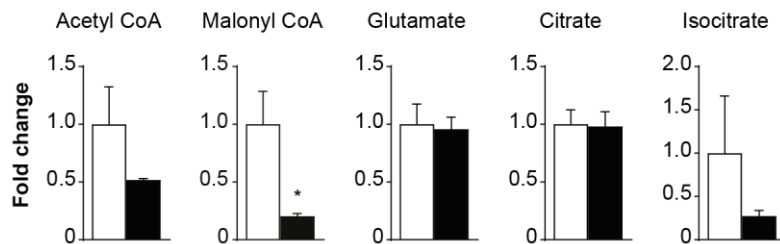


**Supplementary Figure 2:** (A) Fasting plasma glucose levels of S3fl and iSIRT3 mice on CD and HFD [n = 7-10; two-way ANOVA with Tukey's multiple comparisons *post hoc* test; diet, # $P < 0.0001$ ]. (B) Fasting plasma insulin levels of S3fl and iSIRT3 mice on CD and HFD [n = 7-10; two-way ANOVA with Tukey's multiple comparisons *post hoc* test; diet, # $P < 0.0001$ ]. Data are presented as mean values  $\pm$  SEM.

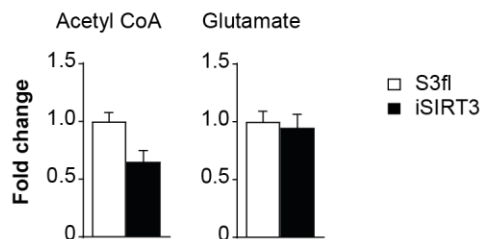
#### A Duodenum



#### B Jejunum



#### C Liver



**Supplementary Figure 3:** LC-MS analysis of metabolites from the (A) duodenum, (B) jejunum, and (C) liver of S3fl and iSIRT3 mice after oleic acid gavage. [n = 3-5; Mann-Whitney test; genotype, ns for all compounds]. Data are presented as mean values  $\pm$  SEM.

## SUPPLEMENTARY TABLES

**Sup table 1: Antibodies for western blotting**

Antibody	Molecular weight	Catalog #	Company	Working Dilution
Sirtuin3 (SIRT3)	28 kDa	5490	Cell Signalling Technology	1:1000
Voltage-dependent anion channel (VDAC)	32 kDa	4661	Cell Signalling Technology	1:1000
Cytochrome-c oxidase subunit-IV (COX IV)	17 kDa	4844	Cell Signalling Technology	1:1000
Anti-rabbit IgG, HRP-linked		7074	Cell Signalling Technology	1:2000

**Sup table 2: Primers for RTqPCR analyses**

Gene name	Primers
3-Hydroxy-3-methylglutaryl-CoA synthase 2 (Hmgcs2)	F: 5' agataccaccaacgcctgtt 3' R: 5' aatgtcaccacagaccacca 3'
Carnitine palmitoyltransferase 1a, liver (CPT1a)	F: 5' gacgaatcggaacaggata 3' R: 5' tggactgtcaaaccacctg 3'
ATP synthase (ATPsyn)	F: 5' aggatgcaatcgacatgga 3' R: 5' aaggccagggaatgttatt 3'
Long chain acyl CoA dehydrogenase (Lcad)	F: 5' gtctggactccggttctgc 3' R: 5' ccgtggagttgcacacatt 3'
Peroxisome proliferative activated receptor, gamma, coactivator 1 alpha (Pgc1a)	F: 5' ttctcgacacaggtcgtgtt 3' R: 5' gtgtgcggtgtctgtagtgg 3'
Peptidylprolyl Isomerase B (Ppib)	F: 5' ttctcataccacagtcagacc 3' R: 5' acctccgtaccacatccat-3'



## **ACKNOWLEDGEMENTS**

This work was supported by the Swiss National Science Foundation, Research Grant 310030\_153149 to WL. We are grateful to Prof. WD Hardt and P Kaiser for the VilCre mice; E Karimian, F Mouttet, E Weber, F Mueller, L Michel, and M Heyner for assistance in experimentation or genotyping, to JP Krieger for his support in editing the manuscript and the SLA animal facility for contribution to animal husbandry.

## 2.5 REFERENCES

- [1] World Health Organization, Global Report on Diabetes, Geneva 2016, <http://www.who.int/diabetes/global-report/en/>
- [2] Kahn, S. E., Hull, R. L., Utzschneider, K. M. Mechanisms linking obesity to insulin resistance and type 2 diabetes. *Nature*. 2006,444:840-6.
- [3] Mingrone, G., Cummings, D. E. Changes of insulin sensitivity and secretion after bariatric/metabolic surgery. *Surg Obes Relat Dis*. 2016,12:1199-205.
- [4] Pories, W. J., Swanson, M. S., Macdonald, K. G., Long, S. B., Morris, P. G., Brown, B. M., et al. Who Would Have Thought It - an Operation Proves to Be the Most Effective Therapy for Adult-Onset Diabetes-Mellitus. *Ann Surg*. 1995,222:339-52.
- [5] Pories, W. J., Albrecht, R. J. Etiology of type II diabetes mellitus: role of the foregut. *World J Surg*. 2001,25:527-31.
- [6] Hickey, M. S., Pories, W. J., MacDonald, K. G., Cory, K. A., Dohm, G. L., Swanson, M. S., et al. A new paradigm for type 2 diabetes mellitus - Could it be a disease of the foregut? *Ann Surg*. 1998,227:637-44.
- [7] Saeidi, N., Meoli, L., Nestoridi, E., Gupta, N. K., Kvas, S., Kucharczyk, J., et al. Reprogramming of intestinal glucose metabolism and glycemic control in rats after gastric bypass. *Science*. 2013,341:406-10.
- [8] Yan, Y., Zhou, Z., Kong, F., Feng, S., Li, X., Sha, Y., et al. Roux-en-Y Gastric Bypass Surgery Suppresses Hepatic Gluconeogenesis and Increases Intestinal Gluconeogenesis in a T2DM Rat Model. *Obes Surg*. 2016,26:2683-90.
- [9] Troy, S., Soty, M., Ribeiro, L., Laval, L., Migrenne, S., Fioramonti, X., et al. Intestinal gluconeogenesis is a key factor for early metabolic changes after gastric bypass but not after gastric lap-band in mice. *Cell Metabolism*. 2008,8:201-11.
- [10] Nelson, D. W., Gao, Y., Yen, M. I., Yen, C. L. Intestine-specific deletion of acyl-CoA:monoacylglycerol acyltransferase (MGAT) 2 protects mice from diet-induced obesity and glucose intolerance. *J Biol Chem*. 2014,289:17338-49.

- [11] Schober, G., Arnold, M., Birtles, S., Buckett, L. K., Pacheco-Lopez, G., Turnbull, A. V., et al. Diacylglycerol acyltransferase-1 inhibition enhances intestinal fatty acid oxidation and reduces energy intake in rats. *Journal of Lipid Research*. 2013,54:1369-84.
- [12] Tsuda, N., Kumadaki, S., Higashi, C., Ozawa, M., Shinozaki, M., Kato, Y., et al. Intestine-targeted DGAT1 inhibition improves obesity and insulin resistance without skin aberrations in mice. *PLoS One*. 2014,9:e112027.
- [13] Langhans, W. Fatty acid oxidation in the energostatic control of eating--a new idea. *Appetite*. 2008,51:446-51.
- [14] Mansouri, A., Langhans, W. Enterocyte-afferent nerve interactions in dietary fat sensing. *Diabetes Obes Metab*. 2014,16 Suppl 1:61-7.
- [15] Kondo, H., Minegishi, Y., Komine, Y., Mori, T., Matsumoto, I., Abe, K., et al. Differential regulation of intestinal lipid metabolism-related genes in obesity-resistant A/J vs. obesity-prone C57BL/6J mice. *Am J Physiol Endocrinol Metab*. 2006,291:E1092-9.
- [16] Clara, R., Schumacher, M., Ramachandran, D., Fedele, S., Krieger, J. P., Langhans, W., et al. Metabolic Adaptation of the Small Intestine to Short- and Medium-Term High-Fat Diet Exposure. *J Cell Physiol*. 2017,232:167-75.
- [17] Verdin, E. NAD(+) in aging, metabolism, and neurodegeneration. *Science*. 2015,350:1208-13.
- [18] Rardin, M. J., Newman, J. C., Held, J. M., Cusack, M. P., Sorensen, D. J., Li, B., et al. Label-free quantitative proteomics of the lysine acetylome in mitochondria identifies substrates of SIRT3 in metabolic pathways. *Proc Natl Acad Sci U S A*. 2013,110:6601-6.
- [19] Osborne, B., Bentley, N. L., Montgomery, M. K., Turner, N. The role of mitochondrial sirtuins in health and disease. *Free Radic Biol Med*. 2016,100:164-74.
- [20] Brown, K. D., Maqsood, S., Huang, J. Y., Pan, Y., Harkcom, W., Li, W., et al. Activation of SIRT3 by the NAD(+) precursor nicotinamide riboside protects from noise-induced hearing loss. *Cell Metab*. 2014,20:1059-68.

- [21] Madison, B. B., Dunbar, L., Qiao, X. T., Braunstein, K., Braunstein, E., Gumucio, D. L. Cis elements of the villin gene control expression in restricted domains of the vertical (crypt) and horizontal (duodenum, cecum) axes of the intestine. *J Biol Chem.* 2002,277:33275-83.
- [22] Tschop, M. H., Speakman, J. R., Arch, J. R., Auwerx, J., Bruning, J. C., Chan, L., et al. A guide to analysis of mouse energy metabolism. *Nature methods.* 2012,9:57-63.
- [23] Fischer, K., Ruiz, H. H., Jhun, K., Finan, B., Oberlin, D. J., van der Heide, V., et al. Alternatively activated macrophages do not synthesize catecholamines or contribute to adipose tissue adaptive thermogenesis. *Nature Medicine.* 2017,23:623-30.
- [24] McGuinness, O. P., Ayala, J. E., Laughlin, M. R., Wasserman, D. H. NIH experiment in centralized mouse phenotyping: the Vanderbilt experience and recommendations for evaluating glucose homeostasis in the mouse. *Am J Physiol Endocrinol Metab.* 2009,297:E849-55.
- [25] Nik, A. M., Carlsson, P. Separation of intact intestinal epithelium from mesenchyme. *BioTechniques.* 2013,55:42-4.
- [26] Frezza, C., Cipolat, S., Scorrano, L. Organelle isolation: functional mitochondria from mouse liver, muscle and cultured fibroblasts. *Nat Protoc.* 2007,2:287-95.
- [27] Livak, K. J., Schmittgen, T. D. Analysis of relative gene expression data using real-time quantitative PCR and the 2<sup>(-ΔΔC<sub>T</sub>)</sup> method. *Methods.* 2001,25:402-8.
- [28] Sirakov, M., Borra, M., Cambuli, F. M., Plateroti, M. Defining Suitable Reference Genes for RT-qPCR Analysis on Intestinal Epithelial Cells. *Molecular biotechnology.* 2013.
- [29] Langhans, W. Hepatic and intestinal handling of metabolites during feeding in rats. *Physiol Behav.* 1991,49:1203-9.
- [30] Riera-Borrull, M., Rodriguez-Gallego, E., Hernandez-Aguilera, A., Luciano, F., Ras, R., Cuyas, E., et al. Exploring the Process of Energy Generation in

Pathophysiology by Targeted Metabolomics: Performance of a Simple and Quantitative Method. *J Am Soc Mass Spectrom.* 2016,27:168-77.

[31] Abplanalp, J., Laczko, E., Philp, N. J., Neidhardt, J., Zuercher, J., Braun, P., et al. The cataract and glucosuria associated monocarboxylate transporter MCT12 is a new creatine transporter. *Hum Mol Genet.* 2013,22:3218-26.

[32] Hirschey, M. D. Old enzymes, new tricks: sirtuins are NAD(+)-dependent deacetylases. *Cell Metab.* 2011,14:718-9.

[33] Bai, P., Canto, C., Oudart, H., Brunyanszki, A., Cen, Y. N., Thomas, C., et al. PARP-1 Inhibition Increases Mitochondrial Metabolism through SIRT1 Activation. *Cell Metabolism.* 2011,13:461-8.

[34] Foster, D. W. Malonyl-CoA: the regulator of fatty acid synthesis and oxidation. *Journal of Clinical Investigation.* 2012,122:1958-9.

[35] Abu-Elheiga, L., Matzuk, M. M., Abo-Hashema, K. A., Wakil, S. J. Continuous fatty acid oxidation and reduced fat storage in mice lacking acetyl-CoA carboxylase 2. *Science.* 2001,291:2613-6.

[36] Hirschey, M. D., Shimazu, T., Jing, E., Grueter, C. A., Collins, A. M., Aouizerat, B., et al. SIRT3 deficiency and mitochondrial protein hyperacetylation accelerate the development of the metabolic syndrome. *Mol Cell.* 2011,44:177-90.

[37] Sundaresan, N. R., Bindu, S., Pillai, V. B., Samant, S., Pan, Y., Huang, J. Y., et al. SIRT3 Blocks Aging-Associated Tissue Fibrosis in Mice by Deacetylating and Activating Glycogen Synthase Kinase 3beta. *Mol Cell Biol.* 2015,36:678-92.

[38] Baldassano, S., Amato, A., Cappello, F., Rappa, F., Mule, F. Glucagon-like peptide-2 and mouse intestinal adaptation to a high-fat diet. *The Journal of endocrinology.* 2013,217:11-20.

[39] Collins, S., Martin, T. L., Surwit, R. S., Robidoux, J. Genetic vulnerability to diet-induced obesity in the C57BL/6J mouse: physiological and molecular characteristics. *Physiol Behav.* 2004,81:243-8.

- [40] Ellacott, K. L., Morton, G. J., Woods, S. C., Tso, P., Schwartz, M. W. Assessment of feeding behavior in laboratory mice. *Cell Metab.* 2010,12:10-7.
- [41] Longo, K. A., Charoenthongtrakul, S., Giuliana, D. J., Govek, E. K., McDonagh, T., DiStefano, P. S., et al. The 24-hour respiratory quotient predicts energy intake and changes in body mass. *Am J Physiol-Reg I.* 2010,298:R747-R54.
- [42] Bjursell, M., Gerdin, A. K., Lelliott, C. J., Egecioglu, E., Elmgren, A., Tornell, J., et al. Acutely reduced locomotor activity is a major contributor to Western diet-induced obesity in mice. *Am J Physiol-Endoc M.* 2008,294:E251-E60.
- [43] Zhang, D., Liu, Z. X., Choi, C. S., Tian, L., Kibbey, R., Dong, J., et al. Mitochondrial dysfunction due to long-chain Acyl-CoA dehydrogenase deficiency causes hepatic steatosis and hepatic insulin resistance. *Proc Natl Acad Sci U S A.* 2007,104:17075-80.
- [44] Koves, T. R., Ussher, J. R., Noland, R. C., Slentz, D., Mosedale, M., Ilkayeva, O., et al. Mitochondrial overload and incomplete fatty acid oxidation contribute to skeletal muscle insulin resistance. *Cell Metab.* 2008,7:45-56.
- [45] Hirschey, M. D., Shimazu, T., Goetzman, E., Jing, E., Schwer, B., Lombard, D. B., et al. SIRT3 regulates mitochondrial fatty-acid oxidation by reversible enzyme deacetylation. *Nature.* 2010,464:121-U37.
- [46] Shimazu, T., Hirschey, M. D., Hua, L., Dittenhafer-Reed, K. E., Schwer, B., Lombard, D. B., et al. SIRT3 deacetylates mitochondrial 3-hydroxy-3-methylglutaryl CoA synthase 2 and regulates ketone body production. *Cell Metab.* 2010,12:654-61.
- [47] Vice, E., Privette, J. D., Hickner, R. C., Barakat, H. A. Ketone body metabolism in lean and obese women. *Metabolism.* 2005,54:1542-5.
- [48] Soeters, M. R., Sauerwein, H. P., Faas, L., Smeenge, M., Duran, M., Wanders, R. J., et al. Effects of insulin on ketogenesis following fasting in lean and obese men. *Obesity (Silver Spring).* 2009,17:1326-31.
- [49] Satapati, S., He, T., Inagaki, T., Potthoff, M., Merritt, M. E., Esser, V., et al. Partial resistance to peroxisome proliferator-activated receptor-alpha agonists in ZDF rats is

associated with defective hepatic mitochondrial metabolism. *Diabetes*. 2008,57:2012-21.

[50] Satapati, S., Sunny, N. E., Kucejova, B., Fu, X., He, T. T., Mendez-Lucas, A., et al. Elevated TCA cycle function in the pathology of diet-induced hepatic insulin resistance and fatty liver. *J Lipid Res*. 2012,53:1080-92.

[51] Azari, E. K., Leitner, C., Jaggi, T., Langhans, W., Mansouri, A. Possible Role of Intestinal Fatty Acid Oxidation in the Eating-Inhibitory Effect of the PPAR-alpha Agonist Wy-14643 in High-Fat Diet Fed Rats. *PLoS One*. 2013,8.

[52] Azari, E. K., Ramachandran, D., Weibel, S., Arnold, M., Romano, A., Gaetani, S., et al. Vagal afferents are not necessary for the satiety effect of the gut lipid messenger oleoylethanolamide. *Am J Physiol Regul Integr Comp Physiol*. 2014,307:R167-78.

[53] Gao, S., He, L., Ding, Y., Liu, G. Mechanisms underlying different responses of plasma triglyceride to high-fat diets in hamsters and mice: roles of hepatic MTP and triglyceride secretion. *Biochem Biophys Res Commun*. 2010,398:619-26.

[54] Newman, J. C., Verdin, E. beta-hydroxybutyrate: Much more than a metabolite. *Diabetes Res Clin Pr*. 2014,106:173-81.

[55] Puchalska, P., Crawford, P. A. Multi-dimensional Roles of Ketone Bodies in Fuel Metabolism, Signaling, and Therapeutics. *Cell Metab*. 2017,25:262-84.

## **CHAPTER 3:**

# **ENTEROCYTE EXPRESSION OF MUTATED CARNITINE PALMITOYLTRANSFERASE-1 INSENSITIVE TO MALONYL COA INHIBITION IN MICE AFFECTS GLYCEMIC CONTROL DEPENDING ON DIETARY FAT**

Deepti Ramachandran<sup>1</sup>, Rosmarie Clara<sup>1</sup>, Shahana Fedele<sup>1</sup>, Ladina Michel<sup>1</sup>,  
Johannes Burkard<sup>1</sup>, Sharon Kaufman<sup>1</sup>, Alvarado Diaz Abdiel<sup>2</sup>, Nadja Weissfeld<sup>1</sup>,  
Katrien De Bock<sup>2</sup>, Carina Prip-Buus<sup>3,4,5</sup>, Wolfgang Langhans<sup>1</sup>, Abdelhak Mansouri<sup>1,\*</sup>

<sup>1</sup>Physiology and Behavior Laboratory, ETH Zurich, Schwerzenbach, Switzerland

<sup>2</sup>Excercise and Health Laboratory, ETH Zurich, Schwerzenbach, Switzerland

<sup>3</sup>Inserm, U1016, Institut Cochin, Paris, France

<sup>4</sup>CNRS, UMR 8104, Paris, France

<sup>5</sup>Université Paris Descartes, Sorbonne Paris Cité, Paris, France

**STATUS**

*In preparation*

---



**ABSTRACT:**

**Objective:** Studies indicate that modulating enterocyte metabolism might affect whole body glucose homeostasis and the development of diet-induced obesity (DIO). We tested whether enhancing enterocyte fatty acid oxidation (FAO) could protect mice from DIO and impaired glycemic control.

**Methods:** We used mice expressing a mutant form of carnitine palmitoyltransferase-1a (CPT1mt), insensitive to inhibition by malonyl-CoA in their enterocytes (iCPT1mt) and fed them low-fat control diet (CD) or high-fat diet (HFD) chronically.

**Results:** CPT1mt expression led to an upregulation of FAO in the enterocytes. On CD, iCPT1mt mice had impaired glycemic control and showed concomitant activation of lipogenesis, glycolysis and gluconeogenesis in their enterocytes. On HFD, both iCPT1mt and control mice developed DIO, but iCPT1mt mice showed improved glycemic control and reduced visceral fat mass.

**Conclusion:** Modulating enterocyte metabolism in iCPT1mt mice affects glycemic control in a body weight-independent, but dietary fat-dependent manner.

### 3.1 INTRODUCTION

Obesity and its related comorbidities, such as type-2-diabetes (T2D), hypertension, and cardiovascular disease, are major global health concerns [1]. With a rise in the consumption of western diets, and with decreasing physical activity, the incidence of obesity is increasing dramatically world over. Currently, the only treatments for morbid obesity that lead to sustained weight loss are invasive and costly interventions such as gastric bypass surgery [2]. The success of these surgical procedures comes with several unresolved side effects, including malabsorption of essential micronutrients and early or late post-surgical complications [2]. Interestingly, one of the consistent benefits of bariatric surgery is improved glycemic control based on a reversal of insulin resistance (IR). These improvements are seen even before any noticeable weight loss [3]. Results from gastric bypass rodent models as well as human patients suggest that these almost immediate improvements are due to functional and/or morphological changes in the small intestine [4, 5].

Previous pharmacological studies in rodents implicated enhanced fatty acid oxidation (FAO) in the small intestine in the control of eating, which might then also prevent weight gain and the development of DIO [6-8]. We recently reported evidence that a constitutive overexpression of the mitochondrial protein Sirtuin 3 (SIRT3) in mouse enterocytes was associated with enhanced FAO and ketogenesis and reduced fatty acid synthesis in these cells when the mice were fed a fat-rich diet [9]. Interestingly, constitutive enterocyte SIRT3 overexpression had no effect on daily food intake and did not protect the mice from developing diet-induced obesity (DIO), but did protect them from developing IR. SIRT3, however, is a post-translational regulator of several other pathways in addition to FAO, including reactive oxygen species (ROS) scavenging, the tri-carboxylic acid (TCA) cycle, urea cycle and ketogenesis [10].

To more specifically upregulate FAO in mouse enterocytes, we used the CPT1mt protein, a mutated form of the rat carnitine palmitoyltransferase-1a (CPT1a) enzyme that is insensitive to its endogenous inhibitor malonyl-CoA [11]. Several studies have used the CPT1mt protein *in vitro* as well as *in vivo* to enhance mitochondrial FAO flux in target cells or tissues [12-17]. We crossed the established transgenic mouse line with *loxP*-STOP-*loxP*-CPT1mt (Cpt1mt<sup>fl/fl</sup>) [17] with the Villin-Cre mouse line (Vil-Cre) [18] to generate mice with a homozygous expression of CPT1mt in the enterocytes (iCPT1mt). We isolated primary enterocytes from the duodenum and jejunum of these mice to test the metabolic flux of these cells. We fed iCPT1mt and Cpt1mt<sup>fl/fl</sup> mice a low-fat control diet (CD) or a high-fat diet (HFD) for several weeks, and phenotyped them to determine whether enterocyte CPT1mt expression could protect these mice from developing impaired glucose homeostasis, IR and DIO.

## 3.2 MATERIALS AND METHODS

### 3.2.1 Animals

Transgenic mice on the C57Bl6N background homozygous for the Cpt1mt construct, *loxP* - STOP cassette - *loxP* - Cpt1mt (Cptmt<sup>fl/fl</sup>) [17] were crossed with mice on a C57Bl6J background with hemizygous expression of Cre recombinase under the Villin promoter (VilCre<sup>+/-</sup>) [18] to generate mice hemizygous for both the Cpt1mt gene and the Villin-Cre gene (Cptmt<sup>fl/-</sup>/VilCre<sup>+/-</sup>). These mice were backcrossed with the parental line Cptm<sup>fl/fl</sup> to generate male mice homozygous for the Cpt1mt floxed cassette and hemizygous for Villin-Cre (Cptmt<sup>fl/fl</sup>/VilCre<sup>+/-</sup> or iCPT1mt) expressing CPT1mt specifically in the epithelial cells of the intestine. The Cptmt<sup>fl/fl</sup> male littermates

served as controls. All mice were genotyped immediately after weaning (at 3 to 4 weeks of age) and recaged in groups (2-4 mice/cage) such that only mice with the same genotype shared cages. All breedings were carried out in our in-house specified and opportunistic pathogen free (SOPF) facility. At 10 to 12 weeks of age, mice were moved into the experimental room with controlled temperature and humidity ( $22 \pm 1^\circ\text{C}$ ,  $55 \pm 5\%$ ) and a reversed 12 h/12 h dark/light cycle (lights off at 8 am). Animals had *ad libitum* access to food and water unless otherwise specified. The Cantonal Veterinary Office of Zurich approved all animal experiments.

### 3.2.2 Diet

Mice in the SOPF breeding facility were fed autoclaved chow diet (#3807, Kliba). After 1-2 weeks of adaptation to experimental room conditions, all experimental mice were fed either standard chow (#3430, Kliba), refined control diet (CD, #S9213-E001, 10% of energy from fat) or high-fat diet (HFD, # E15742-34, 60% of energy from fat) from ssniff Spezialdiäten GmbH.

### 3.2.3 Body weight measurements

Body weights of mice fed CD and HFD were monitored regularly in the dark phase as indicated in Figure 2 using a generic weighing scale.

### 3.2.4 Insulin sensitivity test (IST)

Mice were fasted for 5-6 h in the middle of the dark phase with *ad libitum* access to water. Actrapid HM human insulin (Novo Nordisk) was injected intraperitoneally (IP), and tail blood glucose was monitored at the indicated time points using the Accu-Chek Aviva blood glucose monitor (Roche). Insulin dose: 0.4 mU/g body weight (CD) and 0.8 mU/g body weight (HFD) [19].

### **3.2.5 Oral glucose tolerance test (OGTT)**

After a 6 h fast from dark phase onset with *ad libitum* access to water [20] mice received a 20% glucose solution by gavage (solvent: water, glucose dose: 2 g/kg body weight). Tail blood glucose was monitored at the time points indicated.

### **3.2.6 Intraperitoneal glucose tolerance test (IPGTT)**

After a 6 h fast from dark phase onset with *ad libitum* access to water [20] mice were injected IP with a 20% glucose solution (solvent: 0.9% saline, glucose dose: 2 g/kg body weight). Tail blood glucose was monitored at the time points indicated.

### **3.2.7 Body composition**

Mice were scanned under isoflurane anesthesia using a high-resolution micro computed tomography (CT) scanner (La Theta LCT-100; Hitachi-Aloka Medical Ltd), to determine body composition and fat distribution.

### **3.2.8 Indirect calorimetry**

Measurements were carried out using the Phenomaster/Labmaster metabolic cages (TSE systems). Mice were adapted to single housing in cages similar to the Phenomaster cages for at least one week prior to measurements. Data displayed were collected after additional 2 days of habituation in the system.

### **3.2.9 Animal sacrifice and tissue collection**

Mice were food deprived for 2 h prior to sacrifice unless specified otherwise. All animals were sacrificed in the dark phase by decapitation, and trunk blood was collected in tubes containing 0.5 M EDTA. The blood samples were centrifuged at 8,700 g for 10 min at 4°C, and plasma was collected and stored at -80°C until required. The intestine and liver were dissected out. Intestinal samples were further processed

as described below, and the liver was flash frozen in liquid nitrogen and stored at -80°C until required. Enterocytes were isolated using a modified protocol described earlier [9, 21] using 12.5mL dritrip maxi syringes (#F164120, Gilson) and ice-cold Cell Recovery solution (#354253, Corning). The cells were scraped into ice cold PBS, pelleted and pellets were snap frozen in liquid nitrogen and stored at -80°C until required.

### **3.2.9.1 Primary enterocyte FAO assay**

Fifteen to 20-week-old iCPT1mt and CPT1mt<sup>fl/fl</sup> mice were fasted overnight. Enterocytes were isolated as described above and scraped into ice cold petri dishes containing DMEM (# A1443001, Gibco, ThermoFisher) supplemented with 100 U/mL penicillin and streptomycin (pen-strep), 1X N-2 supplement, 1X B-27 supplement, 10 µM Y-27632 and 2 µM N-acetyl cysteine (NAC) and phenol red (basal medium). These cells were then transferred to a 50 mL tube and centrifuged at 500 g for 6 min at room temperature. The cell pellet was resuspended in pre-warmed 0.25 % trypsin-EDTA and incubated in a 37°C, 5% CO<sub>2</sub> incubator for 7 min. An equal volume of soybean trypsin inhibitor (# T6414, SIGMA) containing 20 µM Y-27632 was then added to neutralize trypsin activity. The cells were filtered successively through 100 µ and 40 µ filters. The filtrate was kept on ice, the cells were counted, and an appropriate number of cells was collected in a 2 mL Eppendorf tube, centrifuged at 500 g for 5 min and the resulting pellet was resuspended in ice cold basal medium. An equal volume of ice cold growth factor reduced Matrigel (#354230, Corning) diluted 1:2 in the same medium (to an effective concentration of approximately 5 mg/mL) was added to these cells so that the final concentration of matrigel in the cell suspension was 1:4 (2.5 mg/mL). 250000 (250K) cells were plated per well in 40 µL of 1:4 matrigel in a regular 96 well cell culture plate. The plate was incubated on ice for 20 min for the cells to settle down through

the viscous matrigel, then transferred to a 37°C, 5% CO<sub>2</sub> incubator for 20 min for the matrigel to solidify. Basal medium was further supplemented with 1.2X glucose, L-carnitine, fatty acid free BSA, cold palmitic acid and hot (<sup>3</sup>H-9,10)-palmitic acid, now termed as FAO assay medium. Prewarmed FAO assay medium was added to each well (210 µL medium per well) such that each well now had a total volume of 250 µL of medium with a final (1X) concentration of 2.5 mM glucose, 500 µM L-carnitine, 50 µM fatty acid free BSA, 100 µM cold palmitic acid and 2 µCi/ml of hot (<sup>3</sup>H-9,10)-palmitic acid. The cells were incubated for 5 h in a 37°C, 5% CO<sub>2</sub> incubator. Subsequently, 200 µL of medium from each well was transferred into a glass vial and 50 µL of 3 M perchloric acid was added to each vial to stop any metabolic activity. Each vial was closed with a rubber stopper equipped with a hanging well containing a filter paper (1 x 6 cm; #3030-931, Whatman) soaked in 200 µL of water, and then the vials were incubated for 48 h at 37°C. The filter paper was then carefully transferred into a scintillation vial containing 5 mL of Ultima Gold scintillation fluid (# 6013329, Perkin Elmer) along with 100 µL of water used to wash any condensation in the hanging well. The disintegrations per minute were recorded using the 2000CA liquid scintillation analyzer (Tri-Carb). The FAO assay medium containing cold plus hot palmitic acid was used to generate a standard curve using which the FAO flux was calculated from the disintegrations per minute for each sample. Enterocytes from 3 animals were pooled for each genotype (biological replicates) and the n values in the figure legend (Fig 2A) refer to technical replicates.

### **3.2.9.2 Primary enterocyte extracellular flux analysis**

Primary enterocytes were subjected to metabolic flux analysis using the extracellular flux analyzer XFe96 (Agilent Seahorse XF technology) subsequently referred to as the “seahorse”. Enterocytes, from 15- to 20-week old iCPT1mt and

CPT1mt<sup>fl/fl</sup> mice fasted overnight, were isolated as described above and scraped into a petri dish containing DMEM (# A1443001, Gibco, ThermoFisher) supplemented with 5 mM glucose, 100 U/mL pen-strep, 1X glutamax, 1X sodium pyruvate, 1X N-2 supplement, 1X B-27 supplement, 10  $\mu$ M Y-27632 (ROCK inhibitor) and 2  $\mu$ M NAC. The dissociated and filtered cells were counted, centrifuged at 500 g for 6 min and an appropriate number of cells were resuspended in Krebs-Henseleit Buffer (KHB) containing 111 mM NaCl, 4.7 mM KCl, 1.25 mM CaCl<sub>2</sub>, 2 mM MgSO<sub>4</sub>, 1.2 mM NaH<sub>2</sub>PO<sub>4</sub> supplemented with 100 U/mL pen-strep, 1X N-2 supplement, 1X B-27 supplement, 10  $\mu$ M Y27632 and 2  $\mu$ M NAC, pH 7.4) further referred to as experimental medium. The cells were plated into the 96 well seahorse cell plate kept on ice so that each well was seeded with 250K cells in a volume of 20  $\mu$ L of 1:4 matrigel diluted in experimental medium. The plate was incubated on ice for 20 min and in a 37°C, 5% CO<sub>2</sub> incubator for 20 min. Pre-warmed experimental medium (160  $\mu$ L) was then added to each well. The cells were incubated in a CO<sub>2</sub> free incubator at 37°C for 30 min while the machine was calibrated. Basal oxygen consumption rate (OCR) and extracellular acidification rate (ECAR) were measured by the seahorse analyzer followed by the mitochondrial stress test using appropriate concentrations (see figure legends of Fig 2 and Fig 2-Sup1) of the respiratory poisons Oligomycin (Oligo), Carbonyl cyanide-4-phenylhydrazone (FCCP), Antimycin and Rotenone (Anti+Rot) as indicated. It should be noted that some wells showed a leak from one or more of the B, C or D ports of the cartridge due to capillary action initiated by the medium from the wells touching the ports of the cartridge during the mixing process. We believe that this occurred due to the consistency and thickness of the volume of matrigel in the measurement chamber. These wells were easily identifiable by their decrease in OCR due to oligo or Anti+Rot leak or an increase in OCR due to an FCCP leak even when no compounds were injected into the ports. These wells were eliminated from the analysis. Basal OCR,



changes in OCR after oligo or FCCP injections, glycolysis, glycolytic capacity and glycolytic reserve were calculated using the averages of the three measurements made before or after the appropriate compound injection as described earlier [22] as well as in the manufacturer's protocol. In brief, glycolytic flux refers to the difference between the mean of measurements after glucose injection and baseline values. Glycolytic capacity refers to the difference between the mean measurements after oligo injection and baseline values and glycolytic reserve refers to the difference between the mean measurements after oligo injection and after glucose injection. Each well represented a biological replicate of 1, while the n values in the figure legend (Fig 2B and Sup Fig1) refer to technical replicates. Fig 2B to E and Sup Fig1A represent values from two independent experiments pooled together.

### **3.2.10 Western blotting**

Tissue samples were processed for western blotting as described earlier [16]. Briefly, the samples were lysed in RIPA buffer, protein concentrations estimated and denatured in Laemmli buffer containing DTT. Equal amounts of protein samples were run in SDS-PAGE gels and blotted onto PVDF membranes and probed using primary antibodies for CPT1a [23], HMGCS2 (# sc-33828, Santa Cruz Biotechnology) and  $\beta$ -actin (# A2228, Sigma) and the appropriate HRP-linked secondary antibody. The blots were developed using an in-house chemiluminescence-based detection kit and analyzed using the ImageQuant LAS 4000 mini (GE Health Care).

### **3.2.11 Histology - H&E stain**

Two cm pieces of the duodenum and jejunum, and 1 cm<sup>3</sup> liver samples were collected and processed for paraffin embedding and H&E staining as described earlier [9].

### 3.2.12 RT-qPCR analysis

RNA was extracted from tissue samples using the Trizol reagent (#15596018, Life Technologies) following the manufacturer's protocol and treated with DNase (#79254, Quiagen). cDNA was synthesized using the High-Capacity cDNA Reverse Transcription Kit (#4368813, Applied Biosystems) and used for real time quantitative PCR (RT-qPCR) reactions using FAST SYBR green and the Vii7 Real Time PCR system (Applied Biosystems). Each sample was run in triplicate and the best duplicates or triplicates were analyzed using the  $2^{-\Delta\Delta C_T}$  method [24] with Ppib as the reference gene [25]. Primers used are listed in Table 1.

### 3.2.13. Statistical analysis

All data were analyzed using GraphPad Prism (version 7.0.2) or IBM SPSS statistics (version 23). Outliers were identified using the Grubb's test and removed. Data normality was verified using the Shapiro-Wilk test (when  $n \geq 7$ ) and Kolmogorov-Smirnov test (when  $5 \leq n \leq 6$ ). Parametric data was analyzed using an unpaired Student's t-test (two-tailed) or 2 X 2 factorial parametric analysis of variance followed by Sidak's multiple comparison *post hoc* test whenever appropriate or a mixed repeated measures ANOVA followed by a simple effects analysis in the case of a significant interaction or a univariate ANCOVA. The nonparametric test (Mann-Whitney) was used when the data did not meet the criteria of normal distribution. Statistical tests used and *P*-values are mentioned in the figure legends. *P*-values less than 0.05 were considered significant.

**TABLE 1: Primers for RTqPCR analyses.**

Gene name	Primers
Long chain acyl-CoA dehydrogenase ( <i>Lcad</i> )	f: 5' gtctggactccggttctgc 3' r: 5' ccgtggagttgcacacatt 3'
3-Hydroxy-3-methylglutaryl-CoA synthase 2 ( <i>Hmgcs2</i> )	f: 5' agataccaccaacgcctgtt 3' r: 5' aatgtcaccacagaccacca 3'
Peroxisome proliferative activated receptor gamma, coactivator 1 alpha ( <i>Pgc1a</i> )	f: 5' ttctcgacacaggtcgtgtt 3' r: 5' gtgtgcggtgtctgtagtgg 3'
Transcription factor A, mitochondrial ( <i>Tfam</i> )	f: 5' aaggatgattcggctcagg 3' r: 5' ggcttgagacctaactgg 3'
Hexokinase 1 ( <i>Hk1</i> )	f: 5' tgtgggtcacgatgtagcc 3' r: 5' ccacatccaggtaaattcc 3'
Sodium-dependent glucose co-transporter ( <i>Sglt1</i> )	f: 5' aagagcgaatcgacctgga 3' r: 5' gaagcatcctttcttcttctgg 3'
Fatty acid translocase ( <i>Fat/cd36</i> )	f: 5' tgaaaagtctcggacattgag 3' r: 5' tcagatccgaacacagcgta 3'
Fatty acid binding protein 1, liver ( <i>Fabp1</i> )	f: 5' aagtggtccgcaatgagttc 3' r: 5' ctccagcttgacgactgc 3'
Fatty acid binding protein 2, intestinal ( <i>Fabp2</i> )	f: 5' acggaacggagctcactg 3' r: 5' ttaccagaaacctctcggaca 3'

Gene name	Primers
Fatty acid synthase ( <i>Fasn</i> )	f: 5' gctgctgttgaagtcagc 3' r: 5' agtgctcgttcctcggagtg 3'
Acetyl-CoA carboxylase alpha ( <i>Acaca</i> or <i>Acc1</i> )	f: 5' cctgaagaccttaaagccaatgc 3' r: 5' ccagcccacactgcttgta 3'
Acetyl-Coenzyme A carboxylase beta ( <i>Acacb</i> or <i>Acc2</i> )	f: 5' gattcccagttgggcact 3' r: 5' cctcaaagccactaccatgt 3'
Phosphoenolpyruvate carboxykinase 1 ( <i>Pepck1</i> )	f: 5' ggagtaccattgagggtatcat 3' r: 5' gctgagggtctcatagacaag 3'
Peptidylprolyl Isomerase B ( <i>Ppib</i> )	f: 5' ttctcataaccacagtcaagacc 3' r: 5' accttccgtaccacatccat-3'

### 3.3 RESULTS

#### 3.3.1 iCPT1mt mice show increased CPT1a expression in the intestine, but not in the liver.

Western blot analysis of tissue samples from *Cpt1mt<sup>fl/fl</sup>* and iCPT1mt mice fed CD and HFD indicated that the CPT1mt protein was expressed in the enterocytes of the duodenum and jejunum, but not in the liver of iCPT1mt mice ( $P < 0.0001$  for CD duodenum and jejunum;  $P < 0.05$  for HFD duodenum and jejunum) (Fig 1A and B).

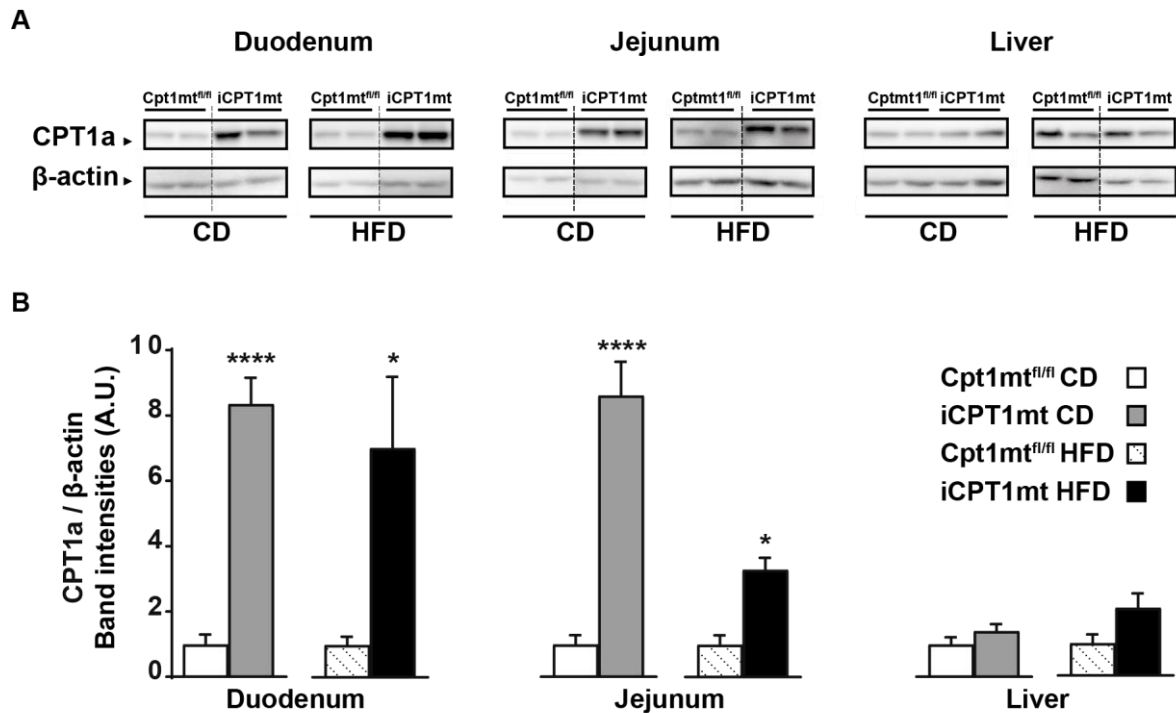


**Figure 1: iCPT1mt mice show increased CPT1a expression in the intestine, but not in the liver.**

Western blot analysis for Carnitine palmitoyltransferase 1, liver isoform (CPT1a) and  $\beta$ -actin protein expression from tissue samples of *Cpt1mt<sup>fl/fl</sup>* and *iCPT1mt* mice fed control diet (CD) or high-fat diet (HFD) as indicated for 20 weeks. (A) Representative pictures of western blot bands from the duodenum, jejunum and liver. The dotted line separates discontinuous lanes from the same gel. (B) Quantification of band intensities. (n = 4 to 5, Unpaired t test; \* $P < 0.05$  and \*\*\*\* $P < 0.0001$  for Duodenum CD and HFD, Jejunum CD and Liver CD and HFD; Mann-Whitney test; \* $P < 0.05$  for Jejunum HFD). Data are presented as mean values  $\pm$  SEM.

### 3.3.2 Primary enterocytes from *iCPT1mt* mice have a higher rate of FAO, mitochondrial respiration and glycolysis than *Cpt1mt<sup>fl/fl</sup>* control mice.

Primary enterocytes isolated from *iCPT1mt* mice fed standard chow showed an increased flux of palmitate oxidation in the duodenum and jejunum compared to *Cpt1mt<sup>fl/fl</sup>* mice ( $P < 0.05$ ) (Fig 2A). When fed HFD for 3 days, primary enterocytes from the duodenum of *iCPT1mt* mice showed a lower rate of palmitate oxidation compared to *Cpt1mt<sup>fl/fl</sup>* mice ( $P < 0.001$ ), but the enterocytes from the jejunum of *iCPT1mt* mice showed an enhanced palmitate oxidation rate compared to controls ( $P < 0.0001$ ) (Fig 2A). In a mitochondrial stress test with the seahorse analyzer, primary enterocytes isolated from the duodenum and jejunum of *iCPT1mt* mice fed standard chow showed an increased basal respiration ( $P < 0.0001$ ) (Fig 2B and C) and an increased sensitivity

to ATP synthase inhibition by oligomycin ( $P < 0.001$ ) (Fig 2B and D) compared to primary enterocytes from Cpt1mt<sup>fl/fl</sup> mice. Enterocytes from iCPT1mt mice also showed an increased maximal respiration in response to the uncoupler carbonyl cyanide-4-(trifluoromethoxy)-phenylhydrazone (FCCP) compared to controls ( $P < 0.0001$ ) (Fig 2B and E). The basal extracellular acidification rate (ECAR) of enterocytes from these chow-fed iCPT1mt mice was also higher than that of cells from Cpt1mt<sup>fl/fl</sup> controls ( $P < 0.0001$ ) (Fig 2-Sup1A and B) as well as after the addition of oligomycin ( $P < 0.01$ ) (Fig 2-Sup 1A and B). The addition of 2-deoxyglucose (2-DG), the competitive inhibitor of the enzyme hexokinase (Hk1), abrogated the increased maximal respiration as well as the increase in ECAR seen after the addition of glucose, oligomycin and FCCP in these cells. This indicates that enterocytes from iCPT1mt mice fed standard chow diet have an increased rate of glycolysis ( $P < 0.05$ ) and glycolytic reserve ( $P < 0.05$ ) with no difference in the glycolytic capacity (Fig 2-Sup1C and D).

### **3.3.3 Intestinal CPT1mt expression reduces visceral fat with HFD feeding without affecting body weight gain.**

HFD feeding increased body weight (significant after 1 week,  $P < 0.0001$ ), lean body mass ( $P < 0.0001$ ) and subcutaneous fat mass ( $P < 0.0001$ ) (microcomputed tomography (CT) measurement after 19 weeks on the diets) compared to CD feeding in all mice irrespective of genotype (Fig 3A and B). Total fat mass and visceral fat mass showed an interaction effect ( $P < 0.05$ , diet x genotype for both) such that iCPT1mt mice had less visceral fat than Cpt1mt<sup>fl/fl</sup> mice when fed HFD for 19 weeks ( $P < 0.05$ ) (Fig 3B).

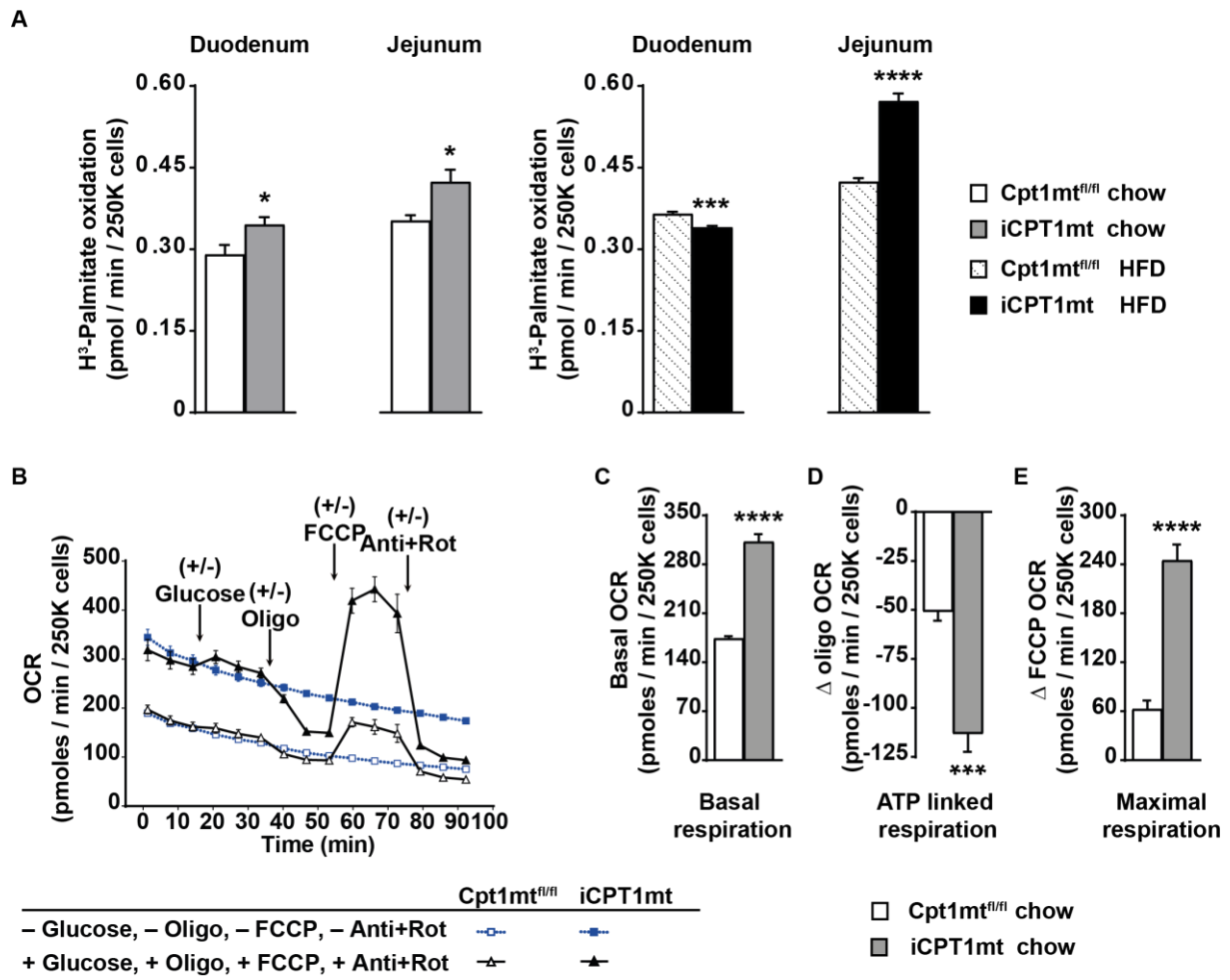


**Figure 2: Primary enterocytes from iCPT1mt mice have a higher rate of FAO, mitochondrial respiration and glycolysis than Cpt1mt<sup>fl/fl</sup> control mice.**

(A) Rate of oxidation of H<sup>3</sup>-Palmitic acid by of 250000 (250K) primary enterocytes isolated from the duodenum or jejunum of Cpt1mt<sup>fl/fl</sup> and iCPT1mt mice. Left two bars: Mice fed standard chow. Right two bars: Mice fed HFD for 3 days (n = 5-6, Unpaired t test, \*P < 0.05, \*\*\*P < 0.001, \*\*\*\*P < 0.0001). (B) Oxygen consumption rate (OCR) of primary enterocytes per well, isolated from the (duodenum + jejunum) of Cpt1mt<sup>fl/fl</sup> and iCPT1mt mice, incubated in KHB medium and subsequently injected with KHB medium or with an effective concentration of 5mM glucose, 10 µg/mL Oligomycin (Oligo), 8 µmol/L FCCP and 5 µg/mL antimycin + 3.75 µmol/L rotenone (Anti+Rot). (C) Basal OCR of cells in B before the addition of glucose with values for the same genotype pooled (n = 18-19, Mann Whitney test, \*\*\*\*P < 0.0001). (D and E) The change in OCR (Δ OCR) in B induced by (D) oligo and (E) FCCP (n = 5-6, Unpaired t test, \*\*\*P < 0.001, \*\*\*\*P < 0.0001). Data are presented as mean values ± SEM.

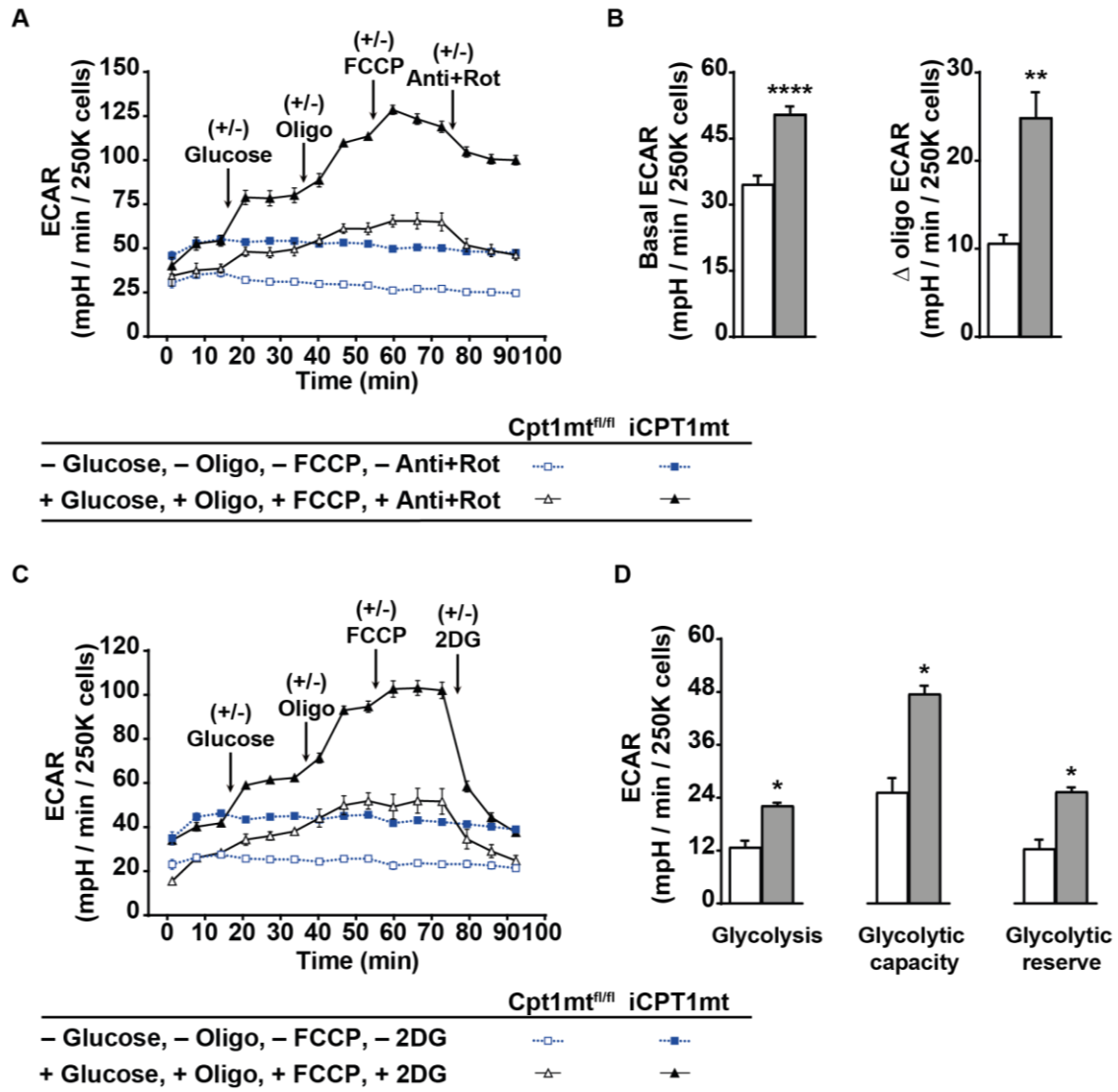


**Figure 2-Supplement 1: Primary enterocytes from iCPT1mt mice fed standard chow show increased glycolysis and glycolytic reserve compared to Cpt1mt<sup>fl/fl</sup> control mice.**

(A) Extra cellular acidification rate (ECAR) of 250000 (250K) primary enterocytes per well, isolated from the small intestine (duodenum + jejunum) of Cpt1mt<sup>fl/fl</sup> and iCPT1mt mice, incubated in KHB medium and subsequently injected with KHB medium (squares) or with an effective concentration of 5mM glucose, 10  $\mu$ g/mL Oligomycin (Oligo), 8  $\mu$ mol/L FCCP and 5  $\mu$ g/mL antimycin + 3.75  $\mu$ mol/L rotenone (Anti+Rot) (triangles). (B) Left: Basal ECAR of cells in (A) before the addition of glucose with values for the same genotype pooled (n = 18-19). Right: The change in ECAR ( $\Delta$  ECAR) in (A) induced by oligo (n = 5-6). (C) Extra cellular acidification rate (ECAR) of 250K primary enterocytes isolated from the small intestine (duodenum + jejunum) of Cpt1mt<sup>fl/fl</sup> and iCPT1mt mice incubated in KHB medium and subsequently injected with KHB medium (squares) or with an effective concentration of 5mM glucose, 10  $\mu$ g/mL Oligomycin (Oligo), 8  $\mu$ mol/L FCCP and 100mM 2-deoxyglucose (2-DG) (triangles). (D) Glycolysis, glycolytic capacity and glycolytic reserve calculated from the values in (C) (n = 3-5). (B) Unpaired t test and (D) Mann-Whitney test. \* $P$  < 0.05, \*\* $P$  < 0.01, \*\*\*\* $P$  < 0.0001. Data are presented as mean values  $\pm$  SEM.



A morphological analysis of the small intestine of iCPT1mt and Cpt1mt<sup>fl/fl</sup> mice fed CD or HFD revealed an interaction effect in the villi lengths of their duodenum ( $P < 0.05$ , diet x genotype), such that iCPT1mt mice on CD had longer duodenal villi compared to Cpt1mt<sup>fl/fl</sup> mice ( $P < 0.05$ ) (Fig 3C and D). HFD feeding led to an increase in the length of villi in the jejunum of all mice ( $P < 0.01$ ) compared to CD feeding, with no genotype effects (Fig 3C and D). The livers of these mice showed no genotype differences, but all mice on HFD, irrespective of genotype, showed markers of hepatic steatosis compared to CD fed mice (Fig 3C).

### **3.3.4 iCPT1mt mice and Cpt1mt<sup>fl/fl</sup> control mice show similar energy intake and whole body energy metabolism when fed CD and when switched to HFD.**

Both iCPT1mt and Cpt1mt<sup>fl/fl</sup> mice showed a similar decrease in the respiratory exchange ratio (RER) ( $P < 0.0001$ ) when switched from CD to HFD feeding (Fig 4A). No differences were observed in daily energy intake (Fig 4B), energy expenditure (Fig 4C) or locomotor activity (Fig 4D) between the genotypes or on either of the two diets.

### **3.3.5 Intestinal CPT1mt expression compromises glycemic control on the CD, but improves it over time on HFD.**

An insulin sensitivity test (IST) on iCPT1mt and Cpt1mt<sup>fl/fl</sup> control mice fed CD or HFD for 12 weeks did not reveal any differences between the two genotypes (Fig 5A). Both HFD-fed iCPT1mt and Cpt1mt<sup>fl/fl</sup> mice had developed IR as indicated by the increased baseline glucose levels (Fig 5B). An oral glucose tolerance test (OGTT) after 13 weeks on the diets revealed that iCPT1mt mice on CD had impaired glucose clearance compared to Cpt1mt<sup>fl/fl</sup> control mice ( $P < 0.01$ , time x genotype) (Fig 5C).

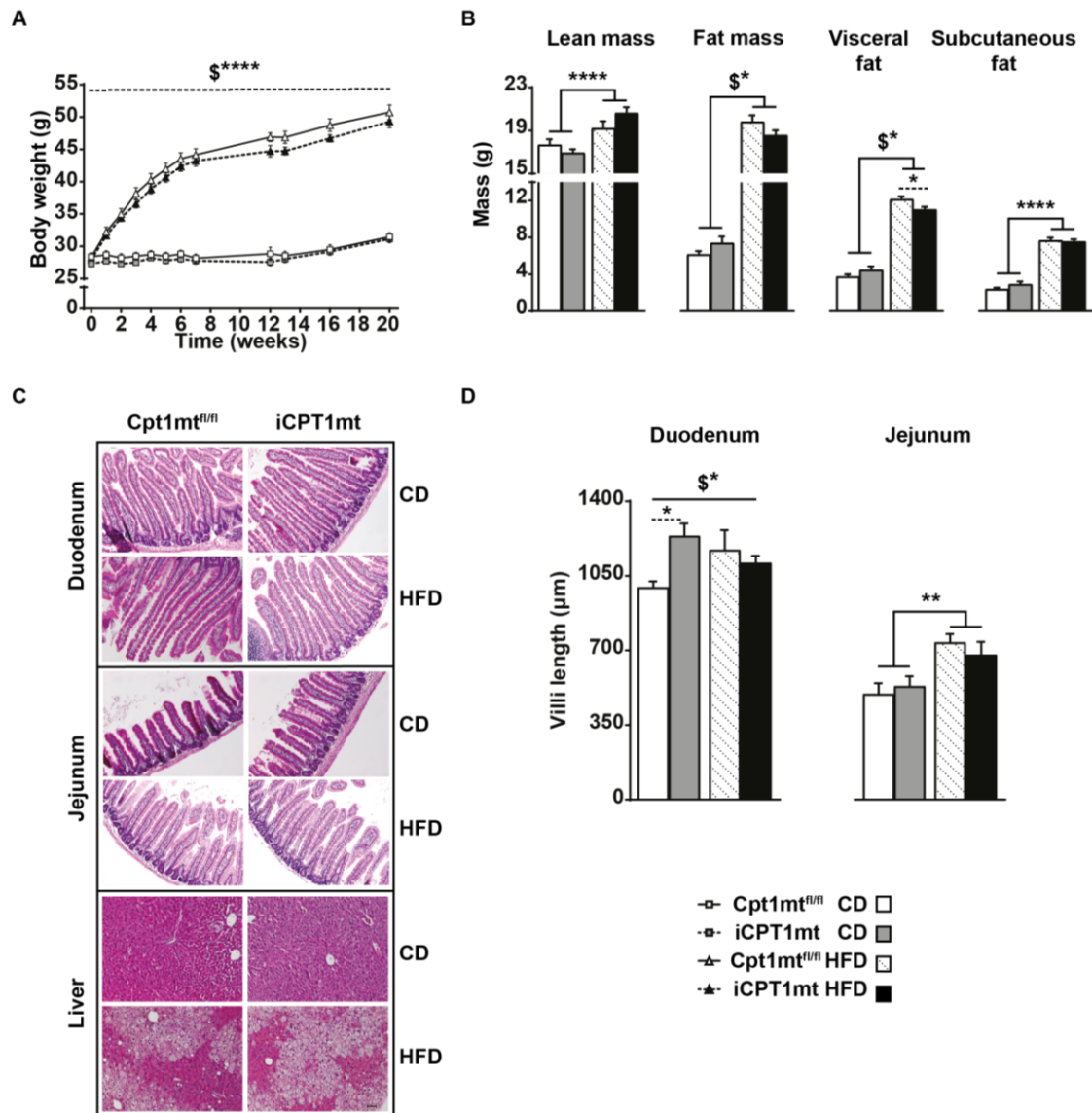


**Figure 3: Intestinal CPT1mt expression reduces visceral fat with HFD feeding without affecting body weight gain.**

(A) Body weights of Cpt1mt<sup>fl/fl</sup> and iCPT1mt mice on CD or HFD monitored over time (n = 11-17; Mixed-repeated measures (RM) ANOVA (time x diet x genotype), \*\*\*\*P < 0.0001 for interaction effects of diet x genotype (\$)). (B) CT scan analyses of Cpt1mt<sup>fl/fl</sup> and iCPT1mt mice fed CD or HFD for 19 weeks (n = 5-10; 2 x 2 factorial ANOVA (diet x genotype). \*P < 0.05, \*\*\*\*P < 0.0001 for main effect of diet and *post hoc* tests (dashed lines) and interaction effects of diet x genotype (\$)). (C) Representative bright field microscopy images of H&E stained duodenum, jejunum and liver sections of Cpt1mt<sup>fl/fl</sup> and iCPT1mt mice fed CD or HFD for 20 weeks at 20X magnification. (D) Measurements of the villi lengths of Cpt1mt<sup>fl/fl</sup> and iCPT1mt mice from H&E stained sections. Left: Duodenum, Right: Jejunum (n = 3-5; 2 x 2 factorial ANOVA (diet x genotype). \*P < 0.05, \*\*P < 0.01 for main effect of diet and *post hoc* tests (dashed lines) and interaction effects of diet x genotype (\$)). Data are presented as mean values ± SEM.

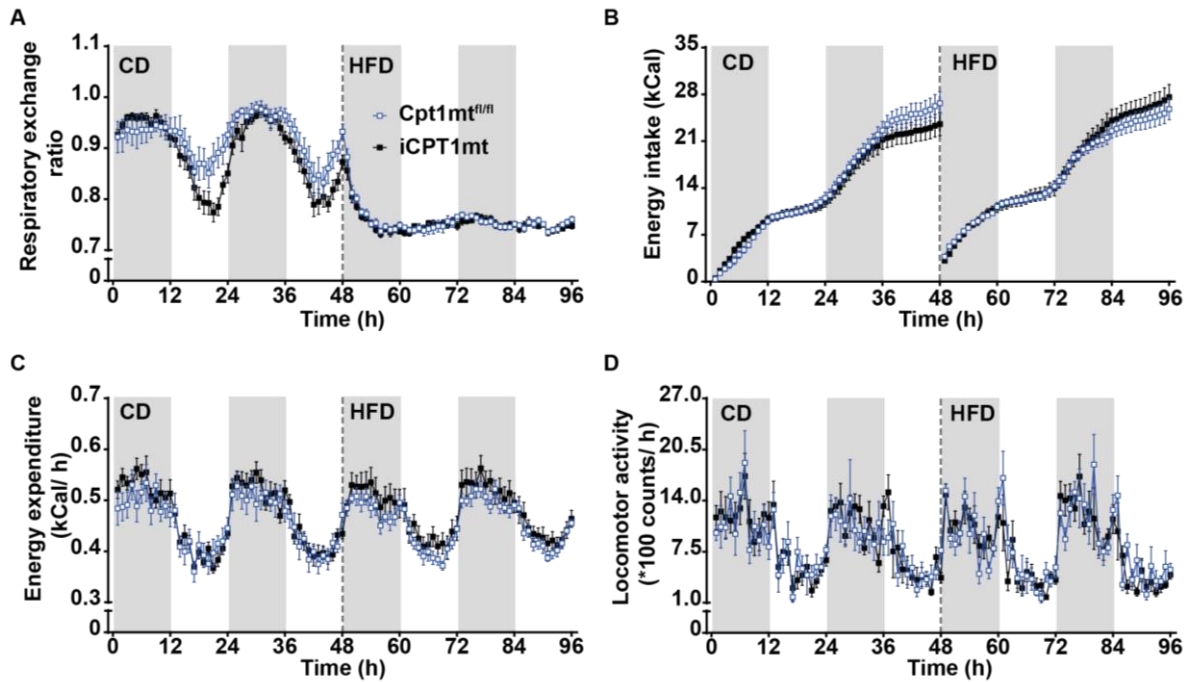


**Figure 4: iCPT1mt mice and Cpt1mt<sup>fl/fl</sup> control mice show similar energy intake and whole body energy metabolism when fed CD and when switched to HFD.**

(A-D) Indirect calorimetry data of Cpt1mt<sup>fl/fl</sup> and iCPT1mt mice on CD for 48 h and HFD for the next 48 h. The grey and white bars in the background represent the periods of dark and light phases respectively. The dashed lines indicate when the mice were switched from CD to HFD feeding. (A) Respiratory exchange ratio as mean values of 1 h bins. (B) Cumulative energy intake in 1 h bins. (C) Energy expenditure (EE) as mean values of 1 h bins. (D) Locomotor activity as mean values of 1 h bins. (n = 8-11, Mixed RM ANOVA (diet x time x genotype, repeated measures for time and diet for A, B and D; ANCOVA for mean values per day with BW as the covariate for C). Data are presented as mean values ± SEM.

A pairwise comparison at each time point showed that iCPT1mt mice had higher circulating glucose levels compared to Cpt1mt<sup>fl/fl</sup> mice, at every time point measured post glucose gavage (at t = 15 and 120 min,  $P < 0.05$ ; at t = 30,  $P < 0.0001$ ; at t = 60 and 90 min,  $P < 0.01$ ). With HFD feeding, iCPT1mt mice also showed impaired glucose tolerance compared to Cpt1mt<sup>fl/fl</sup> mice, though with a smaller difference between the two genotypes (Fig 5D, time x genotype,  $P < 0.05$ ), with iCPT1mt mice showing higher circulating glucose levels at 30 min ( $P < 0.01$ ) and 120 min ( $P < 0.05$ ) post glucose gavage.

After 16 weeks on the diets, mice fed CD continued to show a similar difference, with iCPT1mt mice exhibiting higher levels of circulating glucose in an intraperitoneal GTT (IPGTT) ( $P < 0.01$ , time x genotype) (Fig 5E), specifically at 30 ( $P < 0.05$ ) and 60

min ( $P < 0.01$ ) post IP glucose injection. HFD-fed iCPT1mt mice, however, showed a reversal of glucose tolerance in the IPGTT. iCPT1mt mice cleared the IP-injected glucose better than Cpt1mt<sup>fl/fl</sup> mice ( $P < 0.01$ , time x genotype) (Fig 5F), with lower glycemia at 30 ( $P < 0.05$ ), 60 ( $P < 0.01$ ), 90 ( $P < 0.01$ ) and 120 min ( $P < 0.01$ ) post glucose injection.

### **3.3.6 iCPT1mt mice have reduced circulating non-esterified fatty acid (NEFA) levels compared to Cpt1mt<sup>fl/fl</sup> control mice.**

An analysis of circulating post-prandial plasma metabolites after 20 weeks on CD or HFD revealed a main effect of diet such that all HFD-fed mice showed lower levels of circulating triacylglycerol (TAG) ( $P < 0.0001$ ),  $\beta$ -hydroxybutyrate (BHB) ( $P < 0.05$ ) and NEFA ( $P < 0.0001$ ) than mice on CD, with no genotype differences (Fig 6A to C). Plasma NEFA levels also showed a main effect of genotype ( $P < 0.05$ ), but the *post hoc* tests did not reveal a significant difference between the genotypes on either diet (Fig 6C). Plasma cholesterol as well as plasma glucose levels were higher in all HFD-fed mice than in CD-fed mice, irrespective of genotype ( $P < 0.0001$ ) (Fig 6D to E).

### **3.3.7 iCPT1mt mice on CD, but not on HFD, show an upregulation of fatty acid synthesis, glycolysis and gluconeogenic genes in jejunal enterocytes compared to Cpt1mt<sup>fl/fl</sup> mice.**

A gene expression analysis of the jejunal enterocytes of iCPT1mt and Cpt1mt<sup>fl/fl</sup> mice after 20 weeks on CD and HFD revealed increased expression of genes involved in fatty acid uptake (*Fat/cd36*) ( $P < 0.001$ ), fatty acid binding (*Fabp1*), FAO (*Lcad*), ketogenesis (*Hmgcs2*) ( $P < 0.0001$ ) and malonyl-CoA synthesis (*Acc2*) ( $P < 0.0001$ ) in all HFD-fed mice compared to CD-fed mice (Fig 7, Fig 7-Sup1 and Table 1).

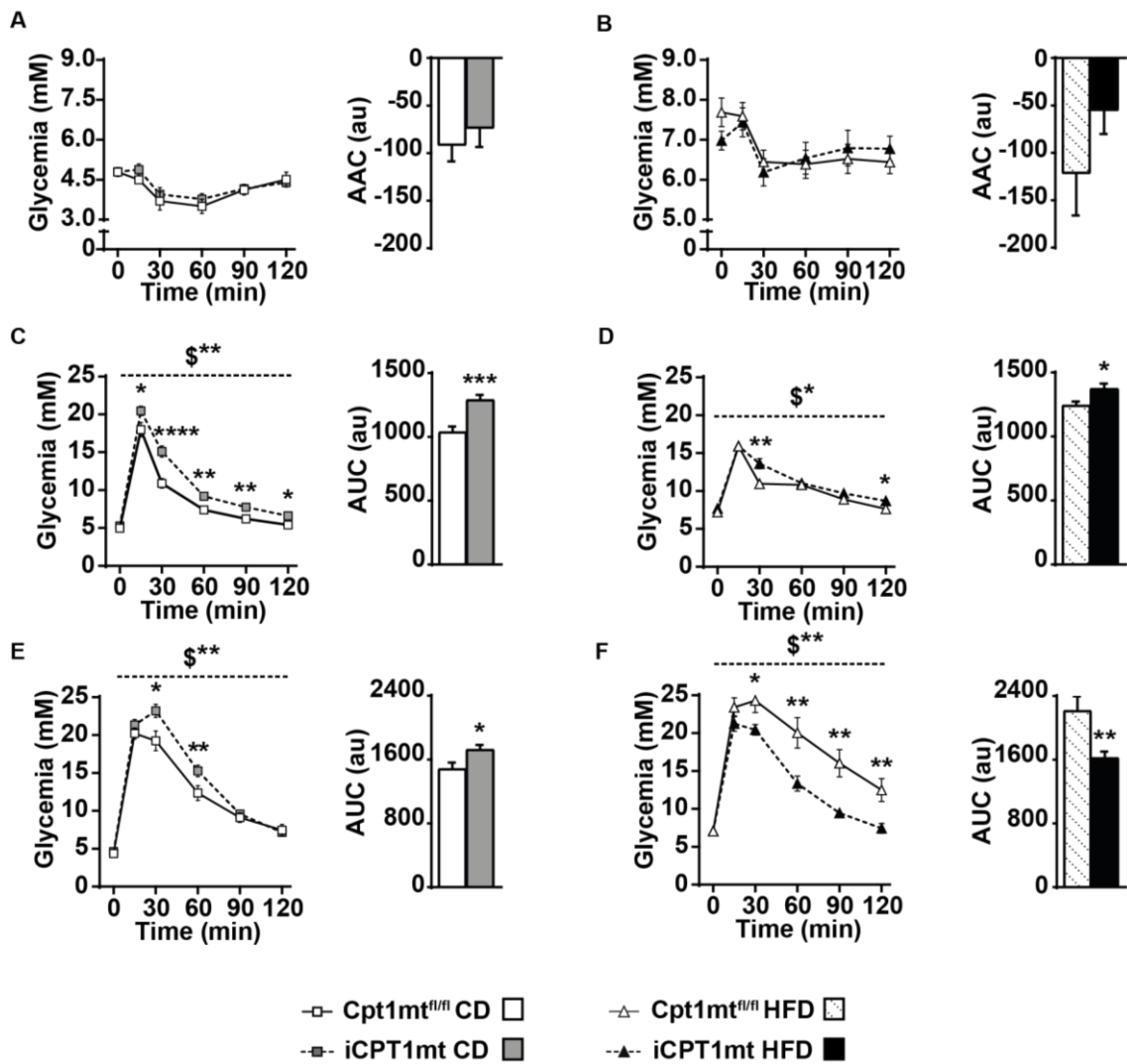


**Figure 5: Intestinal CPT1mt expression compromises glycemic control on the CD, but improves it over time on HFD.**

(A-B) Insulin sensitivity test (IST) for *Cpt1mt<sup>fl/fl</sup>* and *iCPT1mt* mice on CD and HFD, respectively. (A) Left: Tail blood glucose values for CD-fed mice at the time points indicated ( $n = 10-13$ ). (B) Left: Tail blood glucose values for HFD-fed mice at the time points indicated. Right: Area above the curve (AAC) for the data on the left ( $n = 16-17$ ). (C-D) Oral glucose tolerance test (OGTT) for *Cpt1mt<sup>fl/fl</sup>* and *iCPT1mt* on CD and HFD respectively. (C) Left: Tail blood glucose values for CD-fed mice at the time points indicated. Right: Area under the curve (AUC) for the data on the left ( $n = 11-15$ ). (D) Left: Tail blood glucose values for HFD-fed mice at the time points indicated. Right: Area under the curve (AUC) for the data on the left ( $n = 11-15$ ). (E-F) Intra-peritoneal glucose tolerance test (IPGTT) for *Cpt1mt<sup>fl/fl</sup>* and *iCPT1mt* on CD and HFD respectively. (E) Left: Tail blood glucose values for CD-fed mice at the time points indicated. Right: Area under the curve (AUC) for the data on the left ( $n = 11-15$ ). (F) Left: Tail blood glucose values for HFD-fed mice at the time points indicated. Right: Area under the curve (AUC) for the data on the left ( $n = 11-15$ ). (A-F) Mixed RM ANOVA (time  $\times$  genotype) with repeated measures for time for the line graphs and unpaired t test for the bar graphs. \* $P < 0.05$ , \*\* $P < 0.05$ , \*\*\* $P < 0.001$ , \*\*\*\* $P < 0.0001$  for main effect of genotype and simple effects analysis of genotype at each time point in the case of a significant interaction between time and genotype (\$).

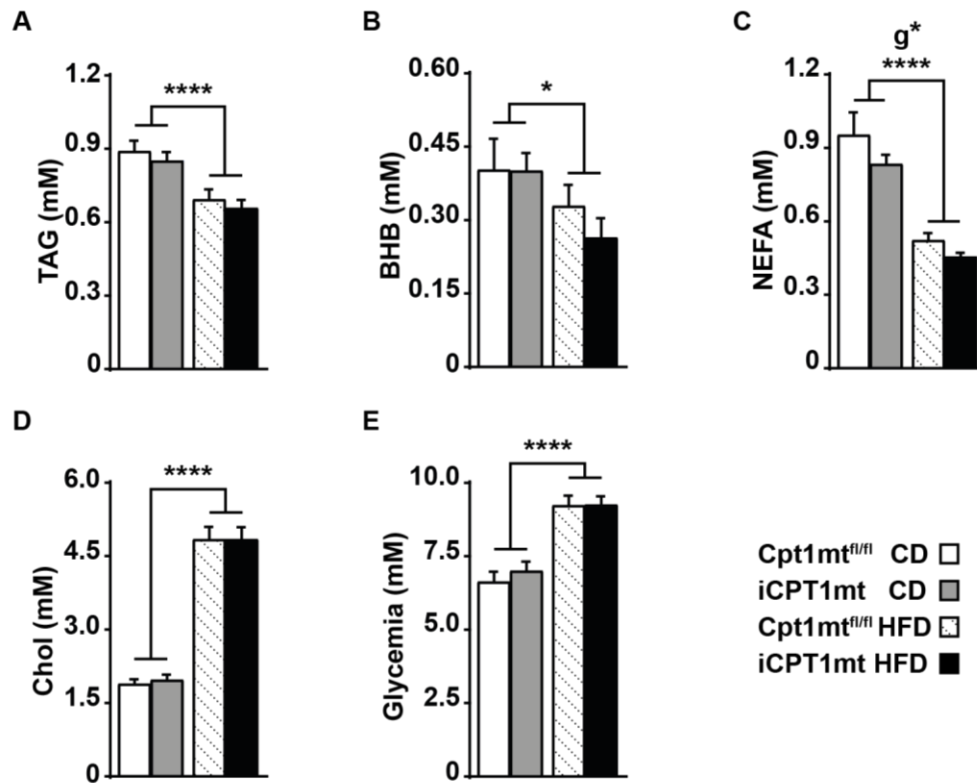


**Figure 6: iCPT1mt mice have reduced circulating non-esterified fatty acid (NEFA) levels compared to Cpt1mt<sup>fl/fl</sup> control mice.**

(A-E) Post prandial trunk blood plasma metabolite levels of Cpt1mt<sup>fl/fl</sup> and iCPT1mt mice on CD and HFD. (A) Triacylglycerol (TAG). (B)  $\beta$ -hydroxybutyrate (BHB). (C) Non-esterified fatty acids (NEFA). (D) Cholesterol (Chol). (E) Glucose. (A-E) n = 11-17, 2 x 2 factorial ANOVA (diet x genotype). \* $P < 0.05$ , \*\*\*\* $P < 0.0001$  for main effect of diet and genotype (g). Data are presented as mean values  $\pm$  SEM.

The genes involved in glucose absorption through the apical enterocyte membrane (*Sglt1*) ( $P < 0.0001$ ), glycolysis (*Hk1*) ( $P < 0.05$ ) and *de novo* fatty acid synthesis (*Acc1*) ( $P < 0.0001$ ) were downregulated in all HFD-fed mice compared to CD-fed mice (Fig 7 and Table 1). Genes involved in mitochondrial biogenesis were downregulated (*Pgc1a*) ( $P < 0.0001$ ), or remained unchanged (*Tfam*) in all HFD-fed mice. All iCPT1mt mice showed an upregulation of glycolysis (*Hk1*), fatty acid binding (*Fabp2*) ( $P < 0.05$ ), *de novo* fatty acid synthesis (*Fasn* ( $P < 0.01$ ) and *Acc1* ( $P < 0.001$ )) compared to Cpt1mt<sup>fl/fl</sup> mice, and *post hoc* tests revealed that these effects were significant on the CD ( $P < 0.05$  for *Hk1*, *Fabp2* and *Fasn*;  $P < 0.01$  for *Acc1*). The gluconeogenic gene phosphoenolpyruvate carboxykinase 1 (*Pepck1*) showed an interaction effect in the

jejunum ( $P < 0.01$ , diet x genotype) such that *Pepck1* was upregulated in the CD-fed iCPT1mt mice compared to *Cpt1mt<sup>fl/fl</sup>* mice ( $P < 0.05$ ), whereas there was no difference between the genotypes when fed HFD (Fig 7, Fig 7-Sup1 and Table 1).

The duodenal enterocytes of all HFD-fed mice showed increased expression of *Lcad*, *Hmgcs2*, *Fat/cd36*, *Fabp1*, *Fabp2*, *Acc2* ( $P < 0.0001$ ) and *Fasn* ( $P < 0.05$ ) and reduced expression of *Pgc1a* ( $P < 0.0001$ ) compared to CD-fed mice (Fig 7-Sup1). The expressions of *Pgc1a* ( $P < 0.05$ ) and *Acc2* ( $P < 0.01$ ) were further downregulated in all iCPT1mt mice compared to *Cpt1mt<sup>fl/fl</sup>* controls, and a *post hoc* test showed that this effect was significant for *Pgc1a* in iCPT1mt mice fed CD ( $P < 0.05$ ) and for *Acc2* in iCPT1mt mice fed HFD ( $P < 0.01$ ) (Fig 7-Sup1). *Acc1* showed a genotype effect ( $P < 0.05$ ), but the *post hoc* comparisons were not significant when compared within each diet (Fig 7-Sup1). Expression of *Sglt1* showed an interaction effect ( $P < 0.01$ , diet x genotype) with its levels specifically upregulated in iCPT1mt mice fed CD ( $P < 0.01$ ) (Fig 7-Sup1).

The livers of iCPT1mt and *Cpt1mt<sup>fl/fl</sup>* mainly showed an upregulation of all the genes tested in HFD-fed mice, compared to those fed CD ( $P < 0.05$  for *Hmgcs2*,  $P < 0.01$  for *Fasn* and  $P < 0.0001$  for the other genes), except for *Pgc1a* and *Pepck1*, which showed no differences between the genotypes or diets (Fig 7-Sup2).

A western blot analysis of these tissue samples showed that protein level of the ketogenic marker HMGCS2 was downregulated in the duodenal and jejunal enterocytes but not in the liver of iCPT1mt mice on CD ( $P < 0.01$  for duodenum,  $P < 0.05$  for jejunum). HMGCS2 protein level was also downregulated in the jejunal enterocytes ( $P < 0.05$ ), but not in the duodenal enterocytes or in the liver, of HFD-fed iCPT1mt mice compared to *Cpt1mt<sup>fl/fl</sup>* controls (Fig 7-Sup3).

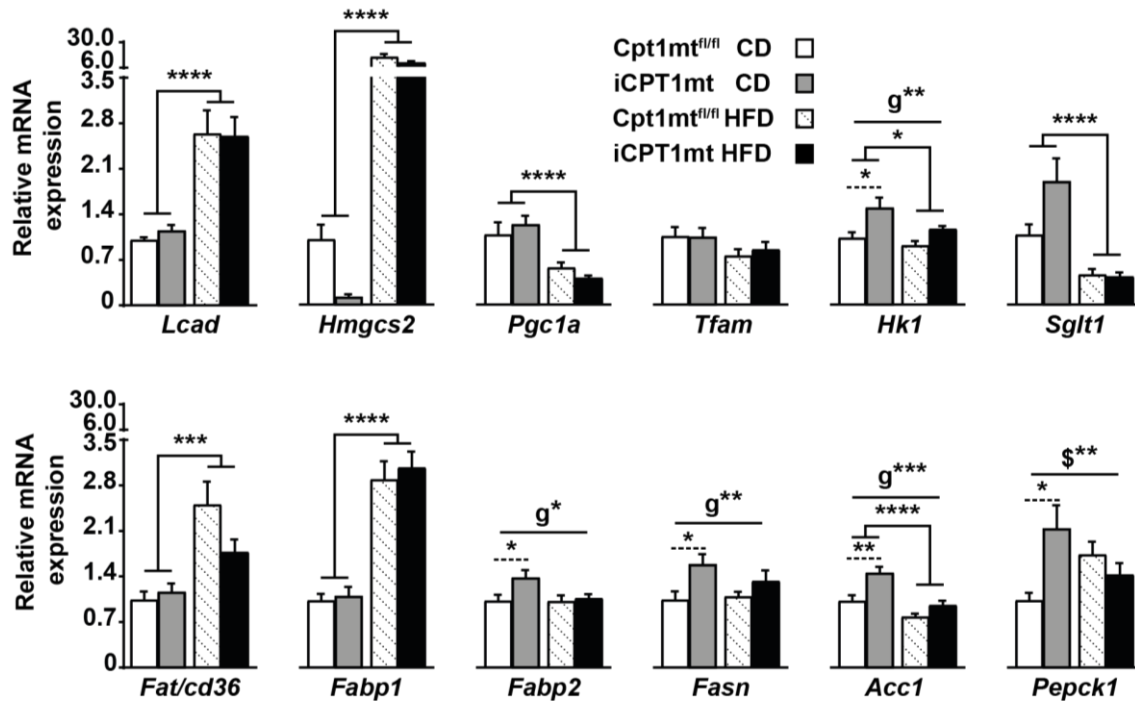


**Figure 7: iCPT1mt mice on CD show an upregulation of fatty acid synthesis, glycolysis and gluconeogenic genes in jejunal enterocytes compared to Cpt1mt<sup>fl/fl</sup> mice.**

Relative mRNA expression of genes in the jejunum of CPT1mt<sup>fl/fl</sup> and iCPT1mt mice fed CD or HFD for 20 weeks (n = 6-10, 2 x 2 factorial ANOVA (diet x genotype)). \* $P < 0.05$ , \*\* $P < 0.001$ , \*\*\* $P < 0.001$ , \*\*\*\* $P < 0.0001$  for main effects of diet or genotype (g) and *post hoc* tests (dashed lines) and interaction effects of diet x genotype (\$). Data are presented as mean values  $\pm$  SEM.





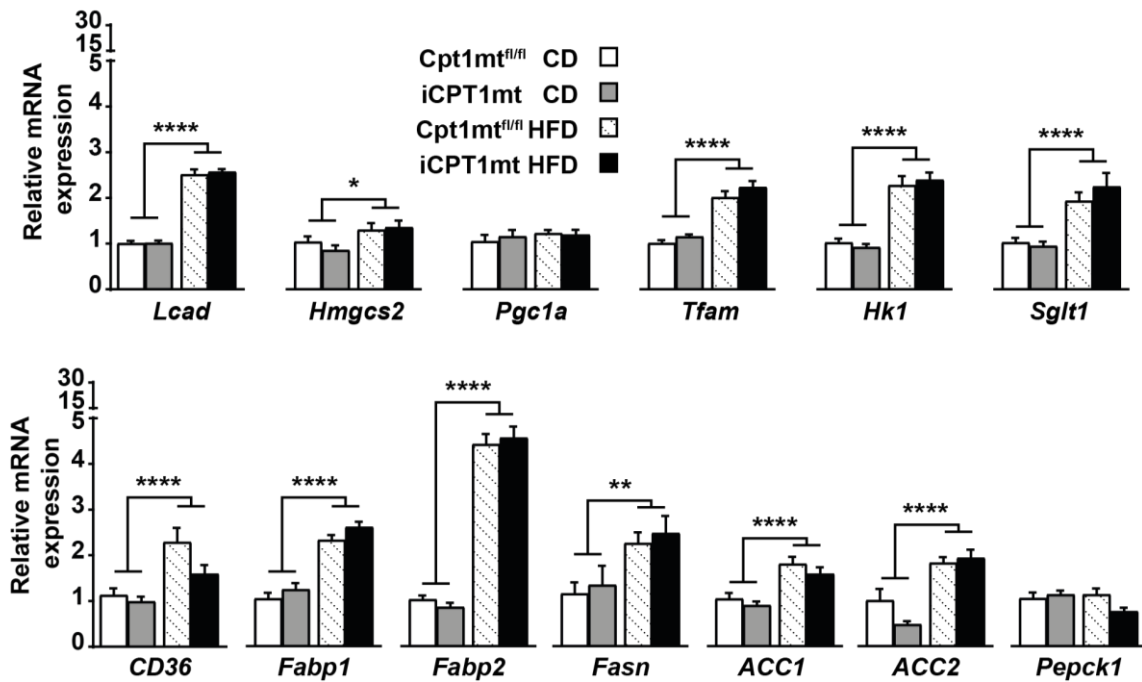


Figure 7-Supplement 2: iCPT1mt mice showed no gene expression differences from Cpt1mt<sup>fl/fl</sup> control mice when fed CD or HFD.

Relative mRNA expression of genes in the liver of CPT1mt<sup>fl/fl</sup> and iCPT1mt mice fed CD or HFD for 20 weeks. (n = 6-10, 2 x 2 factorial ANOVA (diet x genotype). \**P* < 0.05, \*\**P* < 0.001, \*\*\**P* < 0.001, \*\*\*\**P* < 0.0001 for main effects of diet or genotype (g) and *post hoc* tests (dashed lines) and interaction effects of diet x genotype (\$). Data are presented as mean values ± SEM.

### 3.4 DISCUSSION

Studies using pharmacological approaches in rodents suggest that metabolic changes in the small intestine can reduce food intake and hence improve DIO [6, 7]. Metabolic changes in the intestine may also contribute to the improvements in glucose homeostasis seen immediately after bariatric surgery in humans and rodents [4]. Here we report that enterocyte CPT1mt expression impaired glycemic control in CD-fed mice, but improved it in HFD-fed mice. These effects were independent of changes in body weight, but were accompanied by increased expressions of genes involved in

fatty acid synthesis, glucose uptake, glycolysis and gluconeogenesis, especially in CD-fed iCPT1mt mice.

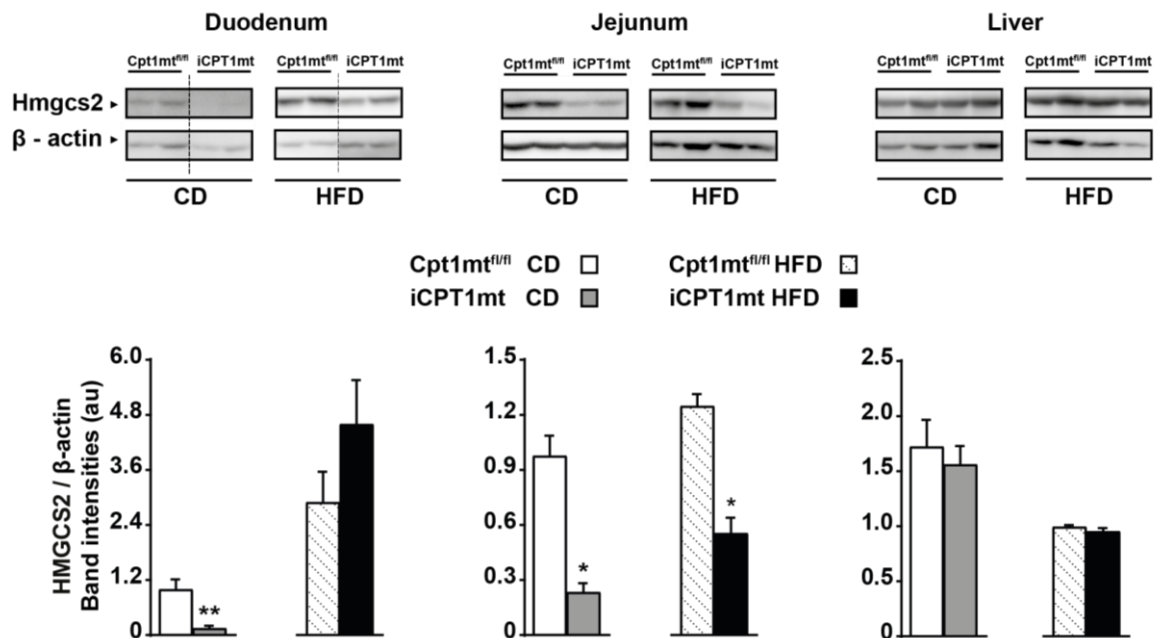


**Figure 7-Supplement 3: iCPT1mt mice show reduced HMGCS2 protein expression in the duodenum and jejunum**

Western blot analysis for 3-Hydroxy-3-Methylglutaryl-CoA Synthase 2, (HMGCS2) and  $\beta$ -actin protein expression from tissue samples of Cpt1mt<sup>fl/fl</sup> and iCPT1mt mice fed control diet (CD) or high-fat diet (HFD) as indicated for 20 weeks. (A) Representative pictures of western blot bands from the duodenum, jejunum and liver. The dotted line separates discontinuous lanes from the same gel. (B) Quantification of band intensities. (n = 5, Unpaired t test; \*\* $P < 0.01$  for Duodenum CD. n = 4-5, Mann-Whitney test; \* $P < 0.05$  for Jejunum CD and HFD and Liver CD and HFD). Data are presented as mean values  $\pm$  SEM.

Using a previously established method, we isolated primary enterocytes from iCPT1mt and Cpt1mt<sup>fl/fl</sup> mice [9, 21], and successfully processed and embedded them in a diluted matrigel matrix such that we could study their metabolic flux *in vitro*. The increased FAO flux in enterocytes isolated from chow-fed iCPT1mt mice compared to those from Cpt1mt<sup>fl/fl</sup> mice is consistent with previous studies using the CPT1mt protein [12-17]. HFD feeding for 3 days seemed to increase the FAO flux of both duodenal and jejunal enterocytes of both Cpt1mt<sup>fl/fl</sup> and iCPT1mt mice. This is consistent with previous data from our lab, which showed that the gene expression of FAO enzymes

was upregulated in the duodenum and jejunum of mice fed HFD for 3 days [22]. Interestingly, the duodenal enterocytes of iCPT1mt mice showed similar rates of FAO compared to those fed chow, whereas the jejunum of these mice showed an enhanced FAO flux that was even higher than the HFD induced increase seen in the enterocytes of Cpt1mt<sup>fl/fl</sup> mice. Together these results suggest that the enterocytes of iCPT1mt mice are capable of oxidizing more fatty acids than the enterocytes of control Cpt1mt<sup>fl/fl</sup> mice when fed a low-fat diet. When fed HFD, the jejunal enterocytes of iCPT1mt can enhance their FAO capacity even further. This is consistent with previous data from isolated rat hepatocytes expressing the CPT1mt protein, where these cells had a higher FAO flux even in the presence of high concentrations of glucose and insulin [12].

The extracellular flux analysis revealed that pooled duodenal and jejunal enterocytes of chow-fed iCPT1mt mice had an overall increased basal metabolism, in the absence of any added substrate in the medium, compared to enterocytes from Cpt1mt<sup>fl/fl</sup> mice. Providing glucose increased the rate of glycolysis and mitochondrial respiration in enterocytes from iCPT1mt mice, indicating that their glycolytic as well as oxidative respiration capacity were upregulated compared to enterocytes from Cpt1mt<sup>fl/fl</sup> mice. It would be interesting to see how HFD feeding would affect these metabolic fluxes.

At the whole body level, we saw no differences in body weight gain between iCPT1mt and Cpt1mt<sup>fl/fl</sup> mice when fed CD or HFD for up to 20 weeks. This is similar to what we observed in intestinal SIRT3 overexpressing (iSIRT3) mice [9], suggesting that increasing FAO flux in the enterocytes of mice does not cause a change in body weight gain. A body composition analysis revealed, however, that HFD-fed obese iCPT1mt mice had less visceral fat than Cpt1mt<sup>fl/fl</sup> mice. Both iCPT1mt and Cpt1mt<sup>fl/fl</sup>

control mice showed similar changes in postprandial circulating TAG, BHB, cholesterol and glucose levels when fed HFD vs CD. These effects were similar to those seen in iSIRT3 mice on HFD and CD, and were consistent with the species-specific effects observed in long-term HFD-fed mice [26, 27]. We saw no genotype differences in energy intake or energy homeostasis when the mice were fed CD or switched to HFD. This was also similar to our findings in iSIRT3 mice [9], indicating that a constitutive upregulation of FAO in the enterocytes does not affect energy intake or whole body energy metabolism. It would be interesting to see how the energy metabolism in these mice might change after feeding them CD or HFD for several weeks.

Both iCPT1mt and Cpt1mt<sup>fl/fl</sup> control mice showed similar responses to exogenous insulin after 12 weeks of CD or HFD feeding. iCPT1mt mice however responded differently to exogenous glucose depending on the diet, the route of glucose administration and/or the duration of CD or HFD feeding. These differences could be related to the mode of glucose administration, but may also indicate that adult iCPT1mt mice that may have already been intolerant to glucose, slowly reversed this phenotype when fed HFD chronically. If so, it may explain why the iCPT1mt mice were still comparatively intolerant to exogenous glucose after 13 weeks on HFD, but had reversed this phenotype by 16 weeks. The idea of a biphasic response of glucose intolerance in HFD fed C57Bl6 mice seen after 3 days of HFD feeding and then between 12 to 16 weeks of HFD feeding fits with our idea of a gradual change in glucose tolerance [28]. The reduced visceral fat mass in HFD-fed iCPT1mt mice could also be involved in the improved glucose tolerance, since visceral fat is well known to be associated with the incidence of metabolic syndrome [29]. These results were partly similar and partly different from our findings in iSIRT3 mice. Enterocyte overexpression

of SIRT3 had no effect in mice fed CD but did protect them from developing IR and glucose intolerance under conditions of DIO [9].

Expressions of genes for fatty acid binding and fatty acid synthesis were upregulated specifically in iCPT1mt mice compared to Cpt1mt<sup>fl/fl</sup> controls on CD. This could indicate that CPT1mt expression in the jejunal enterocytes led to increased *de novo* fatty acid synthesis in these cells, perhaps to funnel fatty acids into the mitochondria for the constitutively active FAO. This assumption is consistent with data from isolated rat hepatocytes expressing the CPT1mt protein. Even in the presence of high glucose and insulin that favor lipogenesis, these cells were able to oxidize *de novo* synthesized LCFA [12].

Interestingly, the glycolytic gene *Hk1* was upregulated in the jejunal enterocytes of iCPT1mt mice fed CD. This is consistent with the Seahorse data from isolated enterocytes, which showed that enterocytes from iCPT1mt mice had a higher rate of glycolysis than enterocytes from Cpt1mt<sup>fl/fl</sup> mice when provided with glucose. Mitochondrial acetyl-CoA generated via FAO cannot directly leave the mitochondria and fuel fatty acid synthesis. It needs to enter the TCA cycle to generate citrate, which can then leave the mitochondria via the citrate shuttle to fuel *de novo* lipogenesis [30]. The pyruvate derived from enhanced glycolysis undergoes oxidative decarboxylation, and the resulting Acetyl-CoA also enters the mitochondria to fuel the TCA cycle. When TCA cycle intermediates become limiting, accumulating mitochondrial acetyl-CoA form ketone bodies. In the enterocytes of CD-fed iCPT1mt mice, however, the protein levels of ketogenic HMGCS2 were significantly downregulated. This supports the assumption that the accumulating acetyl-CoA could be funneled into the TCA cycle which would eventually fuel lipogenesis. Interestingly, the expression of the gluconeogenic gene *Pepck1* was also increased in the jejunal enterocytes of iCPT1mt mice, indicating that

these cells were producing glucose. Together these results indicate that the jejunal enterocytes of CD-fed iCPT1mt mice had developed futile cycles of FAO and lipogenesis, as well as glycolysis and gluconeogenesis.

Concomitantly, in the duodenal enterocytes of CD-fed iCPT1mt mice, we saw an increase in *Sglt1* expression. SGLT1 is the glucose transporter in the apical membrane that absorbs glucose from the intestinal lumen, thus supporting the idea of increased glucose absorption. The increased villi length in the duodenum of iCPT1mt mice fed CD as well as the higher levels of blood glucose seen in iCPT1mt mice, 15 minutes after oral, but not IP glucose bolus support the idea of increased glucose absorption from the intestine of iCPT1mt mice fed CD.

On HFD, all mice showed an overall increase in the expressions of genes related to fatty acid uptake, fatty acid binding, FAO and ketogenesis in their duodenal and jejunal enterocytes. Expressions of genes related to glucose absorption, glycolysis and gluconeogenesis were either downregulated in all mice or remained unchanged. Together these results indicate that the futile cycles generated in CD-fed iCPT1mt mice were absent in HFD-fed mice. How these enterocyte metabolic changes might affect whole body glucose homeostasis is still unclear.

In iSIRT3 mice fed HFD, increased ketogenesis in the small intestine was associated with the improved insulin sensitivity and glucose tolerance [9]. In iCPT1mt mice, however, HMGCS2 protein levels were significantly lower and circulating BHB levels were unchanged, indicating that these effects on improved glycemic control were unrelated to ketogenesis. We believe that the increased glucose absorption in the duodenum and the upregulated gluconeogenesis in the jejunum might contribute to the reduced glucose tolerance seen in iCPT1mt mice fed CD. Unlike hepatic gluconeogenesis that is inhibited by insulin, intestinal gluconeogenesis is known to be

enhanced in the post absorptive period [31]. The enhanced intestinal gluconeogenesis supposedly provides more glucose for hepatic portal vein glucose sensors that may signal the brain to inhibit eating as reviewed in [32]. Perhaps the higher glucose levels observed in the OGTT and IPGTT are the result of substantially enhanced glucose absorption and/or gluconeogenesis in the enterocytes of iCPT1mt mice. Another possible explanation is that the permanently enhanced gluconeogenesis and glycolysis in the enterocytes of iCPT1mt mice fed CD limits their capacity to utilize large oral or intraperitoneal loads of glucose properly, leading to impaired glycemic control. Data from rodent models shows that gluconeogenesis in the gut can contribute anywhere from 5 to 25 % of whole body endogenous glucose production depending on the diet as reviewed in [33]. Mice with a liver specific or liver and intestinal specific knock out of the gluconeogenic gene glucose-6-phosphatase, catalytic subunit (*G6pc*) showed that in the absence of hepatic gluconeogenesis, intestinal gluconeogenesis is essential to maintain physiological levels of blood glycemia [34]. Together these data indicate that changes in enterocyte metabolism can contribute to and influence systemic glucose concentrations substantially, which supports our idea that enterocyte gluconeogenesis is capable of contributing to the glycemic dysregulation we see in iCPT1mt mice.

Perhaps on HFD, iCPT1mt mice have enough LCFA and carbohydrate intermediates to fuel the constitutive upregulation of FAO and the TCA cycle and therefore do not need a massive upregulation of glucose absorption or gluconeogenesis to fuel the *de novo* synthesis of fatty acids. The constitutive upregulation of FAO under these conditions could slowly reverse the adverse effects seen under CD fed conditions. It would be interesting to see whether iCPT1mt mice might be prevented from developing DIO and/or impaired glycemia if they were directly



weaned onto the HFD. Consistent with this idea hepatic CPT1mt expression was able to prevent the development of DIO and IR in adult mice fed HFHS diet after the expression of CPT1mt using an adeno-associated virus [14]. Also both hepatic and skeletal muscle expressions of CPT1mt were able to reverse already established IR and impaired glycemia in DIO mouse models without affecting body weight [15, 17]. In fact, these studies did not show any adverse effects of CPT1mt expression in mice fed standard chow. The main difference between these mouse models and our intestinal transgenic mice, other than the obvious difference in the organs we targeted, is that our mice express CPT1mt constitutively from embryonic development, whereas in these other models the CPT1mt expression was induced in adulthood. An inducible Villin-Cre model, in which we could specifically express CPT1mt in the mouse enterocytes in adulthood, might provide a clearer picture to whether an upregulation of enterocyte FAO would protect from the development of DIO and IR, without the negative effects seen on CD.

In sum, these results show that persistent changes in mouse enterocyte FAO do not influence daily energy intake or energy homeostasis and body weight, but affect whole body glucose homeostasis under different dietary conditions. Further studies should try to elucidate the exact mechanism of these effects and dissociate the contribution of the molecular and metabolic changes in the gut versus other organs.

## **ACKNOWLEDGEMENTS**

This work was supported by the Swiss National Science Foundation, Research Grant 310030\_153149 to WL. We are grateful to Prof. WD Hardt and P Kaiser for the Villin-Cre mice; F Mouttet, E Weber and F Mueller for assistance in experimentation or genotyping and the SLA animal facility for contribution to animal husbandry.

### 3.5 REFERENCES

- [1] Ng, M., Fleming, T., Robinson, M. Global, regional, and national prevalence of overweight and obesity in children and adults during 1980-2013: a systematic analysis for the Global Burden of Disease Study 2013 (vol 384, pg 766, 2014). *Lancet*. 2014,384:746-.
- [2] Vairavamurthy, J., Cheskin, L. J., Kraitchman, D. L., Arepally, A., Weiss, C. R. Current and cutting-edge interventions for the treatment of obese patients. *Eur J Radiol*. 2017,93:134-42.
- [3] Pories, W. J., Swanson, M. S., Macdonald, K. G., Long, S. B., Morris, P. G., Brown, B. M., et al. Who Would Have Thought It - an Operation Proves to Be the Most Effective Therapy for Adult-Onset Diabetes-Mellitus. *Ann Surg*. 1995,222:339-52.
- [4] Cavin, J. B., Couvelard, A., Lebtahi, R., Ducroc, R., Arapis, K., Voitellier, E., et al. Differences in Alimentary Glucose Absorption and Intestinal Disposal of Blood Glucose After Roux-en-Y Gastric Bypass vs Sleeve Gastrectomy. *Gastroenterology*. 2016,150:454-64 e9.
- [5] Cavin, J. B., Bado, A., Le Gall, M. Intestinal Adaptations after Bariatric Surgery: Consequences on Glucose Homeostasis. *Trends Endocrinol Metab*. 2017,28:354-64.
- [6] Schober, G., Arnold, M., Birtles, S., Buckett, L. K., Pacheco-Lopez, G., Turnbull, A. V., et al. Diacylglycerol acyltransferase-1 inhibition enhances intestinal fatty acid oxidation and reduces energy intake in rats. *Journal of Lipid Research*. 2013,54:1369-84.
- [7] Azari, E. K., Leitner, C., Jaggi, T., Langhans, W., Mansouri, A. Possible Role of Intestinal Fatty Acid Oxidation in the Eating-Inhibitory Effect of the PPAR-alpha Agonist Wy-14643 in High-Fat Diet Fed Rats. *PLoS One*. 2013,8.
- [8] Azari, E. K., Ramachandran, D., Weibel, S., Arnold, M., Romano, A., Gaetani, S., et al. Vagal afferents are not necessary for the satiety effect of the gut lipid messenger oleoylethanolamide. *Am J Physiol Regul Integr Comp Physiol*. 2014,307:R167-78.

- [9] Ramachandran, D., Clara, R., Fedele, S., Hu, J., Lackzo, E., Huang, J. Y., et al. Intestinal SIRT3 overexpression in mice improves whole body glucose homeostasis independent of body weight. *Mol Metab.* 2017,6:1264-73.
- [10] Rardin, M. J., Newman, J. C., Held, J. M., Cusack, M. P., Sorensen, D. J., Li, B., et al. Label-free quantitative proteomics of the lysine acetylome in mitochondria identifies substrates of SIRT3 in metabolic pathways. *Proc Natl Acad Sci U S A.* 2013,110:6601-6.
- [11] Morillas, M., Gomez-Puertas, P., Bentebibel, A., Selles, E., Casals, N., Valencia, A., et al. Identification of conserved amino acid residues in rat liver carnitine palmitoyltransferase I critical for malonyl-CoA inhibition - Mutation of methionine 593 abolishes malonyl-CoA inhibition. *Journal of Biological Chemistry.* 2003,278:9058-63.
- [12] Akkaoui, M., Cohen, I., Esnous, C., Lenoir, V., Sournac, M., Girard, J., et al. Modulation of the hepatic malonyl-CoA-carnitine palmitoyltransferase 1A partnership creates a metabolic switch allowing oxidation of de novo fatty acids. *Biochem J.* 2009,420:429-38.
- [13] Henique, C., Mansouri, A., Fumey, G., Lenoir, V., Girard, J., Bouillaud, F., et al. Increased mitochondrial fatty acid oxidation is sufficient to protect skeletal muscle cells from palmitate-induced apoptosis. *J Biol Chem.* 2010,285:36818-27.
- [14] Orellana-Gavalda, J. M., Herrero, L., Malandrino, M. I., Paneda, A., Sol Rodriguez-Pena, M., Petry, H., et al. Molecular therapy for obesity and diabetes based on a long-term increase in hepatic fatty-acid oxidation. *Hepatology.* 2011,53:821-32.
- [15] Monsenego, J., Mansouri, A., Akkaoui, M., Lenoir, V., Esnous, C., Fauveau, V., et al. Enhancing liver mitochondrial fatty acid oxidation capacity in obese mice improves insulin sensitivity independently of hepatic steatosis. *Journal of Hepatology.* 2012,56:632-9.
- [16] Henique, C., Mansouri, A., Vavrova, E., Lenoir, V., Ferry, A., Esnous, C., et al. Increasing mitochondrial muscle fatty acid oxidation induces skeletal muscle remodeling toward an oxidative phenotype. *FASEB J.* 2015,29:2473-83.

- [17] Vavrova, E., Lenoir, V., Alves-Guerra, M. C., Denis, R. G., Castel, J., Esnous, C., et al. Muscle expression of a malonyl-CoA-insensitive carnitine palmitoyltransferase-1 protects mice against high-fat/high-sucrose diet-induced insulin resistance. *Am J Physiol Endocrinol Metab.* 2016,311:E649-60.
- [18] Madison, B. B., Dunbar, L., Qiao, X. T., Braunstein, K., Braunstein, E., Gumucio, D. L. Cis elements of the villin gene control expression in restricted domains of the vertical (crypt) and horizontal (duodenum, cecum) axes of the intestine. *J Biol Chem.* 2002,277:33275-83.
- [19] McGuinness, O. P., Ayala, J. E., Laughlin, M. R., Wasserman, D. H. NIH experiment in centralized mouse phenotyping: the Vanderbilt experience and recommendations for evaluating glucose homeostasis in the mouse. *Am J Physiol Endocrinol Metab.* 2009,297:E849-55.
- [20] Andrikopoulos, S., Blair, A. R., Deluca, N., Fam, B. C., Proietto, J. Evaluating the glucose tolerance test in mice. *Am J Physiol Endocrinol Metab.* 2008,295:E1323-32.
- [21] Nik, A. M., Carlsson, P. Separation of intact intestinal epithelium from mesenchyme. *BioTechniques.* 2013,55:42-4.
- [22] Clara, R., Schumacher, M., Ramachandran, D., Fedele, S., Krieger, J. P., Langhans, W., et al. Metabolic Adaptation of the Small Intestine to Short- and Medium-Term High-Fat Diet Exposure. *J Cell Physiol.* 2017,232:167-75.
- [23] Prip-Buus, C., Cohen, I., Kohl, C., Esser, V., McGarry, J. D., Girard, J. Topological and functional analysis of the rat liver carnitine palmitoyltransferase 1 expressed in *Saccharomyces cerevisiae*. *FEBS Lett.* 1998,429:173-8.
- [24] Livak, K. J., Schmittgen, T. D. Analysis of relative gene expression data using real-time quantitative PCR and the  $2^{-\Delta\Delta C_T}$  method. *Methods.* 2001,25:402-8.
- [25] Sirakov, M., Borra, M., Cambuli, F. M., Plateroti, M. Defining suitable reference genes for RT-qPCR analysis on intestinal epithelial cells. *Molecular biotechnology.* 2013,54:930-8.
- [26] Satapati, S., He, T., Inagaki, T., Potthoff, M., Merritt, M. E., Esser, V., et al. Partial resistance to peroxisome proliferator-activated receptor-alpha agonists in ZDF rats is

associated with defective hepatic mitochondrial metabolism. *Diabetes*. 2008,57:2012-21.

[27] Satapati, S., Sunny, N. E., Kucejova, B., Fu, X., He, T. T., Mendez-Lucas, A., et al. Elevated TCA cycle function in the pathology of diet-induced hepatic insulin resistance and fatty liver. *J Lipid Res*. 2012,53:1080-92.

[28] Williams, L. M., Campbell, F. M., Drew, J. E., Koch, C., Hoggard, N., Rees, W. D., et al. The development of diet-induced obesity and glucose intolerance in C57BL/6 mice on a high-fat diet consists of distinct phases. *PLoS One*. 2014,9:e106159.

[29] Kwon, H., Kim, D., Kim, J. S. Body Fat Distribution and the Risk of Incident Metabolic Syndrome: A Longitudinal Cohort Study. *Sci Rep*. 2017,7:10955.

[30] Shi, L., Tu, B. P. Acetyl-CoA and the regulation of metabolism: mechanisms and consequences. *Curr Opin Cell Biol*. 2015,33:125-31.

[31] Soty, M., Gautier-Stein, A., Rajas, F., Mithieux, G. Gut-Brain Glucose Signaling in Energy Homeostasis. *Cell Metab*. 2017,25:1231-42.

[32] Mithieux, G. A novel function of intestinal gluconeogenesis: central signaling in glucose and energy homeostasis. *Nutrition*. 2009,25:881-4.

[33] Mithieux, G., Gautier-Stein, A. Intestinal glucose metabolism revisited. *Diabetes Res Clin Pract*. 2014,105:295-301.

[34] Penhoat, A., Fayard, L., Stefanutti, A., Mithieux, G., Rajas, F. Intestinal gluconeogenesis is crucial to maintain a physiological fasting glycemia in the absence of hepatic glucose production in mice. *Metabolism-Clinical and Experimental*. 2014,63:104-11.

## **CHAPTER 4:**

### **GENERAL DISCUSSION**

---

#### **4.1 Overview of the main findings**

The two manuscripts compiled in this thesis clearly indicate that modulating enterocyte metabolism affects glycemic control in mice. Both transgenic mouse models, namely iSIRT3 and iCPT1mt mice, showed changes in insulin resistance and/or glucose tolerance. These changes occurred without any effect on 24 h food intake or body weight. Enterocyte overexpression of SIRT3 caused no changes in mice fed CD, but improved IR and glucose tolerance in DIO. In contrast, iCPT1mt mice had impaired glucose tolerance when fed CD, but improved glucose tolerance under conditions of DIO. The mechanisms of these effects remain elusive, but all available data indicate that they involve different processes/mechanisms. For instance, the improved glycemia in iSIRT3 mice under conditions of DIO was associated with increased intestinal ketogenesis, whereas iCPT1mt mice showed a downregulation of intestinal ketogenic enzymes and no differences in circulating BHB levels compared to control mice. Moreover, iCPT1mt mice fed CD developed futile cycles of glycolysis/gluconeogenesis and FAO/*de novo* fatty acid synthesis, which were absent when the mice were fed HFD. Together, these data indicate that the metabolic pathways activated in the enterocytes influence glycemic control in mice and that the fat content of the diet in part affects glycemic control through enterocyte metabolism.

#### **4.2 Limitations of our transgenic manipulation**

A major limitation of the two studies is the use of the Villin-Cre mouse line with constitutive Cre recombinase expression [1]. Our transgenes of interest (Sirt3 or Cpt1mt) were (over)expressed in these mice since embryogenesis. This most likely led to developmental compensations in these mice, which would have been absent if we

had been able to express these transgenes in a conditional manner. Using an inducible Vil-Cre mouse line [2], we could add temporal regulation to tissue specificity, which would also more closely resemble the acute pharmacological treatments that led to upregulation of intestinal FAO and ketogenesis in rats [3-5]. This could in turn reveal whether increased FAO in the enterocytes can really affect eating behavior and body weight gain.

Another point of consideration is the expression profile of the villin promoter in all cell types of the intestinal epithelium. Our Vil-Cre mouse line drives the expression of our transgene of interest in all the cells of the intestinal epithelium in both the vertical axis (crypt to villus) as well as the horizontal axis (duodenum to colon) [1]. In our study we only addressed the effects seen in the duodenum and jejunum of these mice, which limits our understanding of how the distal portions of the intestine might be contributing to the observed phenomena. Previous experiments in enteroendocrine cells *in vitro* and *in vivo* indicate that gut peptides are differentially released from these cells under different metabolic conditions [6-8]. These studies indicate that modifications of enteroendocrine cell metabolism might affect the release of gut peptides, which would also affect whole body glucose metabolism - a factor we did not consider in our study.

We also have no data on how intestinal SIRT3 or CPT1mt (over)expression might be affecting the microbiota in these mice. It seems logical that there is a crosstalk between microbial metabolism and enterocyte metabolism. Moreover, we are missing any information on possible sex differences, which are conceivable because some of the metabolic enzymes in enterocytes have a sexually dimorphic expression pattern [9]. During our initial experiments, we did start working with male and female mice. But we were unable to establish DIO and IR in female mice in the time that we saw the effects manifest in male mice. We therefore decided to discontinue the experiments in



female mice. We believe, however, that it is important to consider possible sex differences in the observed effects in the future.

### **4.3 Intestinal ketogenesis**

#### **4.3.1 Looking beyond hepatic ketogenesis**

Ketone bodies are a vital alternative fuel for non-hepatic tissues such as brain, heart and skeletal muscles under conditions of long-term fasting or starvation [10]. Traditionally, the liver was considered the only source of ketone bodies. Later it became clear, however, that the ketogenic enzyme HMGCS2 is also expressed in the intestine and kidney as well as in cortical astrocytes of suckling rats [11-14]. In fact, mRNA levels of *Hmgcs2* were shown to be regulated in the intestine and kidney of rats depending on the fat content in the diet. When fed a high carbohydrate low fat diet, *Hmgcs2* expression was completely lost in the intestine and kidneys of weaned rats, but could be restored when the animals were fed HFD for a week [13]. Data from our own lab showed that *Hmgcs2* mRNA as well as protein levels are upregulated in the duodenal and jejunal enterocytes of mice after 3 days of HFD feeding, while their levels were unchanged in the liver [15]. In fact, the presence of higher levels of BHB in blood sampled from the hepatic portal vein versus the vena cava in rat studies from our lab also confirm that the intestine is capable of producing ketone bodies [3-5].

#### **4.3.2 Regulation of ketogenesis in pathophysiology**

Ketone bodies are derived from the acetyl-CoA produced by the  $\beta$ -oxidation of fatty acids [16]. HMGCS2, the rate limiting enzyme of ketogenesis, is localized to the mitochondria and commits acetyl-CoA to the ketogenic fate to produce acetoacetate, acetone and D- $\beta$ -hydroxybutyrate (BHB), together called ketone bodies [17]. Ketone

bodies are transported across cell membranes by monocarboxylate transporters (MCT) and sodium-coupled monocarboxylate transporters (SMCT) along their concentration gradient [18]. In diabetic patients, insulin insufficiency leads to an upregulation of FAO and gluconeogenesis and an accumulation of mitochondrial acetyl-CoA in the liver. This accelerates ketogenesis to extremely high levels causing ketoacidosis, which is toxic. In contrast, non-diabetic obese patients with hyperinsulinemia and IR have lower plasma BHB levels than lean controls. This is attributed to an insulin-mediated suppression of hepatic ketogenesis, even under conventional signs of IR, suggesting that there might be a differential regulation of ketogenesis by insulin during the transition from prediabetes to diabetes as well as a differential sensitivity to insulin in different tissues [19].

Consistent with these findings, in both of our studies, all diet-induced obese mice showed signs of IR and decreased circulating BHB levels compared to CD-fed mice. iSIRT3 mice fed HFD, however, tended to show increased circulating BHB levels compared to the HFD-fed S3fl controls, but this increase did not reach statistical significance. iSIRT3 mice also showed dramatically increased ketogenic gene expression levels specifically in their duodenal and jejunal enterocytes, but not in their livers. Considering that hepatic ketogenesis is a major contributor to circulating ketone body levels, the increased intestinal ketogenesis could have been masked by reduced hepatic ketogenesis. One of the caveats of increased *Hmgcs2* expression in response to an upregulation of SIRT3 is that SIRT3 is a post-translational regulator of its target proteins, including HMGCS2 [20]. A transcriptional upregulation of *Hmgcs2* therefore indicates that this effect was not directly mediated by SIRT3. This increased *Hmgcs2* expression at the mRNA level could be related to the high demand for mitochondrial NAD<sup>+</sup> due to increased SIRT3 activity [21]. SIRT3 breaks down a molecule of NAD<sup>+</sup>

for every deacetylation reaction, and this increased demand for NAD<sup>+</sup> in the mitochondria could be fueled by the production of BHB where NADH is converted to NAD<sup>+</sup> by D-β-hydroxybutyrate dehydrogenase [10].

### 4.3.3 Ketone bodies and glycemic control

In the manuscript describing our findings in iSIRT3 mice (Chapter 2), we hypothesized that the increased enterocyte ketogenesis might play a role in the improved IR and glucose tolerance seen in these mice with DIO. More and more evidence suggests that ketone bodies play a role beyond a secondary fuel source [19]. In fact, data indicate that both central and peripheral ketone bodies could regulate energy homeostasis through currently unknown mechanisms [22, 23]. BHB has been shown to inhibit histone deacetylases *in vitro*. BHB is structurally similar to the short-chain fatty acid (SCFA) butyrate. Chronic supplementation of butyrate, a global HDAC inhibitor, in the diet, causes HFD-fed rats to remain metabolically healthy [24]. This was also true for rat models of T1D [25]. BHB can also bind to at least two different G-protein-coupled receptors that regulate lipid metabolism [26, 27]. The oxidation of BHB in peripheral tissues leads to the generation of NADH and acetyl-CoA, and alters the NAD<sup>+</sup>/NADH ratio of peripheral tissues. Both acetyl-CoA and NAD<sup>+</sup>/NADH ratio themselves can regulate metabolic function. Succinyl-CoA:3-oxoacid CoA transferase (SCOT) is the extrahepatic mitochondrial enzyme involved in oxidizing ketone bodies. SCOT knock-out mice cannot use ketone bodies as a fuel, and within 48 h of birth develop hyperketonemic hypoglycemia [28]. Preliminary unpublished data from Peter Crawford's lab also indicate that a knockdown of hepatic *Hmgcs2* using antisense oligonucleotides leads to ketogenic insufficiency, which causes dysregulation of glucose homeostasis in chow-fed mice and of lipid metabolism in HFD-fed mice as mentioned in [19].

Studies with high fat, very low carb ketogenic diets (KD) are known to have beneficial effects in obesogenic environments in mice [29, 30]. In humans, ketogenic diets have been extensively used to treat childhood epilepsy [31] as well as PCOS in women [32]. The mechanisms of these effects remain unclear, but the improvement in insulin sensitivity and weight reduction in these women suggests that a ketogenic diet has beneficial metabolic effects. Whether the beneficial effects of ketogenic diets are mainly due to increased circulating ketone body levels remains to be determined.

#### **4.3.4 Rising ketone body levels - friend or foe?**

One of the discrepancies about whether increased circulating ketones are a health benefit or a health hazard comes from the fact that high levels of ketone bodies can cause ketoacidosis, often seen during Type 1 diabetes or T2D. Ketoacidosis, caused by an uncontrolled increase of acidic ketone bodies in circulation, if left unchecked, can be fatal. The insulin-deficient conditions in diabetes mimic starvation, leading to uncontrolled hepatocyte ketogenesis as well as gluconeogenesis. The concomitant high plasma glucose levels might also contribute to the toxic effects of ketoacidosis. The increased circulating levels of ketones with chronic KD feeding remain at physiological levels and can still be controlled by insulin [33]. Also, KD is a very low carbohydrate diet, which means the plasma glucose and insulin levels remain relatively low. Perhaps the rise in BHB levels seen in iSIRT3 mice under post-prandial conditions could increase significantly under fasting conditions and generate a ketotic state, which might in turn lead to the improved insulin sensitivity and glucose tolerance seen in iSIRT3 mice, by as yet unknown mechanisms.

## **4.4 Intestinal gluconeogenesis**

### **4.4.1 Intestinal gluconeogenesis – physiological relevance**

As mentioned earlier, the mechanisms of glucose homeostasis regulation in iCPT1mt mice do not seem to be related to intestinal ketogenesis. The impaired glycemic control on CD could be linked to the upregulated gluconeogenesis in the jejunum of iCPT1mt mice. That the intestine can generate glucose was first discovered nearly 20 years ago [34]. In rodent models, intestinal gluconeogenesis supposedly contributes to the satiety effect of protein-rich foods mainly by increasing the release of glucose into the hepatic portal vein. The glucose sensors in the hepatic portal vein in turn signal to hypothalamic nuclei in the brain, and their activation presumably inhibits food intake [35]. In the absence of liver glycogen mobilization and gluconeogenesis, intestinal and renal gluconeogenesis could combine to maintain normal whole body glucose levels during prolonged fasting [36]. Intestinal gluconeogenesis was markedly upregulated in diabetic mice after gastric bypass surgeries, but not after gastric banding, and was associated with the metabolic benefits seen in these mice. This increase was mainly in the ileum and the metabolic benefits of gastric bypass disappeared after the inactivation of portal neural afferents [37]. These effects, however, could not be clearly dissociated from the increased gut peptide levels seen after RYGB [38].

### **4.4.2 Intestinal gluconeogenesis and glycemic control**

Because intestinal gluconeogenesis is upregulated post-prandially, we believe that the increased gluconeogenesis that we observed in iCPT1mt mice on CD contributes to the impaired glucose tolerance seen in these animals after a glucose bolus. This seems to contradict the original idea of intestinal glucose production being

beneficial, but we believe it is situationally different. Increasing intestinal gluconeogenesis in diabetic or IR conditions may in fact be beneficial. But a constitutive upregulation of the futile cycles of gluconeogenesis and glycolysis (and FAO and lipogenesis) that we found in CD-fed iCPT1mt mice, might be overtaxing or limiting the metabolic capacity of these cells, reducing their capability to respond to a large bolus of glucose. The increased expression of the apical glucose transporter *Sglt1* presumably contributes to enhanced glucose absorption, meaning that iCPT1mt mice have to deal with a greater glucose load that needs to be cleared for the same amount of glucose bolus. On the other hand, the downregulation of the constitutive futile cycle of glycolysis/gluconeogenesis in the enterocytes might also be the major reason for the improved glucose homeostasis seen in HFD-fed iCPT1mt mice, which was established only after 16 weeks of HFD feeding. Perhaps these compensatory mechanisms caused by the constitutive CPT1mt expression since embryonic stages do require several weeks to be completely reversed. An inducible expression of CPT1mt in adult mice might circumvent these negative effects and lead to improved glycemic control as seen in mice in which CPT1mt expression was induced in adulthood skeletal muscles [39-41].

#### **4.5 Intestinal crosstalk - how does the intestine signal to the rest of the body?**

Considering that the intestine is the organ responsible for absorbing and repackaging nutrients for the rest of the body, it is not surprising that changes in intestinal metabolism could affect the whole body. We already know that a robust bidirectional gut-brain axis exists with sympathetic and parasympathetic neural connections between the two organs [42]. Afferent signals from the gut to the brain can in turn lead to efferent signals from the brain to the rest of the body. The enteric nervous

system is also crucial for this cross-talk [43]. In addition, neuroendocrine gut hormones enter the circulation via the hepatic portal vein [44]. Sensors in the hepatic portal vein, the enteric nervous system or further upstream supposedly sense these hormones as well as metabolites and lead to downstream effects.

The gut can also signal to the rest of the body via its immune system [45]. The lymphatic vessels collect information from the gut and transport nutrients and immune cells to the rest of the body and affect metabolic function. Gut microbiota play a big role in how the gut signals to the rest of the body [46]. They are involved in producing the neurotransmitters serotonin and gamma-aminobutyric acid (GABA). They also produce SCFA such as butyric acid, propionic acid and acetic acid, capable of stimulating the autonomic nervous system. Altered gut permeability can lead to inflammation and endotoxin release into circulation, both of which are risk factors for disease [47]. Altering the metabolism of enterocytes has the potential to regulate one or more of these pathways, thereby signaling to the rest of the body and affecting whole body metabolism.

In both studies described in this thesis, the main phenotypic differences were related to changes in glycemic control in response to exogenous insulin and/or glucose bolus. Based on our analysis of the molecular and morphological changes in the enterocytes and liver of these mice, we assumed that our effects were primarily caused by metabolic changes in the enterocytes. We cannot, however, exclude the possibility that the insulin sensitivity of other tissues such as muscle, liver and adipose tissue, might also be affected and contribute to the observed effects. Though both intestinal ketogenesis and gluconeogenesis might contribute to the insulin signaling or glucose metabolism of the intestinal cells themselves, signals from the intestine could also be affecting the metabolic response of other tissues in the body. This could be mediated

by BHB, gut peptide hormones or intestinal glucose production via circulation or via nerve signals. One indication of tissue crosstalk was the change in adiposity seen in iCPT1mt mice fed HFD. These mice had lower visceral fat mass compared to control Cpt1mt<sup>fl/fl</sup> mice fed HFD. Excess visceral or ectopic fat is associated with an increased risk for IR and metabolic syndrome. These reduced levels could therefore be contributing to the improved glucose tolerance we see in iCPT1mt mice after 16 weeks of HFD feeding. Evidence supporting this idea comes from the link between intestinal inflammation and increased visceral adiposity seen in humans and animal models, as well as a link between gut microbiota differences in lean and obese humans and rodents as reviewed in [48]. Together these studies indicate that changes in intestinal metabolic function are highly correlated with the incidence of obesity and metabolic disease.

#### **4.6 Future prospects**

I hope this thesis is convincing of the fact that modulating enterocyte metabolism affects whole body glucose metabolism. In particular, the studies described here suggest that modulating enterocyte metabolism can affect glycemic control without affecting body weight. This supports the idea that the improved glycemic control seen in gastric bypass surgery models, well before any weight loss, could at least partly be due to the metabolic changes seen in the small intestinal epithelium.

Future experiments need to address if an acute or chronic upregulation of specific metabolic pathways in the enterocytes might have similar or different effects. They should also try to address the exact mechanism by which enterocyte metabolism could affect whole body glucose homeostasis, i.e., whether the effects on the systemic



readouts that we observed were in fact solely due to the changes in enterocyte metabolism or whether it also affected the metabolic response of other peripheral tissues besides the liver. This could be achieved by using glucose clamps and labelled substrates to determine the metabolic fate of these substrates in the intestine as well as in the liver, muscle and adipose tissue in response to changes in enterocyte metabolism. It would also be interesting to test if modulating enterocyte metabolism could lead to changes in gut – brain signaling with subsequent autonomic responses affecting whole body glycemic control. In conclusion, our results support the view that targeting enterocyte metabolism might have a therapeutic potential in the battle against metabolic disease.

## 4.7 REFERENCES

- [1] Madison, B. B., Dunbar, L., Qiao, X. T., Braunstein, K., Braunstein, E., Gumucio, D. L. Cis elements of the villin gene control expression in restricted domains of the vertical (crypt) and horizontal (duodenum, cecum) axes of the intestine. *J Biol Chem.* 2002,277:33275-83.
- [2] el Marjou, F., Janssen, K. P., Chang, B. H., Li, M., Hindie, V., Chan, L., et al. Tissue-specific and inducible Cre-mediated recombination in the gut epithelium. *Genesis.* 2004,39:186-93.
- [3] Schober, G., Arnold, M., Birtles, S., Buckett, L. K., Pacheco-Lopez, G., Turnbull, A. V., et al. Diacylglycerol acyltransferase-1 inhibition enhances intestinal fatty acid oxidation and reduces energy intake in rats. *Journal of Lipid Research.* 2013,54:1369-84.
- [4] Azari, E. K., Leitner, C., Jaggi, T., Langhans, W., Mansouri, A. Possible Role of Intestinal Fatty Acid Oxidation in the Eating-Inhibitory Effect of the PPAR-alpha Agonist Wy-14643 in High-Fat Diet Fed Rats. *PLoS One.* 2013,8.
- [5] Azari, E. K., Ramachandran, D., Weibel, S., Arnold, M., Romano, A., Gaetani, S., et al. Vagal afferents are not necessary for the satiety effect of the gut lipid messenger oleoylethanolamide. *Am J Physiol Regul Integr Comp Physiol.* 2014,307:R167-78.
- [6] Clara, R., Langhans, W., Mansouri, A. Oleic acid stimulates glucagon-like peptide-1 release from enteroendocrine cells by modulating cell respiration and glycolysis. *Metabolism.* 2016,65:8-17.
- [7] Sayers, S. R., Reimann, F., Gribble, F. M., Parker, H., Zac-Varghese, S., Bloom, S. R., et al. Proglucagon Promoter Cre-Mediated AMPK Deletion in Mice Increases Circulating GLP-1 Levels and Oral Glucose Tolerance. *PLoS One.* 2016,11:e0149549.
- [8] Dusaulcy, R., Handgraaf, S., Skarupelova, S., Visentin, F., Vesin, C., Heddad-Masson, M., et al. Functional and Molecular Adaptations of Enteroendocrine L-Cells in Male Obese Mice Are Associated With Preservation of Pancreatic alpha-Cell Function and Prevention of Hyperglycemia. *Endocrinology.* 2016,157:3832-43.

- [9] Luxon, B. A., Weisiger, R. A. Sex differences in intracellular fatty acid transport: role of cytoplasmic binding proteins. *Am J Physiol.* 1993,265:G831-41.
- [10] Robinson, A. M., Williamson, D. H. Physiological roles of ketone bodies as substrates and signals in mammalian tissues. *Physiol Rev.* 1980,60:143-87.
- [11] Hahn, P., Taller, M. Ketone formation in the intestinal mucosa of infant rats. *Life Sci.* 1987,41:1525-8.
- [12] Hahn, P., Taller, M., Srubiski, L., Kirby, L. Regulation of ketone formation and phosphoenolpyruvate carboxykinase activity in the small intestinal mucosa of infant rats. *Biol Neonate.* 1991,60:1-6.
- [13] Thumelin, S., Forestier, M., Girard, J., Pegorier, J. P. Developmental changes in mitochondrial 3-hydroxy-3-methylglutaryl-CoA synthase gene expression in rat liver, intestine and kidney. *Biochem J.* 1993,292 ( Pt 2):493-6.
- [14] Cullingford, T. E., Dolphin, C. T., Bhakoo, K. K., Peuchen, S., Canevari, L., Clark, J. B. Molecular cloning of rat mitochondrial 3-hydroxy-3-methylglutaryl-CoA lyase and detection of the corresponding mRNA and of those encoding the remaining enzymes comprising the ketogenic 3-hydroxy-3-methylglutaryl-CoA cycle in central nervous system of suckling rat. *Biochemical Journal.* 1998,329:373-81.
- [15] Clara, R., Schumacher, M., Ramachandran, D., Fedele, S., Krieger, J. P., Langhans, W., et al. Metabolic Adaptation of the Small Intestine to Short- and Medium-Term High-Fat Diet Exposure. *J Cell Physiol.* 2017,232:167-75.
- [16] McGarry, J. D., Foster, D. W. Regulation of hepatic fatty acid oxidation and ketone body production. *Annu Rev Biochem.* 1980,49:395-420.
- [17] Dashti, N., Ontko, J. A. Rate-limiting function of 3-hydroxy-3-methylglutaryl-coenzyme A synthase in ketogenesis. *Biochem Med.* 1979,22:365-74.
- [18] Iwanaga, T., Takebe, K., Kato, I., Karaki, S., Kuwahara, A. Cellular expression of monocarboxylate transporters (MCT) in the digestive tract of the mouse, rat, and humans, with special reference to slc5a8. *Biomed Res.* 2006,27:243-54.

- [19] Puchalska, P., Crawford, P. A. Multi-dimensional Roles of Ketone Bodies in Fuel Metabolism, Signaling, and Therapeutics. *Cell Metab.* 2017,25:262-84.
- [20] Shimazu, T., Hirschey, M. D., Hua, L., Dittenhafer-Reed, K. E., Schwer, B., Lombard, D. B., et al. SIRT3 deacetylates mitochondrial 3-hydroxy-3-methylglutaryl CoA synthase 2 and regulates ketone body production. *Cell Metab.* 2010,12:654-61.
- [21] Hirschey, M. D. Old enzymes, new tricks: sirtuins are NAD(+)-dependent deacylases. *Cell Metab.* 2011,14:718-9.
- [22] Le Foll, C., Dunn-Meynell, A. A., Mizioro, H. M., Levin, B. E. Regulation of hypothalamic neuronal sensing and food intake by ketone bodies and fatty acids. *Diabetes.* 2014,63:1259-69.
- [23] Carneiro, L., Geller, S., Fioramonti, X., Hebert, A., Repond, C., Leloup, C., et al. Evidence for hypothalamic ketone body sensing: impact on food intake and peripheral metabolic responses in mice. *Am J Physiol-Endoc M.* 2016,310:E103-E15.
- [24] Mattace Raso, G., Simeoli, R., Russo, R., Iacono, A., Santoro, A., Paciello, O., et al. Effects of sodium butyrate and its synthetic amide derivative on liver inflammation and glucose tolerance in an animal model of steatosis induced by high fat diet. *PLoS One.* 2013,8:e68626.
- [25] Khan, S., Jena, G. B. Protective role of sodium butyrate, a HDAC inhibitor on beta-cell proliferation, function and glucose homeostasis through modulation of p38/ERK MAPK and apoptotic pathways: Study in juvenile diabetic rat. *Chem-Biol Interact.* 2014,213:1-12.
- [26] Rahman, M., Muhammad, S., Khan, M. A., Chen, H., Ridder, D. A., Muller-Fielitz, H., et al. The beta-hydroxybutyrate receptor HCA2 activates a neuroprotective subset of macrophages. *Nat Commun.* 2014,5:3944.
- [27] van der Westhuizen, E. T., Valant, C., Sexton, P. M., Christopoulos, A. Endogenous allosteric modulators of G protein-coupled receptors. *J Pharmacol Exp Ther.* 2015,353:246-60.

- [28] Cotter, D. G., d'Avignon, D. A., Wentz, A. E., Weber, M. L., Crawford, P. A. Obligate role for ketone body oxidation in neonatal metabolic homeostasis. *J Biol Chem.* 2011,286:6902-10.
- [29] Kennedy, A. R., Pissios, P., Otu, H., Roberson, R., Xue, B., Asakura, K., et al. A high-fat, ketogenic diet induces a unique metabolic state in mice. *Am J Physiol Endocrinol Metab.* 2007,292:E1724-39.
- [30] Roberts, M. N., Wallace, M. A., Tomilov, A. A., Zhou, Z., Marcotte, G. R., Tran, D., et al. A Ketogenic Diet Extends Longevity and Healthspan in Adult Mice. *Cell Metab.* 2017,26:539-46 e5.
- [31] Lutas, A., Yellen, G. The ketogenic diet: metabolic influences on brain excitability and epilepsy. *Trends Neurosci.* 2013,36:32-40.
- [32] Mavropoulos, J. C., Yancy, W. S., Hepburn, J., Westman, E. C. The effects of a low-carbohydrate, ketogenic diet on the polycystic ovary syndrome: a pilot study. *Nutr Metab (Lond).* 2005,2:35.
- [33] Manninen, A. H. Metabolic effects of the very-low-carbohydrate diets: misunderstood "villains" of human metabolism. *J Int Soc Sports Nutr.* 2004,1:7-11.
- [34] Rajas, F., Bruni, N., Montano, S., Zitoun, C., Mithieux, G. The glucose-6 phosphatase gene is expressed in human and rat small intestine: Regulation of expression in fasted and diabetic rats. *Gastroenterology.* 1999,117:132-9.
- [35] Mithieux, G., Misery, P., Magnan, C., Pillot, B., Gautier-Stein, A., Bernard, C., et al. Portal sensing of intestinal gluconeogenesis is a mechanistic link in the diminution of food intake induced by diet protein. *Cell Metabolism.* 2005,2:321-9.
- [36] Penhoat, A., Fayard, L., Stefanutti, A., Mithieux, G., Rajas, F. Intestinal gluconeogenesis is crucial to maintain a physiological fasting glycemia in the absence of hepatic glucose production in mice. *Metabolism-Clinical and Experimental.* 2014,63:104-11.
- [37] Troy, S., Soty, M., Ribeiro, L., Laval, L., Migrenne, S., Fioramonti, X., et al. Intestinal gluconeogenesis is a key factor for early metabolic changes after gastric bypass but not after gastric lap-band in mice. *Cell Metabolism.* 2008,8:201-11.

- [38] Mithieux, G. A Synergy between Incretin Effect and Intestinal Gluconeogenesis Accounting for the Rapid Metabolic Benefits of Gastric Bypass Surgery. *Curr Diabetes Rep.* 2012,12:167-71.
- [39] Monsenego, J., Mansouri, A., Akkaoui, M., Lenoir, V., Esnous, C., Fauveau, V., et al. Enhancing liver mitochondrial fatty acid oxidation capacity in obese mice improves insulin sensitivity independently of hepatic steatosis. *Journal of Hepatology.* 2012,56:632-9.
- [40] Orellana-Gavalda, J. M., Herrero, L., Malandrino, M. I., Paneda, A., Sol Rodriguez-Pena, M., Petry, H., et al. Molecular therapy for obesity and diabetes based on a long-term increase in hepatic fatty-acid oxidation. *Hepatology.* 2011,53:821-32.
- [41] Vavrova, E., Lenoir, V., Alves-Guerra, M. C., Denis, R. G., Castel, J., Esnous, C., et al. Muscle expression of a malonyl-CoA-insensitive carnitine palmitoyltransferase-1 protects mice against high-fat/high-sucrose diet-induced insulin resistance. *Am J Physiol Endocrinol Metab.* 2016,311:E649-60.
- [42] Altaf, M. A., Sood, M. R. The nervous system and gastrointestinal function. *Dev Disabil Res Rev.* 2008,14:87-95.
- [43] Furness, J. B., Callaghan, B. P., Rivera, L. R., Cho, H. J. The enteric nervous system and gastrointestinal innervation: integrated local and central control. *Adv Exp Med Biol.* 2014,817:39-71.
- [44] Hayes, M. R., Mietlicki-Baase, E. G., Kanoski, S. E., De Jonghe, B. C. Incretins and Amylin: Neuroendocrine Communication Between the Gut, Pancreas, and Brain in Control of Food Intake and Blood Glucose. *Annual Review of Nutrition, Vol 34.* 2014,34:237-60.
- [45] Powell, N., Walker, M. M., Talley, N. J. The mucosal immune system: master regulator of bidirectional gut-brain communications. *Nat Rev Gastroenterol Hepatol.* 2017,14:143-59.
- [46] Mayer, E. A., Tillisch, K., Gupta, A. Gut/brain axis and the microbiota. *J Clin Invest.* 2015,125:926-38.

[47] Bischoff, S. C., Barbara, G., Buurman, W., Ockhuizen, T., Schulzke, J. D., Serino, M., et al. Intestinal permeability--a new target for disease prevention and therapy. *BMC Gastroenterol.* 2014,14:189.

[48] Lam, Y. Y., Mitchell, A. J., Holmes, A. J., Denyer, G. S., Gummesson, A., Caterson, I. D., et al. Role of the gut in visceral fat inflammation and metabolic disorders. *Obesity (Silver Spring).* 2011,19:2113-20.